AD-A261 332

(2)

DOCUMENTATION PAGE

Form Approved OMB No. 0704-0188

1a REPORT SECURITY CLASSIFICATION: UNCLASSIFIED (U)	1b RESTRICTIVE MARKINGS:
2a SECURITY CLASSIFICATION AUTHORITY: N/A	3 DISTRIBUTION/AVAILABILITY OF REPORT: "Approved for public release; distribution unlimited."
2b DECLASSIFICATION/DOWNGRADING SCHEDULE:	
4 PERFORMING ORGANIZATION REPORT NUMBER(S):	5 MONITORING ORGANIZATION REPORT NUMBER(S): AFOSR-TR- 93 0036
6a NAME OF PERFORMING ORGANIZATION: HCC SCIENCE & TECHNOLOGY; 6b OFFICE SYMBOL (If applicable): N/A	7a NAME OF MONITORING ORGANIZATION: AIR FORCE OFFICE OF SCIENTIFIC RESEARCH
6c ADDRESS (City, State, and ZIP Code): 86 MORRIS AVENUE, SUMMIT, NJ 07901-3956	7b ADDRESS (City, State, and ZIP Code): BUILDING 410, BOLLING AFB, DC [illegible]
8a NAME OF FUNDING/SPONSORING ORGANIZATION: DEFENSE ADVANCED RESEARCH PROJECTS AGENCY AFOSR; 8b OFFICE SYMBOL (If applicable): NC	9 PROCUREMENT INSTRUMENT IDENTIFICATION NUMBER: F49620-89-C-0097
8c ADDRESS (City, State, and ZIP Code): 3701 NORTH FAIRFAX DRIVE, ARLINGTON, VA 22203-1714	10 SOURCE OF FUNDING NUMBERS: PROGRAM ELEMENT NO 61102F; PROJECT NO 2303; TASK NO A3; WORK UNIT ACCESSION NO

11 TITLE (Include Security Classification): Development of Organic NonLinear Optical Materials (U)

12 PERSONAL AUTHOR(S): J. Sounik, R. Norwood, I. McCulloch, K. Song, R. DeMartino, L. Charbonneau, H. Yoon

13a TYPE OF REPORT	13b TIME COVERED	14 DATE OF REPORT (Year, Month, Day)	15 PAGE COUNT
FINAL	FROM 8/1/89 TO 10/30/92	1992, October 22	166

16 SUPPLEMENTARY NOTATION:

17 COSATI CODES		
FIELD	GROUP	SUB-GROUP

18 SUBJECT TERMS (Continue on reverse if necessary and identify by block number): NonLinear Optics, NLO Polymers, Degenerate Four Wave Mixing Device Fabrication, Waveguide

19 ABSTRACT (Continue on reverse if necessary and identify by block number)

(see reverse side)

93-04272

20 DISTRIBUTION/AVAILABILITY OF ABSTRACT	21 ABSTRACT SECURITY CLASSIFICATION
☒ UNCLASSIFIED/UNLIMITED ☐ SAME AS RPT. ☐ DTIC USERS	UNCLASSIFIED
22a NAME OF RESPONSIBLE INDIVIDUAL: Ashley F. Sabin	22b TELEPHONE (Include Area Code): (908) 522-7631; 22c OFFICE SYMBOL: N/A

DD Form 1473, JUN 86 — Previous editions are obsolete. — SECURITY CLASSIFICATION OF THIS PAGE

93 3 1 044 S/N 0102-LF-014-6603 — UNCLASSIFIED (U)

AFOSR Contract: F49620-89-C-0097

FINAL REPORT

Development of Organic Nonlinear Optical Materials

by

J. Sounik, R. Norwood, I. McCulloch, K. Song, R. DeMartino, L. Charbonneau, and H. Yoon

HCC Science & Technology Company, Inc.
86 Morris Avenue
Summit, NJ 07901-3956

October 1992

Abstract:

The design of organic polymers as active mediums for nonlinear optics has attracted much attention because their nature of versatility in synthetic chemistry and in fabrication. A series of new side chain polymers were synthesized and characterized for the second and third order NLO applications. Linear copolymers containing maleic anhydride as an active functional group on the main chain were prepared in this work. The maleic anhydride group reacts, by ring opening esterification with an appropriate alcohol containing an NLO functionality. These copolymers were also found to be suitable for branching or crosslinking reactions with α,ω-diols. A series of substituted silicon and aluminum phthalocyanines has been synthesized to study their third order nonlinear responses. A nitro/amino substituted aluminum phthalocyanine has been made along with mixtures of benzo substituted silicon phthalocyanines. A synthetic route has been investigated to directly give donor acceptor phthalocyanines. To increase mechanical property of phthalocyanine compounds, copolymers with MMA have been synthesized and characterized. All of the copolymers show excellent film forming characteristics.

Picosecond degenerate four wave mixing was used to study the third order nonlinear optical properties a number of NLO polymers. These polymers include silicon phthalocyanine and naphthalocyanine copolymers, 3 and 5 ring pendant side chain copolymers, and HCC side chain NLO copolymers. The 5-ring pendant copolymer shows both the highest nonlinearity ($\chi^{(3)}_{1111} = 3 \times 10^{-11}$ esu) and the highest value of $\chi^{(3)}_{1111}/\alpha$ for this group of materials. Resonant $\chi^{(3)}_{1111}$ values as large as 2.6×10^{-10} esu were observed for silicon phthalocyanine copolymers with 6 mole percent active chromophore.

It was demonstrated that silicon phthalocyanine/MMA copolymer could be used as an active material in the vertically integrated directional coupler. The waveguide experiment indicates that relatively low loss waveguiding and coupling between the upper and the bottom waveguides can be achieved. The various fabrication techniques of thin film devices were discussed. In order to get defect-free films from the spin coating process, the effects of solvent nature, spinning parameters, and drying conditions on film quality have to be understood. The use of the nonionic long chain surfactant eliminates most of coatings problems and the plasma protection layer could prevent the problem of solvent stress cracking.

FORWARD

This report was prepared at the Hoechst Celanese Research Division, 86 Morris Avenue, Summit, NJ 07901, in a cooperative effort by Drs. Ronald DeMartino, Larry Charbonneau, and Hyun Yoon as principal investigators, and Drs. Iain McCulloch, Robert Norwood, James Sounik, and Kigook Song as coauthors. The work was performed under Contract F49620-89-C-0097 sponsored by Air Force Office of Scientific Research (AFOSR). The contract period is August 1, 1989 to October 30, 1992. Dr. Donald Ulrich and Dr. Charles Lee at the Air Force Office of Scientific Research, Building 410, Bolling Air Force Base, Washington DC 20332 were the program monitors.

ACKNOWLEDGEMENTS

The Hoechst Celanese NLO research group gratefully acknowledges the support and direction provided by D. Ulrich and C. Lee, AFOSR, and L.N. Durvasula and A. Yang, DARPA.

The guidance of Hoechst Celanese management, particularly J. Riggs, Vice President, HCRD; A. Buckley, Research Director; H. Ong, Research Director; E. Steadman, Director/Optoelectronics, J Stamatoff, Manager, NLO Research, and A. Sabin, Manager, Government Program is greatly appreciated. In addition to the authors, the following individuals have worked directly on this project and each has made significant contributions: T. Leslie, D. Holcomb, A. Patel, J. Popolo, R. Keosian, and S. Ghatani.

STATEMENT OF WORK FOR AFOSR

(1) Design, synthesize, and evaluate new molecules as $\chi^{(2)}$ candidates and incorporate the most promising materials into high activity polymers.

(2) Characterize these new macromolecules for second order activity using optical and electro-optical methods.

(3) Synthesize and characterize new and novel small molecules and oligomers/polymers based on the metallated macrocycle family (which includes porphyrins, phthalocyanines, and naphthalocyanines).

(4) Evaluate these materials and other candidates for third order applications using optical methods (including picosecond optical Kerr and degenerate four wave mixing measurements). Other candidates will include polymers synthesized primarily for $\chi^{(2)}$ applications and materials obtained from other AFOSR contractors.

(5) Fabricate NLO materials (e.g. $\chi^{(2)}$ polymers and $\chi^{(3)}$ small molecules/oligomers/polymers) into forms suitable for device development. Examples of these fabrication techniques include spin coating and molding into acceptable structures for evaluation and device construction.

TABLE OF CONTENTS

LIST OF FIGURES

LIST OF TABLES

I. INTRODUCTION

Interest in nonlinear optics has grown tremendously in recent years because developments in the field of nonlinear optics hold promise for important applications in optical information processing, telecommunications, and integrated optics. Organic materials possess many critical attributes for nonlinear optical (NLO) applications. These attributes include large nonresonant susceptibilities, fast response times, and low dielectric constants. Because of their unique chemical structures of π bondings, organic molecules exhibit the largest nonresonant optical nonlinearities. These large nonlinearities have been traced to efficient charge reorganization between the electronic states in the π-electron system of their molecular constituents. For inorganic systems, important higher order NLO effects, such as a third order effect, are resonant. Thus, heat dissipation tends to limit the cycle time of devices derived from these materials. For many device applications, such as in all optical signal processing, the NLO response time is an important consideration. The dielectric constants of organic materials are considerably lower than those of inorganic crystals. This feature also has important implications for electrooptic devices in which a low frequency ac field is used to modulate the refractive index.

Another advantage of organic compounds in the NLO applications is their endless synthetic possibility and the understanding on the relationship between the molecular arrangement in crystals and the operation of NLO devices. However, organic crystals have not yet found widespread utility in integrated optics and waveguide optics mainly because of the difficulty of growing large, high quality single crystals with the required processability, mechanical integrity, and ambient stability. Recently, it has been recognized that, in addition to synthetic flexibility, a wide variety of fabrication techniques are available for organic polymeric materials. Polymeric systems offer mechanical, chemical, and thermal robustness, adhesion to a variety of materials, processability into films, fibers, waveguides, and large area structures, integration with electronics and optical sources and detectors, and low cost. In polymer films, NLO molecules can either be doped in the polymer matrix or be covalently bonded the polymer backbone. The necessary polar alignment is then induced by poling the films in electric fields above the glass transition temperature and subsequently cooling down and freezing in the non-centrosymmetrical order below the glass transition temperature.

The majority of the research and development effort at the Hoechst Celanese Corporation (HCC) in nonlinear optics has been directed toward second order nonlinear optical materials and devices. This is natural since the majority of near to medium term applications of nonlinear optics are in this area, which includes electro-optic devices of all kinds and parametric frequency conversion devices. In this project, in addition to the development of second order NLO polymers, third order NLO polymers have been investigated by presenting several simple design rules that may help in the attainment of materials with large $\chi^{(3)}$'s as well as desirable secondary properties.

There have been a number of reports in the literature on the $\chi^{(3)}$ activity of phthalocyanine derivatives that show relatively high third order NLO responses. These molecules are planar π-conjugated systems that have sharp absorption bands in the visible and near infrared, and exhibit excellent thermal and chemical stability. However, the development of all optical waveguide devices has still suffered from the lack of highly active materials which can be easily processed. It is desirable to develop materials containing these types of phthalocyanine derivatives that show high NLO activity as well as processability. In this report we present the synthesis of silicon phthalocyanine side chain copolymers and the device design which is aimed at producing an all optical switch.

The primary objectives of this project are synthesis and characterization of new NLO polymers for the second order applications; synthesis of novel NLO polymers based on metallated macrocycles; characterizations of these NLO polymers for third order applications; fabrication and evaluation of waveguide devices. In chapter II, a series of linear copolymers containing maleic anhydride as the active functional group on the main chain was prepared to explore the possibility of grafting side chain chromophore units onto a preformed polymer backbone. The second order NLO activity of the copolymers was studied using the electrooptic method. A series of substituted silicon and aluminum phthalocyanines was prepared in order to investigate their second and third order nonlinear responses (chapter III). A general synthetic route to a series of phthalocyanine methylmethacrylate copolymers was developed and the physical and optical properties of these copolymers were characterized. A number of NLO polymers were characterized for third order responses by a technique of the degenerate four wave mixing (chapter IV). These polymers include silicon phthalocyanine and naphthalocyanine copolymers, 3 and 5 ring pendant side chain copolymers, and HCC side chain NLO copolymers. Device designs and evaluation based on the silicon phthalocyanine copolymers in a vertically

integrated waveguide are discussed in the chapter V where the device fabrication techniques for a waveguide of multilayer thin films are explained.

External research and development funds have been used to develop a direct synthetic route to asymmetrical donor acceptor phthalocyanines in the laboratories of Prof. M. Kenney at the Case Western Reserve University. Prof. M. G. Kuzyk at the Washington State University produced nonlinear optical fibers using guest/host doping of various dyes in PMMA. The details of these works are included as appendices.

II. SYNTHESIS AND CHARACTERIZATION OF NEW NLO POLYMERS

2.1 INTRODUCTION

The design of organic polymers as active mediums for nonlinear optics has recently generated much interest. Side chain polymers, in which the active NLO chromophore is a pendant group to the backbone have attracted much attention because their nature combined with the versatility of synthetic chemistry can be used to alter and optimize molecular structure to maximize nonlinear responses and other properties. Other benefits associated with molecular systems derive from the fabrication methods that are available or under development for building thin film structures.

A series of linear copolymers containing maleic anhydride as the active functional group on the main chain were prepared to find out the possibility of grafting side chain chromophore units onto a preformed polymer backbone. It was proposed that incorporation of side chain units could be accomplished by a direct ring opening esterification reaction with a chromophore containing alcohol. In order to ensure a non-electrolytic final polymer, a further esterification reaction on the generated carboxylic acid group was carried out.

Such a reaction scheme may be beneficial for several reasons. Chromophores containing two or more competing vinyl groups may be incorporated by this method into a linear side chain polymer without the complication of crosslinking. Also, the increased chain transfer effects of the nitrobenzene containing monomers, which lowers polymer molecular weight, are circumvented. By correct choice of the starting molecular weight of the polymer, a polymer of predictable molecular weight may be formed. Improvement of the temporal stability of the poled state may be possible by crosslinking. This can be carried out at any stage of the process (including after film formation) by reaction of excess anhydride groups with a diol. The creation of polymer branch points may also improve toughness. A variety of comonomers can be utilized to enhance or tailor a variety of structural, mechanical, physical and optical properties. Among those investigated were styrene and methyl and butyl vinyl ether. Details of the synthesis and physical characterization results on monomers and copolymers were described in the previous interim reports [1,2].

2.2 SYNTHESIS OF MALEIC ANHYDRIDE COPOLYMERS

The synthetic strategy for diester maleic anhydride copolymers are shown in Figures 2.1 and 2.2. The preparation of three alcohols containing NLO chromophores shown in bottom of Figure 2.1 were reported in a previously report [1]. These alcohols were then used to functionalize the maleic anhydride/styrene copolymers by a ring opening esterification reaction as shown in Figure 2.1.

DMAP was used as a nucleophilic catalyst and formed the intermediate amide salt which was displaced by the alcohol. It was necessary to wash the final polymer with acetic acid to remove the catalyst as it was thought to form some kind of complex with the free acrylic acid unit. For this reason also, a molar equivalent of the catalyst was needed. Incorporation percentages were found to be dependent on solvent, temperature and molecular weight of starting polymer. Trifluoroacetic acid was also used as a fugitive acid catalyst, which could be removed either by distillation or reprecipitation of the polymer. This method was necessary when functionalizing polymers containing vinyl ether comonomers. In all cases, care was taken to ensure that the reactions were carried out under anhydrous conditions.

An alternative functionalization procedure was used to form the diesters (Figure 2.2). First, the styrene/maleic anhydride copolymer was monofunctionalized by ethanol to give complete formation of the acid ester. The methacrylic acid unit was then treated with a pyridinium salt which acts as a dehydrating agent. The mechanism involves the formation of an intermediate pyridinium ester which, by nucleophilic substitution with the stilbene alcohol, forms the polymer diester and a pyridone. As the pyridone is a good leaving group, the forward reaction proceeds smoothly.

In order to toughen the films, the polymer was crosslinked by using long chain alcohol molecules. This was achieved by reacting one α,ω-diol with approximately two polymer chains as shown in Figure 2.3. The products from the reaction with both hexane-1,6-diol and bisphenol A were insoluble gels and it was assumed that the polymer had, in effect, crosslinked. On increasing the diol chain length to the extent of poly(THF) (MW = 650 g/mol), a soluble branched polymer was produced. The reaction was carried out either neat, or in THF without addition of any catalyst.

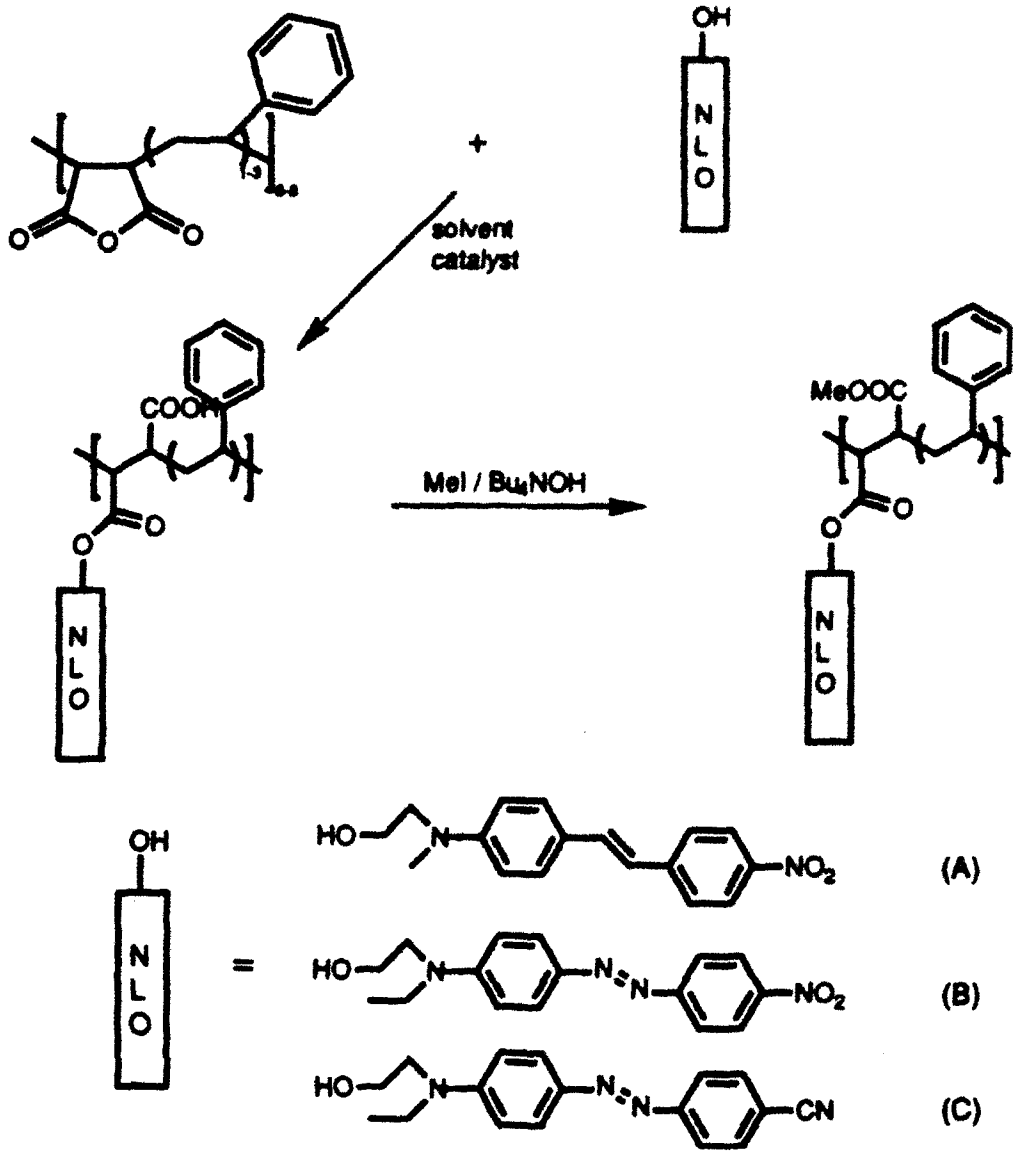

Figure 2.1 First synthetic route for diester maleic anhydride copolymers.

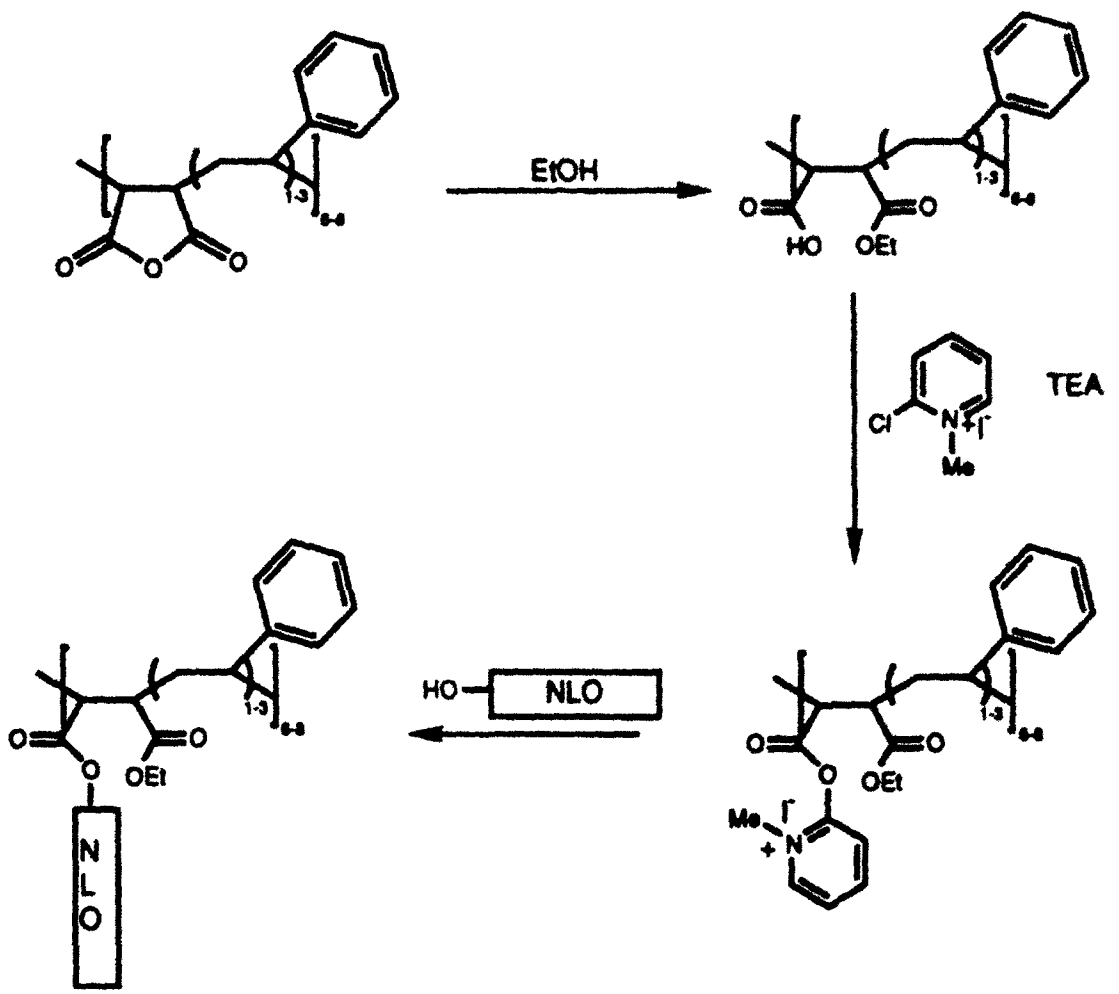

Figure 2.2 Second synthetic route for diester maleic anhydride copolymers.

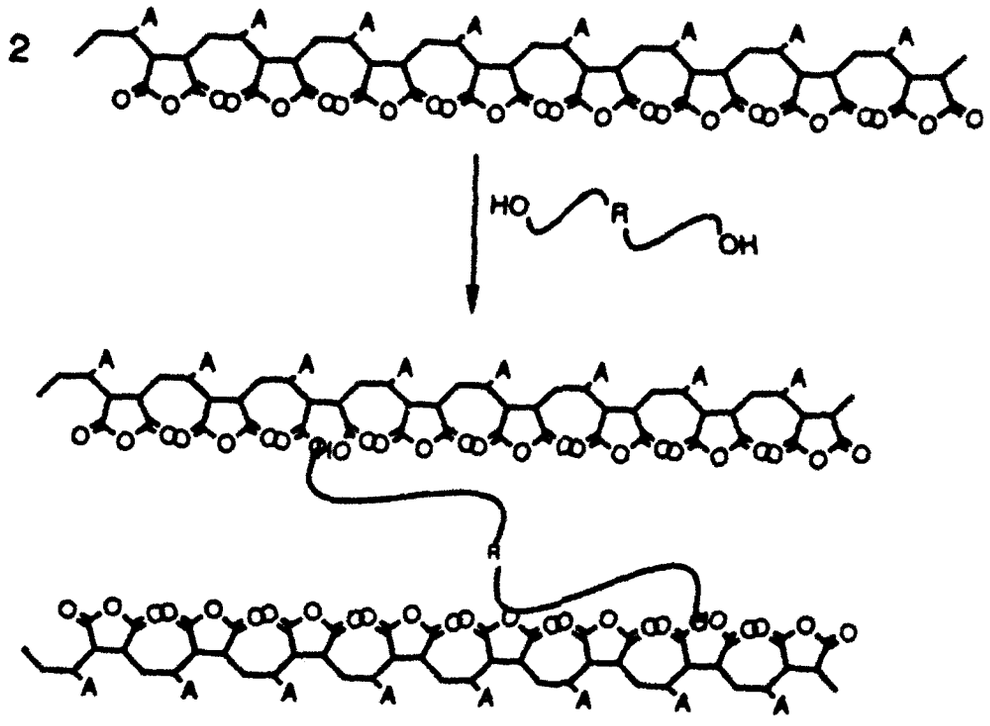

Figure 2.3 Crosslinking of maleic anhydride copolymers

2.3 RESULTS AND DISCUSSION

In all cases, polymerization of maleic anhydride and comonomers such as butyl vinyl ether and styrene resulted in high molecular weight polymer. Introduction of a slight excess of the anhydride in the feed ratio ensured synthesis of an alternating copolymer. The results show that it was possible to functionalize to a respectable degree, maleic anhydride copolymers. Solvation of the polymer was a key issue and use of a solvent which can extend the polymer chain was essential. This allowed greater access into the active anhydride sites by the nucleophiles. In this work, DMAP was recognized as a better catalyst than trifluoroacetic acid. The use of 2-chloro-1-methylpyridinium iodide as a dehydrating agent was also successful. This scheme produced a more soluble diesterified polymer.

Functionalization of the high molecular weight copolymers was also successful. Incorporation levels were generally lower due to high solution viscosity and steric entanglement effects. However the resultant polymer was of such high molecular weight that it formed a gel which proved to be unprocessable. On esterification of the anhydride unit, the backbone became inherently more flexible, resulting in a lower glass transition. However the introduction of bulky stilbene groups counteracts this by hindering movement and Tg is raised. Most glass transitions were in the range 130-150 ^{o}C.

Experiments to investigate the effect of branching the copolymers revealed some interesting preliminary data. It was shown that even for the minimum case of one branch point per chain (one diol per two chain lengths), short diol units produced crosslinked-like material. It was necessary to increase the diol link group length substantially and poly(THF) proved suitable. The resultant polymer was soluble with a lower T_g due to plasticizing effects.

A major cause of concern in this work has been the poor quality of NLO films obtained from the spin coating process. Mechanical failure due to solvent and thermal induced cracking and lack of adhesion on a variety of substrates was evident for most polymer samples. The theory of polymer mechanical property suggests that with an increase of molecular weight, a corresponding improvement in both tensile strength and toughness will result. This was investigated by synthesis of a range of polymer molecular weight precursor samples from 1,800 to 500,000 average molecular weights. However, on functionalization, the solution characteristics of the high molecular weight polymers

were such that a compromise in the solubility and the ease of filtration verses mechanical properties was necessary. The molecular structure also played a significant role in both the solution and bulk behavior. In general, as the concentration of free acid groups increased, the chain hydrodynamic volume decreased resulting in lower solubility and poorer viscosity. The acid group concentration also effected the bulk behavior in that both brittleness and film tendency to crack increased. As a result, the synthetic effort in the diester form was prioritized. Films prepared from initial batches of diesterified polymer show promising improvements in the stress resistance, resulting in fewer cracks. Also, conductivity during poling was lower, which was probably due to a decrease in transient ions scavenged by the carboxylic acid group.

2.4 SECOND ORDER NLO ACTIVITY

For the purposes of characterizing electro-optic properties of these materials, thin films (approximate thicknesses of 1-2 mm) were prepared by the spin-coating technique on indium-tin-oxide (ITO) coated glass slides. The ITO serves as one electrode of our test cell. Our first action is to deposit 1500Å of gold to act as the other electrode. This gold electrode is thermally deposited in an oblong shape of dimensions 10 mm by 3 mm. After attaching very fine wires to both electrodes, orientation of the NLO moiety was carried out through electrical poling. The poling process was carried out by applying a DC electric field across the electrodes while the material is held at a controlled temperature which is slightly above its glass transition temperature (T_g). For the initial poling, the T_g based upon data obtained from differential scanning calorimetry (DSC) was used as the poling temperature. It was found, however, that the T_g supplied by DSC is not always the optimum temperature for poling therefore, after this initial poling, we ran a thermally stimulated discharge (TSD) experiment. The TSD consists simply of heating the sample at a very controlled rate while the current output from the poled area is monitored. We then plotted output current versus temperature and a plot similar to that in Figure 2.4 was obtained. As we can see from the plot, there is a peak in the current around 140°C. It is this peak which determines the optimum poling temperature. We then would normally carry out a study to determine the electro-optic coefficient as a function of poling field. Due to the poor quality of the films, we were only able to pole some samples at a single field level, while other samples could not be poled at all (we experienced electrical breakdown as soon as a field was applied).

The measurement of the electro-optic coefficient utilizes a measurement technique in which a laser beam is directed through the glass substrate, passes through the film and is reflected from the gold electrode. The polarization of the incident laser beam is set at 45° to the plane of incidence causing the parallel and perpendicular components of the reflected light to be equal in amplitude. The reflected beam is passed through a Soleil-Babinet compensator, an analyzer, and into a detector. The modulation in the beam is measured using a lock-in-amplifier. All maleic anhydride copolymer samples investigated show rather low electro-optic properties. The coefficient found from the styrene/maleic anhydride copolymers was about 1 pm/V when poled in a field of 50 volts/μm at 140 °C. These results may indicate that there are problems with the NLO moieties themselves, in the film fabrication, or in the poling processes.

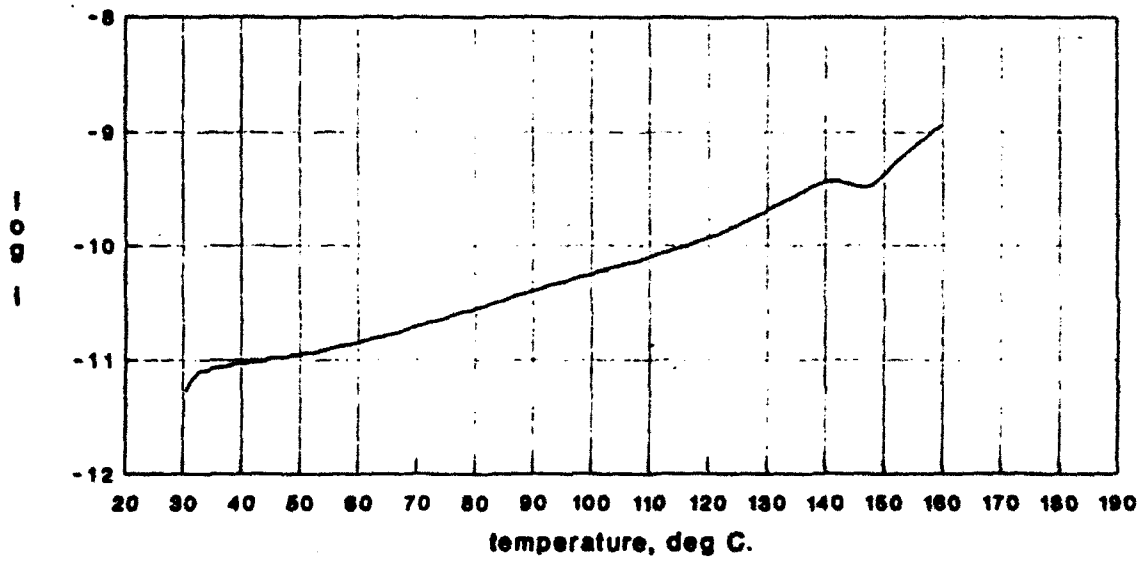

Figure 2.4 Thermally stimulated discharge of Styrene/Maleic anhydride copolymer poled at 130 °C, 50 V/μm, 5 min.

2.5 CONCLUSIONS

A new series of side chain NLO polymers, containing a maleic anhydride copolymer backbone, were prepared in this work. The maleic anhydride group reacts, by ring opening esterification with an appropriate alcohol containing an NLO functionality, to form an acid ester. These copolymers were also found to be suitable for branching or crosslinking reactions with α,ω-diols. On esterification of the anhydride unit, the backbone became inherently more flexible, resulting in a lower glass transition. However, the introduction of bulky stilbene groups counteracts this by hindering movement and T_g is raised.

In all cases, polymerization of maleic anhydride and comonomers such as butyl vinyl ether and styrene resulted in high molecular weight polymer. Introduction of a slight excess of the anhydride in the feed ratio ensured synthesis of an alternating copolymer. The results show that it was possible to functionalize these polymers to a respectable degree. Solvation of the polymer was a key issue and use of a solvent which can chain extend the backbone was essential. This allowed greater access into the active anhydride sites by the nucleophiles.

Experiments to investigate the effect on branching the copolymers revealed some interesting results. It was shown that even for the minimum case of one branch point per chain (one diol per two chain lengths), short diol units produced crosslinked like material. It was necessary to increase the diol link group length substantially and poly(THF) proved suitable. The resultant polymer was soluble with a lower T_g due to plasticizing effects. Initial electro-optic property measurements resulted in rather low activities. However, these results could indicate that there were problems with the NLO moieties themselves, in the film fabrication, or in the poling processes.

III. METALLATED MACROCYCLES

3.1 INTRODUCTION

Organic polymeric materials have received much attention for applications in nonlinear optical devices. Most recent work has focused on the electro-optic applications of glassy polymeric materials in optical waveguide devices whereas the development of all optical waveguide devices has suffered from the lack of highly active materials which can be easily processed [1-4]. There have been a number of reports in the literature on the $\chi^{(3)}$ activity of porphyrin derivatives, namely tetrabenzporphyrins, phthalocyanines and naphthalocyanines, that show relatively high third order nonlinear optical responses. These molecules are planar π-conjugated systems that have sharp absorption bands in the visible and near infrared and exhibit excellent thermal and chemical stability. Most studies have examined these dyes in solution [5-7], sublimed thin films [8,9] or in Langmuir Blodgett thin films [8,10]. Some silicon phthalocyanines have been made into siloxane copolymers that show high third order susceptibilities [11,12]. It would be desirable to develop materials containing these types of porphyrin derivatives that show high activity as well as processability similar to those polymeric materials being developed for electro-optic applications.

As reported in previous interim reports [1,2], a series of substituted silicon and aluminum phthalocyanines has been prepared to study their second and third order nonlinear responses. A nitro/amino substituted aluminum phthalocyanine was synthesized along with mixtures of benzo substituted silicon phthalocyanines. The synthesis and characterization of the benzo substituted silicon phthalocyanines showed that these materials can be made in good yield and that the isomer content along with the major absorption bands in the near infrared can be controlled.

To increase both the physical and mechanical properties of the phthalocyanine compounds a general route to a series of phthalocyanine methylmethacrylate copolymers was developed. These materials give good optical quality thin films by the technique of spin coating which is necessary in the development of $\chi^{(3)}$ waveguide devices. Analysis of the optical properties of these films show that the absorption spectra in the solid state are very similar to the solution spectra. This is due to the smaller amount of aggregation of the dye molecules in the solid state as compared to a guest host polymer thin film. These films also showed areas of low absorption between the Soret and Q bands and at wavelengths

longer than 750 nm which allows for the opportunity to develop devices at these wavelengths. These copolymers also allow for a higher amount of the active material to be incorporated into the film as compared to similar systems based on guest host polymer thin films. This is due to the limited solubility of the dyes in both the spinning solvents as well as the polymer matrix. The development of the side chain copolymers should increase the amount of dye incorporation, the film forming properties, and the solubility of the copolymers in common organic spinning solvents.

Here we present the chemistry and physical properties of a series of silicon phthalocyanine methylmethacrylate copolymers prepared by the modification of the central silicon atom. One advantage of this approach is the ease of application of this chemistry to other macrocyclic systems as there are a number of known porphyrin macrocycles with chelated silicon which could be potential $\chi^{(3)}$ materials. This advantage is demonstrated in the synthesis of silicon naphthalocyanine methylmethacrylate copolymers similar to the silicon phthalocyanine series.

3.2 SYNTHESIS OF PHTHALOCYANINES

3.2.1 Guest/Host Phthalocyanines

The synthetic approach outlined in the first interim reports gave mixtures of not only isomers, but of the nature of the groups substituted. External research and development funds was used to develop a direct route to asymmetrical donor acceptor phthalocyanines in the laboratories of Dr. Malcolm E. Kenney of Case Western Reserve University. He has developed a series of substituted phthalocyanines which can be reacted with substituted or nonsubstituted 1,3-diiminoisoindolines to give a direct synthesis of asymmetrically substituted phthalocyanines, Figure 3.1. A boron subphthalocyanine can be formed by the reaction of the appropriate 1,3-diiminoisoindoline and boron trichloride. The material can then be reacted again with another 1,3-diiminoisoindoline to give the asymmetrical unmetallated phthalocyanine derivative. This is a direct route to asymmetrically substituted phthalocyanines which can be used to make donor acceptor phthalocyanines for electro-optic applications.

A synthesis of a highly organic soluble silicon phthalocyanine was carried out by the modification of the central silicon atom. A group, bismethoxyoctadecylsilane, which would give the macrocycle high organic solvent solubility was chosen based on previous experimental results. The synthesis of the axial substituted silicon phthalocyanine is shown in Figure 3.2. Dihydroxysilicon phthalocyanine is reacted with octadecyltrichlorosilane in pyridine to give bis(dichlorooctadecylsiloxy)silicon phthalocyanine. The reaction mixture is then reacted with methanol to give bis(dimethoxyoctadecylsiloxy)silicon phthalocyanine.

3.2.2 Silicon Phthalocyanine/Methylmethacrylate Copolymers

The synthesis of the diacrylate silicon phthalocyanine copolymers follows directly from dichlorosilicon phthalocyanine (a) made in a template reaction with silicon tetrachloride and 1,3-diiminoisoindoline, Figure 3.3. The dichloride is then treated with sodium octoxide to form the bisoctoxy silicon phthalocyanine (b) which then can be purified by recrystallization. The octoxide is then hydrolyzed to dihydroxy silicon phthalocyanine (c) which is then reacted with methacryloxypropyldimethylchlorosilane to give the diacrylate monomer (d). The phthalocyanine monomer is then polymerized with

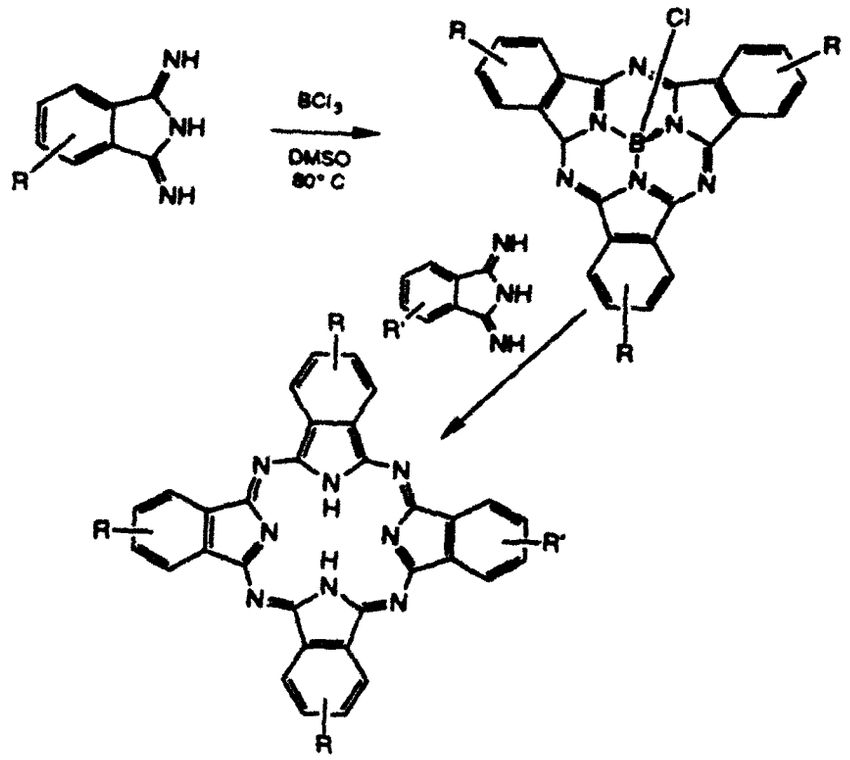

Figure 3.1 Synthesis of asymmetrical phthalocyanines from subphthalocyanines.

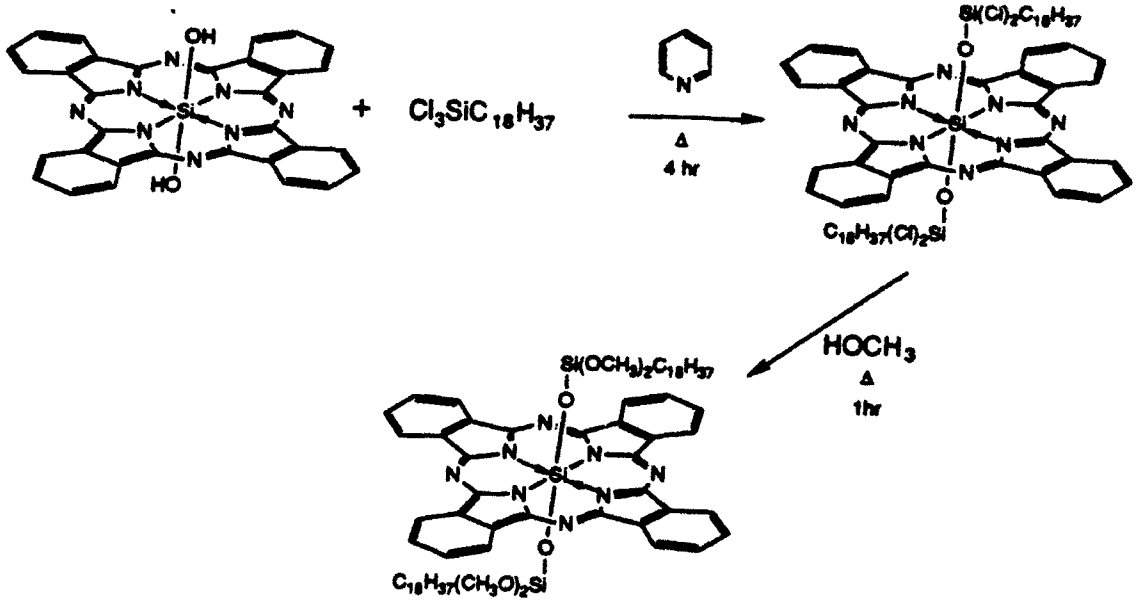

Figure 3.2 Synthesis of bis(dimethoxyoctadecylsiloxy)silicon phthalocyanine.

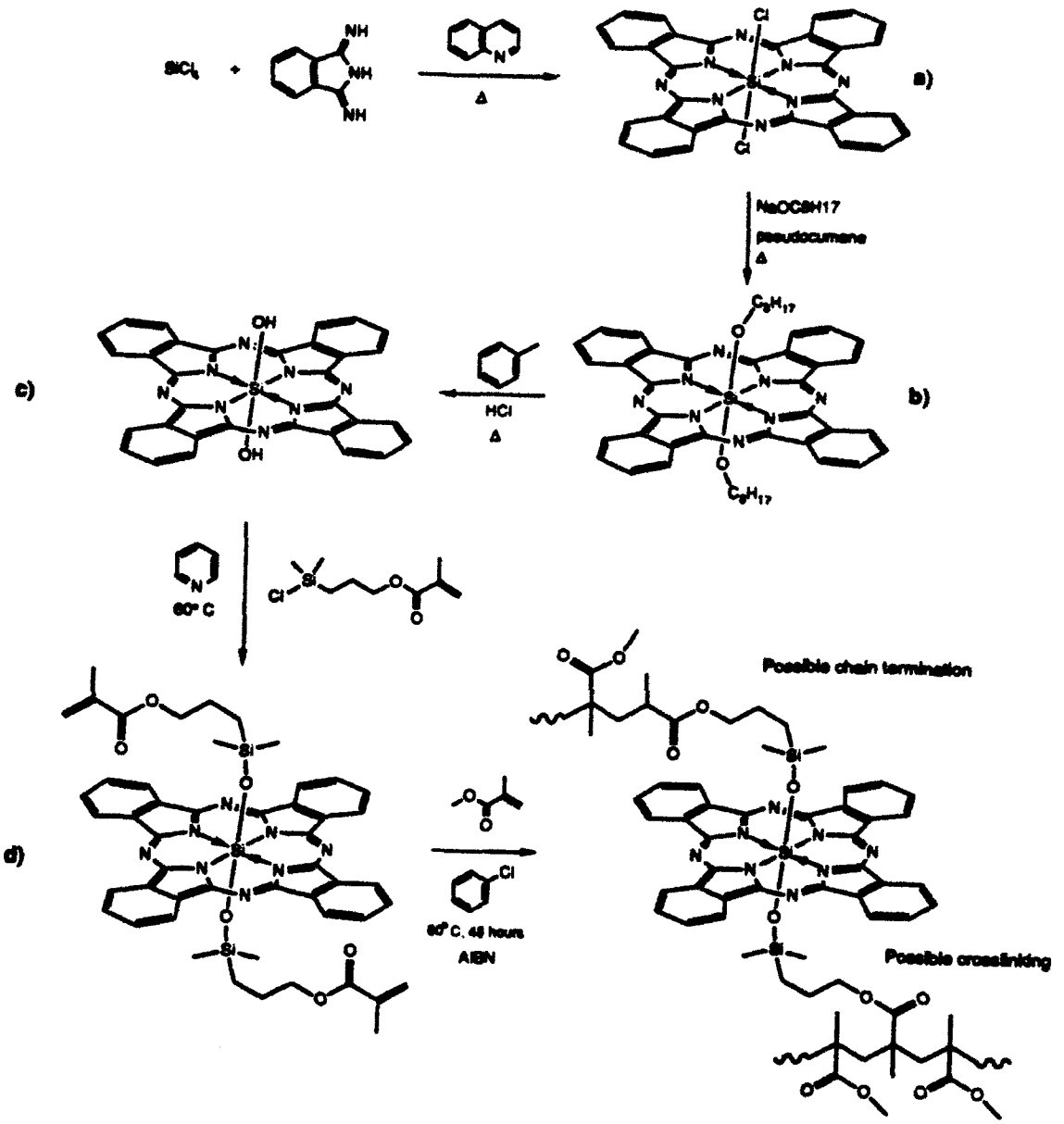

Figure 3.3. Synthesis of diacrylate silicon phthalocyanine/methylmethacrylate copolymers.

methylmethacrylate in chlorobenzene using AIBN as the radical initiator. The copolymers are then precipitated into methanol to give the final product.

The synthesis of the monoacrylate silicon phthalocyanine copolymers also follows directly from dichlorosilicon phthalocyanine (a), Figure 3.4. The dichloride is reacted with tri-*n*-hexyl sodium silanolate to form bis(tri-*n*-hexylsiloxy) silicon phthalocyanine (e). One group is then selectively hydrolyzed using trichloroacetic acid/toluene followed by water/pyridine to form the hydroxy(tri-*n*-hexylsiloxy) derivative (f). The hydroxide is then reacted with the functionalized silane to give the unsymmetrical monoacrylate silicon phthalocyanine monomer (g). The monomer can then be polymerized under similar conditions as the diacrylate monomer to give the copolymers.

3.2.3 Silicon Naphthalocyanine/Methylmethacrylate Copolymers

The synthesis of the diacrylate silicon naphthalocyanine copolymers follows directly from dichlorosilicon naphthalocyanine (h) made in a template reaction with silicon tetrachloride and 1,3-diiminobenz(*f*)isoindoline, Figure 3.5. This procedure is identical to the procedure developed for the silicon phthalocyanine series. The dichloride is then treated with sodium octoxide to form the bisoctoxy silicon naphthalocyanine (i) which then can be recrystallized. The octoxide is then hydrolyzed using HCl/toluene to dihydroxy silicon naphthalocyanine (j) which is then reacted with methacryloxypropyl-dimethylchlorosilane to give the diacrylate silicon naphthalocyanine monomer (k). The monomer can then be polymerized under similar conditions as the diacrylate silicon phthalocyanine monomer to give copolymers, however, dry distilled pyridine is used as the solvent.

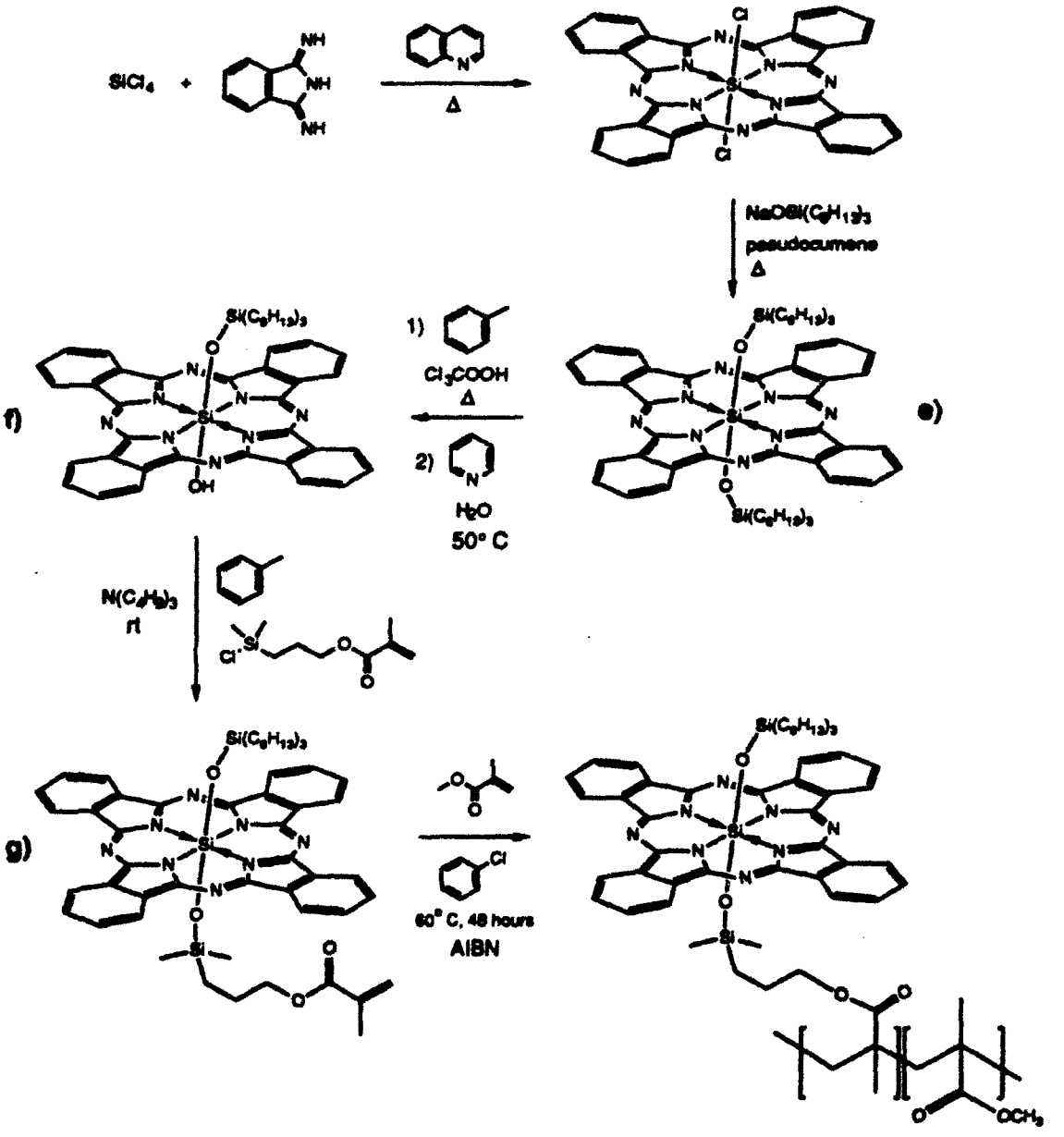

Figure 3.4. Synthesis of monoacrylate silicon phthalocyanine/methylmethacrylate copolymers.

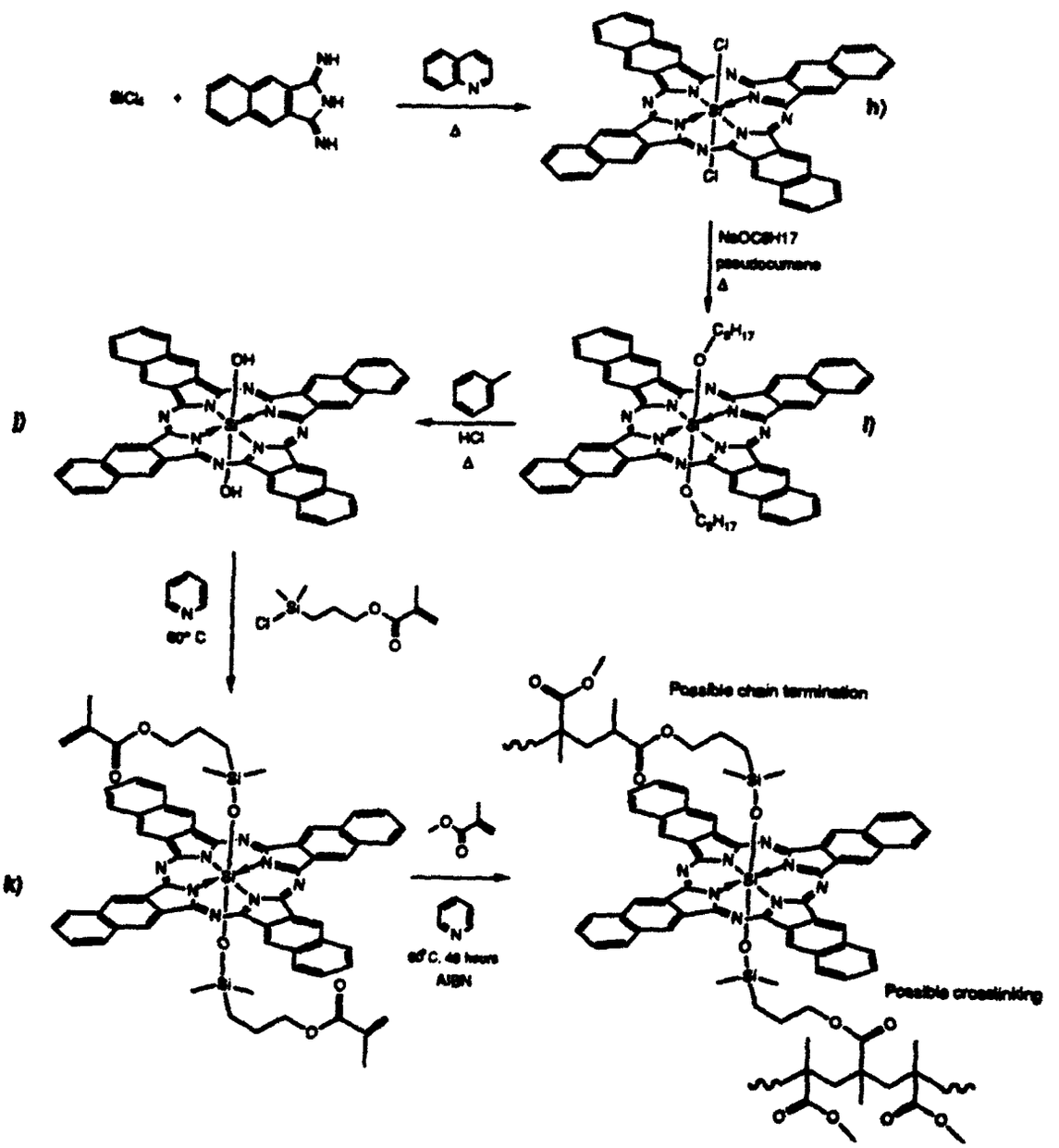

Figure 3.5. Synthesis of diacrylate silicon naphthalocyanine/methylmethacrylate copolymers.

3.3 CHARACTERIZATION

3.3.1 UV-Vis Spectroscopy

Previously we have reported on the characterization and evaluation of a number of silicon phthalocyanine and naphthalocyanine methylmethacrylate copolymers [1,2]. In guest host structures in PMMA, a limited solubility of the guest chromophores in polymer matrix was observed when fabricated by a solution spin coating. As reported in the previous report, the broadening of the strong Q-Band in the UV-Vis spectra (Figure 3.6) was observed with increasing dye concentration from 5 to 10 percent. The data suggest that guest host systems can not retain sharp absorption bands due to intermolecular association. This broadening may effect both the optical damage and the optical clarity at the desired wavelengths for waveguide devices at 1.06 or 1.3 μm. Covalent bonding of the chromophore should eliminate crystallite formation which causes these effects and give materials with higher concentrations of the active chromophore without significant spectral broadening.

In silicon phthalocyanine methylmethacrylate copolymers, the UV-Vis spectra of thin films show a slight shift and broadening of the strong Q-band with increasing phthalocyanine concentration, Figure 3.7. This is due to increased intermolecular interactions at higher concentrations. Solution spectra of the monomer in ethyl acetate shows a band maximum at 670 nm and a FWHM value of 12 nm. All of the copolymers at concentrations of 20 % by weight and below show no effect on the band position and FWHM for both the diacrylate or monoacrylate copolymers.

3.3.2 Thermal Characterization

The analysis of the copolymers by differential scanning calorimetry (DSC) has shown that for the diacrylate silicon phthalocyanine/MMA and silicon naphthalocyanine/MMA copolymers, of up to 10% by weight, the glass transition temperatures are only slightly higher than that seen for polymethylmethacrylate (105 °C), Table 3.1. There is little or no effect of molecular weight or dye concentration on the glass transition temperature which is due to the relatively low amount of chromophore (<1 mole percent) in these systems. DSC analysis of the monomethacrylate silicon

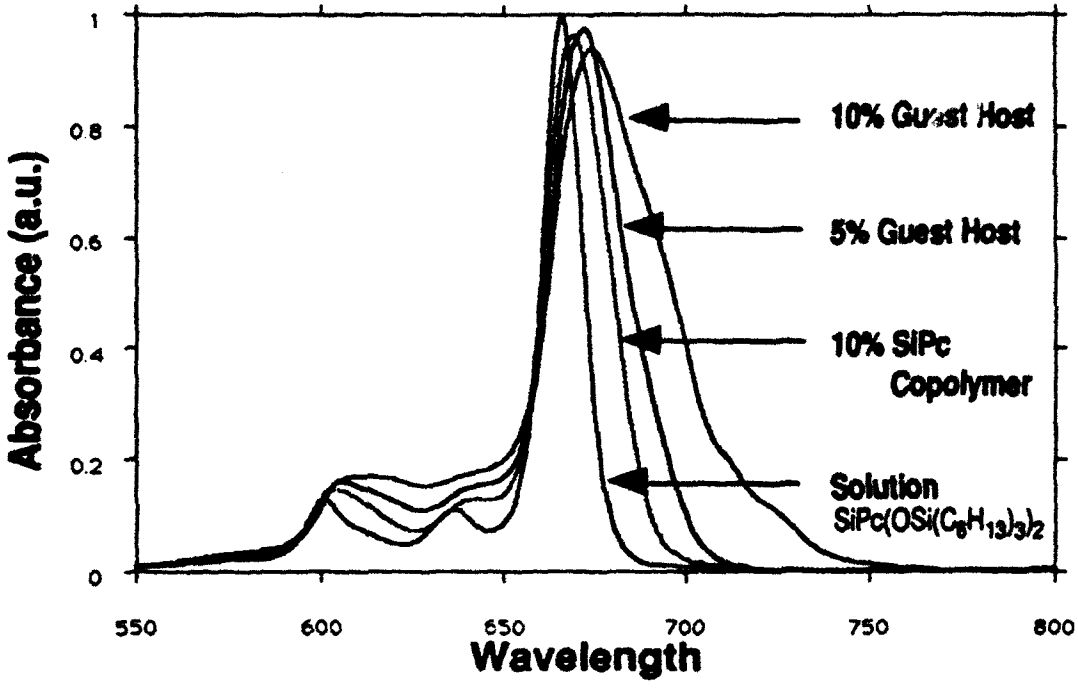

Figure 3.6 UV-Vis-NIR absorption spectra of different concentration guest host thin films, copolymer thin films and $SiPc(OSi(C_6H_{13})_3)_2$ in solution.

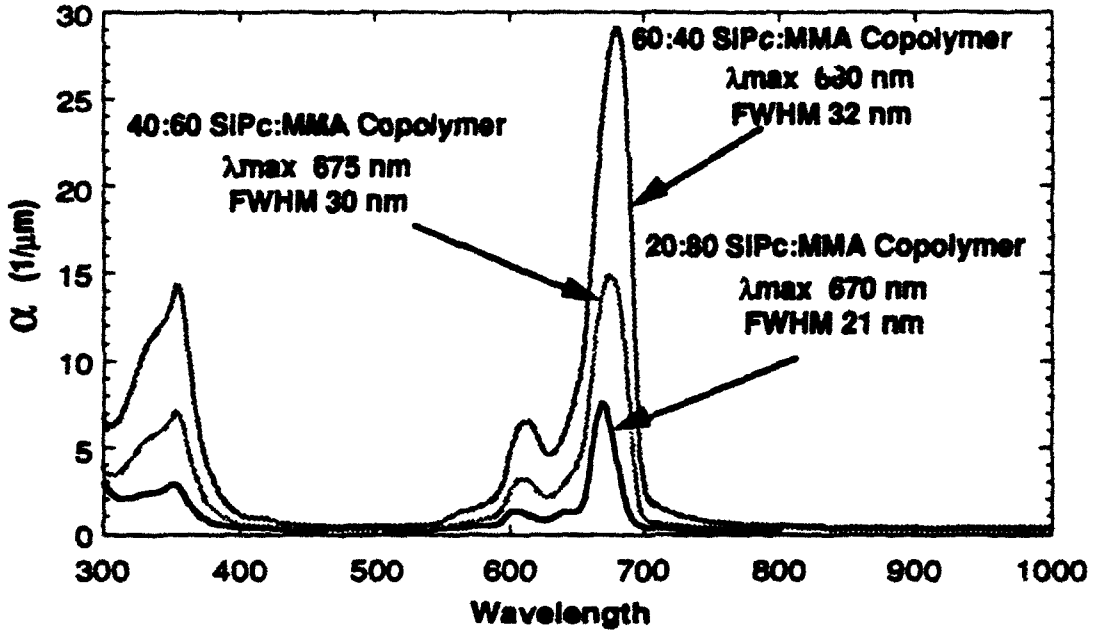

Figure 3.7. UV-Vis-NIR spectra of various concentrations of silicon phthalocyanine methylmethacrylate copolymers.

phthalocyanine/MMA copolymers of as high as 56% by weight have shown that at concentrations of ~30% or lower, the glass transition occurs at temperatures much lower than that seen for PMMA with no other transitions. With concentrations of higher than ~30%, a glass transition and a melting transition is seen, Table 3.2. The DSC trace of the 56% by weight SiPc/MMA copolymer is seen in Figure 3.8. The second scan in the copolymers that initially show melting transitions only show glass transitions. This suggests that the copolymers become amorphous after being heated to temperatures above the melting transition and then cooled. As the concentration of the active chromophore increases, the amount of polymer crystallinity increases which effects both the linear absorption spectrum and the nonlinear response. Linear absorption effects appear, as reported earlier, as inhomogeneous line broadening and shifting of the large Q-band absorption at 680 nm with increased tailing of the band into the near infrared. The nonlinear response effects are seen with a nonlinear increase of $\chi^{(3)}$ with increasing concentrations of the active chromophore. This has been explained by exciton-exciton interactions which is consistent with an increase in molecular association caused by the increased crystallinity in the higher concentration copolymers.

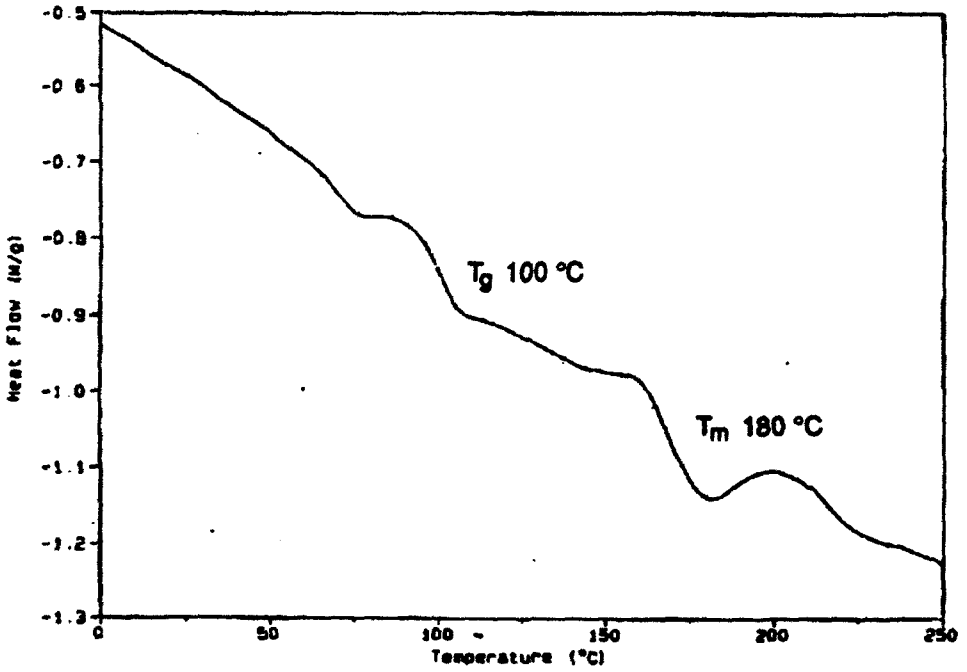

Figure 3.8 DSC trace of a 56% by weight SiPc/MMA copolymer showing both a T_g (100 °C) and T_m (180 °C).

Table 3.1

Silicon Phthalocyanine Bismethacrylate Copolymer Data

Composition[1] (NMR)	T_g (°C)	Molecular Weight	M_w/M_n
2:98	121	41,000	1.8
6:94	124	166,000	4.8
6:94	112	192,000	4.5
11:89	129	307,000	10.4
9:91	117	99,000	5.1

[1] composition SiPc Monomer:MMA monomer as weight %.

Table 3.2

Silicon Phthalocyanine Monomethacrylate Copolymer Data

Composition[1] (NMR)	T_g (°C)	T_m (°C)	Molecular Weight	M_w/M_n
11:89	92	-	21,000	1.3
15:85	94	-	32,000	1.7
16:84	98	-	31,000	1.6
18:82	87	-	24,000	1.4
25:75	73	-	20,000	1.2
40:60	82	190	25,000	1.4
56:44	100	180	25,000	1.4

[1] composition SiPc Monomer:MMA monomer as weight %.

3.3.3 Structural Analysis by X-ray and Infrared Spectroscopy

In order to investigate further the structure of the monomethacrylate silicon phthalocyanine copolymer systems, x-ray powder diffraction was performed on a series of copolymers and polymethylmethacrylate (PMMA). A sample of PMMA (Aldrich, very high molecular weight) and samples of the 18%, 40% and 56% by weight SiPc/MMA copolymers were scanned using a copper K_α source from 5 to 60 degrees 2θ. The results are shown in Figure 3.9. PMMA appears amorphous with two broad bands at 6.46 Å and 3.00 Å, Table 3.3. The 18% by weight SiPc/MMA copolymer shows a similar amorphous pattern with only a slight shift in the largest band, the inter-chain distance, from 6.46 Å to 5.86 Å. As the concentration of the silicon phthalocyanine increases to 40 and 56 percent, the pattern changes significantly showing a increase in crystallinity. A new band appears at 10.04 Å in both samples which becomes more intense in the 56 percent copolymer. The large band shifts even further to 4.93 Å indicating that the amorphous component is more tightly bound. Estimation of the crystallinity based on the integrated area of the crystalline and amorphous peaks gives approximately 10 percent for the 40% SiPc/MMA copolymer and approximately 19 percent for the 56% SiPc/MMA copolymer.

Table 3.3

Silicon Phthalocyanine Monomethacrylate Copolymer
X-ray Powder Diffraction Data

Monomer	Composition[1] (NMR)	Spacing (Å)	Spacing (Å)	Spacing (Å)
PMMA	-	-	6.46	3.00
monomethacrylate	18:82	-	5.86	3.00
monomethacrylate	40:60	10.04	4.93	3.00
monomethacrylate	56:44	10.04	4.93	3.00

[1] composition SiPc Monomer:MMA monomer as weight %.

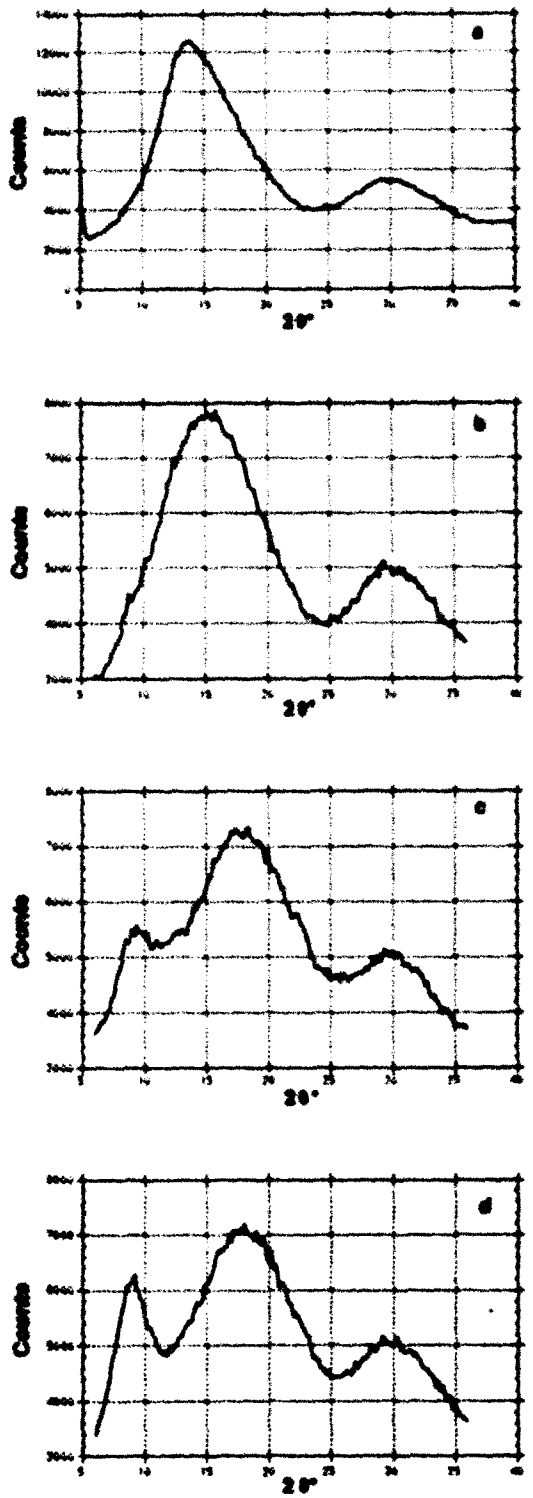

Figure 3.9 X-ray powder diffraction data of a) PMMA (Aldrich, very high molecular weight), b) 20% by weight SiPc/MMA, c) 40% by weight SiPc/MMA, and d) 60% by weight SiPc/MMA. As the chromophore concentration increases, the data shows an increase in crystallinity of copolymers.

Analysis of a series of silicon phthalocyanine copolymers was done to determine the effects of the polymer structure on the infrared absorption spectrum. The FT-infrared absorption spectra of the 18, 40, and 56 percent by weight SiPc/MMA copolymers as Nujol mulls are shown in Figure 3.10. The spectra show clearly the increase in intensity of the silicon phthalocyanine bands at 1612 (aromatic C=C), 1123, 1077, 1040 (Si-O-Si), 910, and 741 cm^{-1} with increasing chromophore content. The presence Si-O-Si band confirms the NMR data which shows no cleavage of the axial ligands in the synthesis of these systems. Significant narrowing of the carbonyl band at 1732 cm^{-1} and the polymethylmethacrylate bands at 1447, 1243 and 1150 cm^{-1} also occur. This is consistent with the increase in crystallinity of these copolymers.

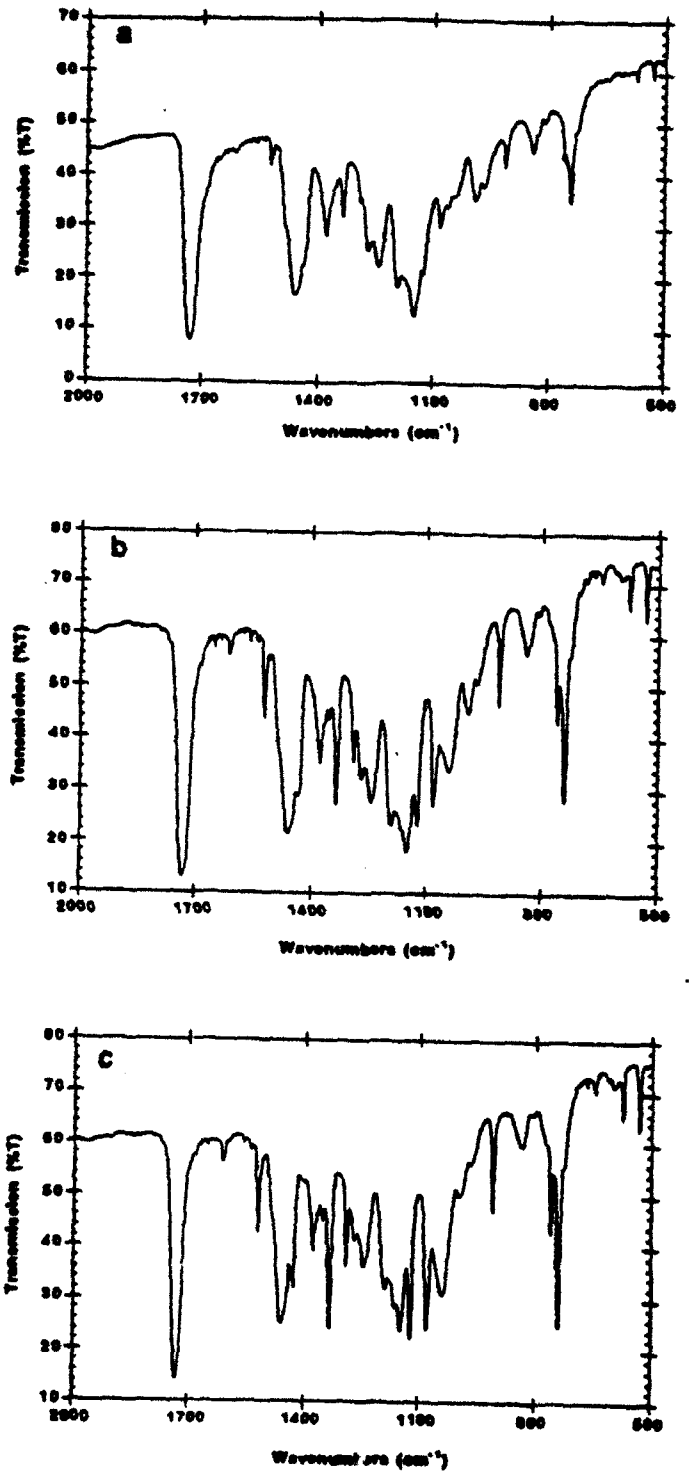

Figure 3.10 Infrared spectra of (a) 18 % SiPc/MMA, (b) 40 % SiPc/MMA, and (c) 60 % SiPc/MMA copolymers in Nujol. Spectra shows the increase of the SiPc bands along with Si-O-Si band at 1040 cm^{-1}.

3.4 CONCLUSIONS

A series of substituted silicon and aluminum phthalocyanines has been made to study their third order nonlinear responses [1,2]. A nitro/amino substituted aluminum phthalocyanine has been prepared along with mixtures of benzo substituted silicon phthalocyanines. The synthesis and characterization of the benzo substituted silicon phthalocyanines has shown that these materials can be prepared in good yield and that the isomer content along with the major absorption bands in the near infrared can be controlled.

To improve both the physical and mechanical properties of the phthalocyanine compounds a general route to a series of phthalocyanine methylmethacrylate copolymers was developed. These materials give good optical quality thin films by the technique of spin coating which is necessary in the development of $\chi^{(3)}$ waveguide devices. Analysis of the optical properties of these films show that the absorption spectra in the solid state are very similar to the solution spectra. This is due to the smaller amount of aggregation of the dye molecules in the solid state as compared to a guest host polymer thin film. These films also show areas of low absorption between the Soret and Q bands and at wavelengths longer than 750 nm which allows for the opportunity to develop devices at these wavelengths. These copolymers also allow for a higher amount of the active material to be incorporated into the film as compared to similar systems based on guest host polymer thin films. This is due to the limited solubility of the dyes in both the spinning solvents as well as the polymer matrix. The development of the side chain copolymers should increase the amount of dye incorporation, the film forming properties, and the solubility of the copolymers in common organic spinning solvents.

When the concentration of the phthalocyanine is higher then approximately 30 percent, the silicon phthalocyanine copolymers exhibit partly crystalline properties. This crystallinity has been observed in the DSC, X-ray and FT-IR data obtained for these systems. Evidence suggest that these systems become amorphous when heated above the melting point which should influence the observed degenerate four wave mixing results. This then may show a linear increase in the third order nonlinear response of these copolymers as well as the degenerate four wave mixing dynamics.

IV. NLO CHARACTERIZATION OF THIRD ORDER POLYMERS

4.1 INTRODUCTION

For nonpoled amorphous polymers, the lowest order nonlinear optical effect is third order in the applied optical field, and the size of the effect is dependent on the size of the third order nonlinear optical susceptibility, a fourth rank tensor called $\chi^{(3)}$. There has been a large amount of interest in the third order NLO properties of polymers, since it is believed that the majority of the nonlinearity present in polymer systems is electronic in origin, and can therefore be very fast (femtosecond response times). The only present application that could use anywhere near this speed is ultrafast switching on telecommunications networks, and even in this case a need will probably not be felt for 5-10 years or so. However, beyond the 5 year time frame and into the farther future, $\chi^{(3)}$ or all-optical materials may play an important role in such diverse areas as telecommunications, optical limiting, parallel processing and optical computing.

One clear advantage of working with $\chi^{(3)}$ polymer materials is that poling and the questions it raises about thermal stability are no longer issues. Furthermore, many applications of $\chi^{(3)}$ materials can be addressed by materials in fiber form, which is consistent with processes that have previously been developed at HCC. A disadvantage is that the optical power handling capability of the material should be much better than for electro-optic applications, since high powers will be needed for switching to occur.

The purpose of this work is to present several simple design rules that may help in the attainment of materials with large $\chi^{(3)}$'s as well as desirable secondary properties and to discuss the measurements on HCC materials and materials supplied by outside contractors. We hope to show that for amorphous polymers incorporating chromophores, the $\chi^{(3)}$ depends primarily on chromophore loading and the strength of the chromophore, as one would expect from a simple model. A number of different systems are discussed in detail including side-chain electro-optic polymers, side chain 5- and 3-ring polymers, guest/host porphyrin derivatives, and side chain polymers incorporating phthalocyanines and naphthalocyanines.

4.2 DEGENERATE FOUR WAVE MIXING

Degenerate four wave mixing (DFWM) in the conventional phase-conjugate geometry (Figure 4.1) was used to perform the measurements on thin film samples of the copolymers cast onto glass slides. The laser pulses used for the experiment were 1-2 psec long, 598 nm wavelength, repetition rate of 10 Hz, and maximum pulse energy densities at the sample of about 1 mJ/cm^2. The diagonal component of the third order nonlinear susceptibility $\chi^{(3)}_{1111}$ is measured by studying the intensity dependence of the phase conjugate signal as a function of input laser intensity. In some cases the off-diagonal component $\chi^{(3)}_{1221}$ was also measured, in which case the backward going pump beam polarization and the signal polarization were perpendicular to the polarizations of the other two beams. Achromatic polarization rotation was achieved by a simple arrangement using two consecutive dichroic sheet polarizers at 45 degrees to one another (see Figure 4.1). One expects that the phase conjugate intensity should go as the cube of the intensity input to the DFWM, but this simple law may not hold because of factors such as light scattering, saturation of the nonlinearity or two-photon absorption. When an appropriate method could be found to extract the cubicly varying portion of the nonlinearity the following expression, appropriate for thin film samples, was used to determine $\chi^{(3)}$

$$\frac{\chi^{(3)}_S}{\chi^{(3)}_R} = \left(\frac{n_S}{n_R}\right)^2 \left(\frac{L_R}{L_S}\right) \frac{\alpha_S L_S}{e^{-\alpha_S L_S/2}(1 - e^{-\alpha_S L_S})} \sqrt{\frac{C_S}{C_R}} \qquad (1)$$

where n_S and n_R are the refractive indices of the sample and the reference (100 μm of carbon disulphide), L_S and L_R the lengths of the sample and reference, respectively; α_S the absorption coefficient of the sample, and C_S and C_R the sample and reference cubic coefficients. Data were often fit in a number of different ways to test the sensitivity of the fitting coefficients to the particular model for the nonlinear response. In cases where significant discrepancies occurred, fitting coefficients from several representative models were averaged. In comparison, the statistical error of the data was generally negligible.

For time-domain measurements of the DFWM response the backward-going beam (attenuated with respect to the other beams by at least a factor of 4) was progressively delayed with respect to the other two beams. The phase conjugate signal amplitude was

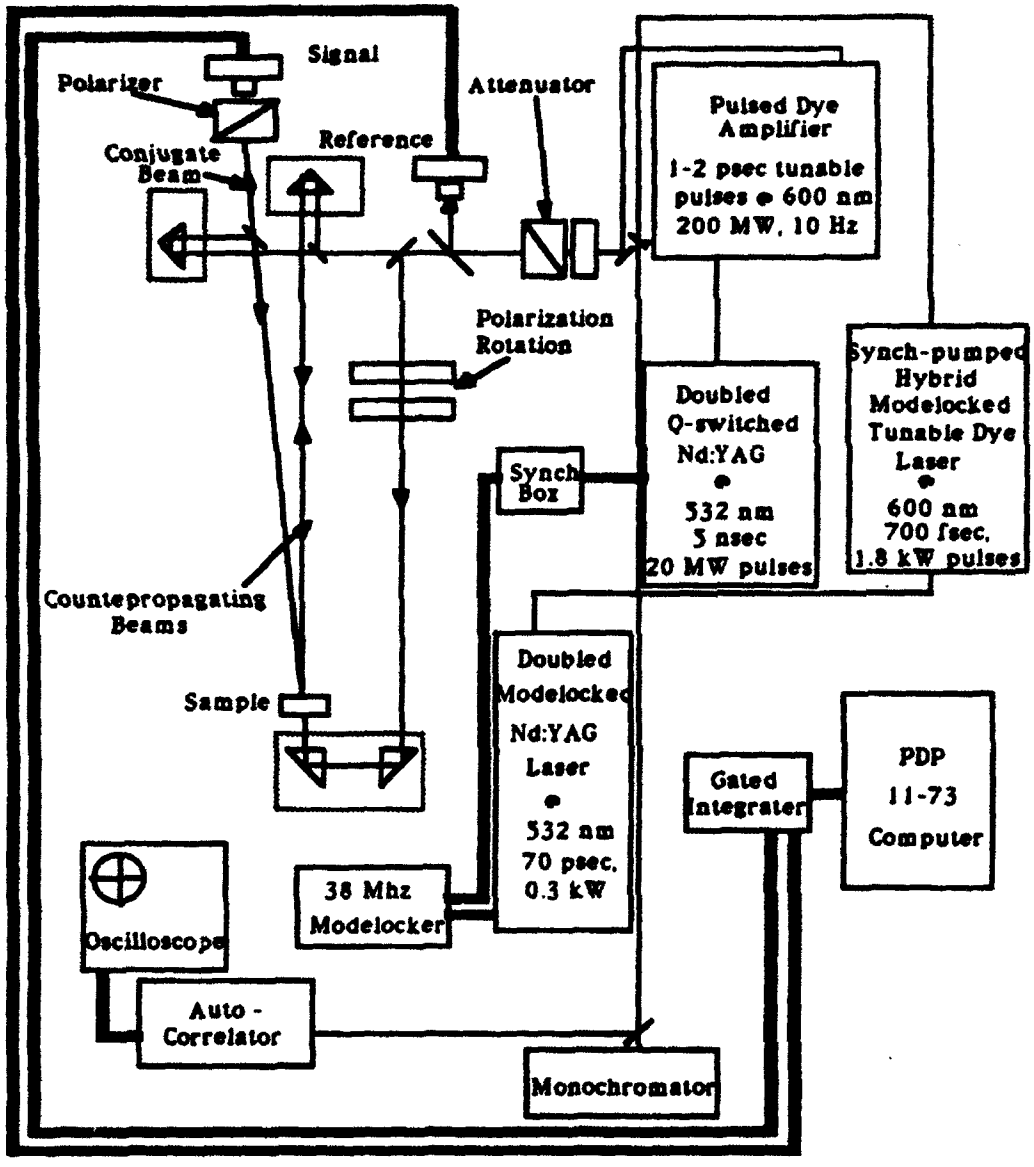

Figure 4.1. Experimental setup for degenerate four wave mixing experiment.

then recorded as a function of this delay. In this case, the dynamics of the grating formed by the two forward-going beams are probed by the backward beam, which is attenuated to avoid additional effects owing to gratings formed between it and the other two beams. In the simplest cases the signal S was analyzed by fitting the data to a sum of instantaneous and noninstantaneous components

$$S(t_D) = A\exp(-t_D/0.91\text{psec}) + B\exp(-2t_D/\tau_r),\ t_D > 0 \qquad (2)$$

where t_D is the delay of the backward going beam with respect to the time origin, A and B are the fractions of the response that are instantaneous and non-instantaneous, respectively, and τ_r is the decay time of the non-instantaneous response. The instantaneous response of the system was determined by measuring the DFWM signal from a thin film sample of a copolymer of 4-amino-4'-nitrostilbene with methyl methacrylate, which is a completely nonresonant response at 598 nm. An inherent assumption in (2) is that the data is not significantly effected by interference between the instantaneous and noninstantaneous components of the grating; this is not the case if the decay time is nearly the same as the pulse length. Often the data could not be accurately fit by (2), in which case an additional component was included that provided for an excited species with a lifetime much longer than the time scale of the experiment.

4.3 SILICON PHTHALOCYANINE COPOLYMERS

4.3.1 Introduction

Quantum-confined systems are known to exhibit exceptionally strong and narrow optical resonances, as witnessed in quantum wells, wires and dots in semiconductor materials. A molecular system with a well-defined dimensionality is obviously analogous to such quantum-confined systems, with the major difference being that the density of electronic states in the molecular system is a series of delta functions, unlike the band that exists in semiconductor systems. Cyclic (2-D) conjugated molecular systems are known that demonstrate extremely large and sharp absorption bands in the visible and near-infrared, namely the porphyrin-phthalocyanine-napthalocyanine series of molecules, depicted in Figure 4.2. The position of the first excited state, dubbed the Q-band, shifts to the red as the fundamental structure increases its conjugation; a further effect is an increase in oscillator strength. These molecules have been of interest for some time owing to their extreme chromophoric intensity, their presence in biological systems, and their high stability to photooxidative and thermal decay.

There have been a number of reports on the third order nonlinear optical properties of porphyrin derivatives, which are two-dimensional π-conjugated macrocyclic molecules [5,6,17]. They are attractive because of their relatively large $\chi^{(3)}$'s, sharp absorption bands in the visible and near-infrared that can be used for resonance enhancement of $\chi^{(3)}$, easy derivatization and central metal substitution, and excellent chemical and thermal stabilities. However, most of these reports involve degenerate four wave mixing (DFWM) measurements on solutions of porphyrins at low concentrations (10^{-4} M) with subsequent extrapolation to what the solid state properties might be [6], or measurements on polycrystalline films that are not viable optical device materials [9].

Calculations have shown that the nonresonant value of $\chi^{(3)}$ should be smaller in cyclic conjugated structures than in linear conjugated structures of the same conjugation length, as a result of the increased dimensionality. However, this increased dimensionality also results in increased sharpening and intensity of the absorption band, thereby making such systems viable as saturable absorbers and as resonantly enhanced $\chi^{(3)}$ media. Indeed, a number of measurements have been done on a variety of phthalocyanines showing the resonance enhancement has a large effect on the $\chi^{(3)}$ as measured by third

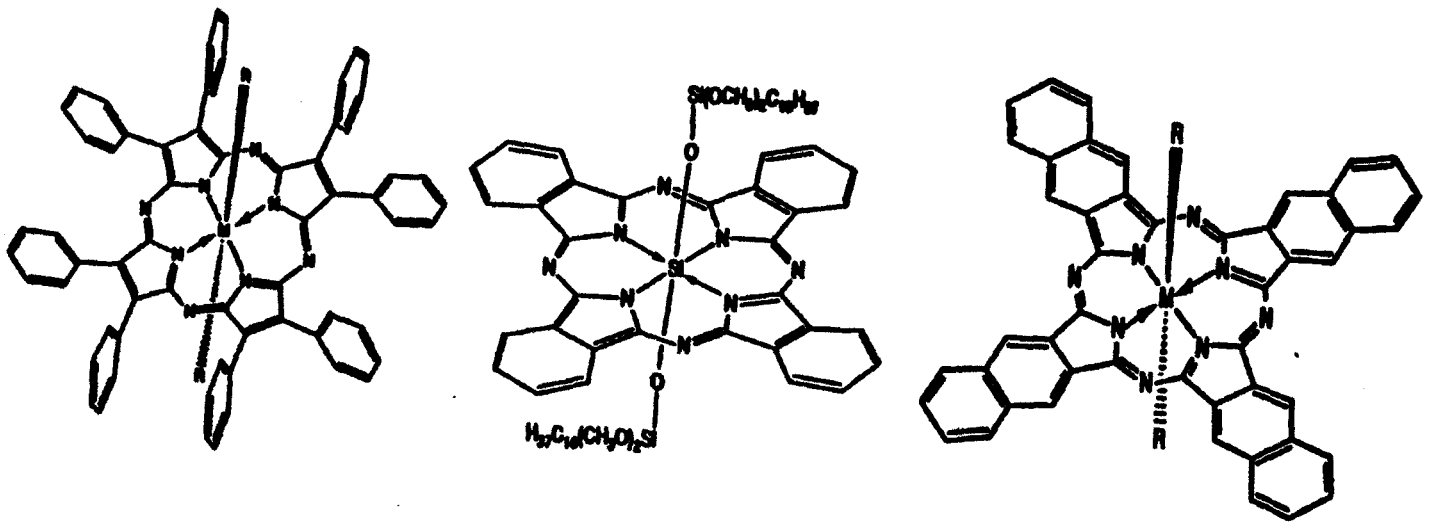

Figure 4.2 Structures of an octaphenyl tetraazaporphyrin, phthalocyanine, and naphthalocyanine.

harmonic generation and by degenerate four wave mixing. Furthermore, the excited state nonlinearities in these systems have received a good deal of study and interest.

Progress has been made in making these chromophores more soluble [5], and also incorporating them in polymers, so that thin film structures of high quality have been made. Furthermore, the near infrared absorption of these materials is small compared to the Q-band absorption. The molecular absorbance of solubilized silicon naphthalocyanine (SiNc) versus wavelength out to 1350 nm was measured by infinite dilution studies of the molecule dissolved in dichloromethane. The results did not fit a Lorentzian indicating that the absorption line is significantly inhomogeneously broadened, as has been discussed for the solid solution case. By making the environment of the chromophores as homogeneous as possible, the narrowest spectra can be obtained and thus the largest resonance enhancement and figure of merit. This is difficult to achieve in guest-host systems because at concentrations of the guest that are high enough for appreciable nonlinear optical effects, aggregation of guest molecules generally results, leading to broadening of the absorption line. However, by covalently bonding the chromophore to a suitable polymer chain the homogeneity can be significantly increased, thereby increasing the molecular figure of merit within the two-level model. Furthermore, these copolymers can have the same advantages that the guest host systems have in terms of fabricability (uniform thin films by spin coating) and increased chemical stability.

4.3.2 Comparison of Guest/Host Systems with Phthalocyanine Copolymers

To investigate the role of excited state population effects and determine the role of the environment of the chromophores, we performed DFWM measurements on two guest host systems and a copolymer, measuring both the magnitudes of the nonlinearity for several different tensor components as well as the dynamics of the nonlinearity. The structures of the two molecules in the guest/host systems and of the copolymer are shown in Figure 4.3, and the specific compositions of the thin films (with chromophore incorporation specified by weight %) were 5% magnesium octaphenyl-tetraazaporphyrin (Mg:OPTAP) /polymethylmethacrylate (PMMA) guest/host, 10% silicon phthalocyanine (SiPc) monomer/methylmethacrylate (MMA) copolymer, and 30% silicon naphthalocyanine (SiNc) /PMMA guest/host. This SiPc/MMA copolymer is a cross-linked system with the

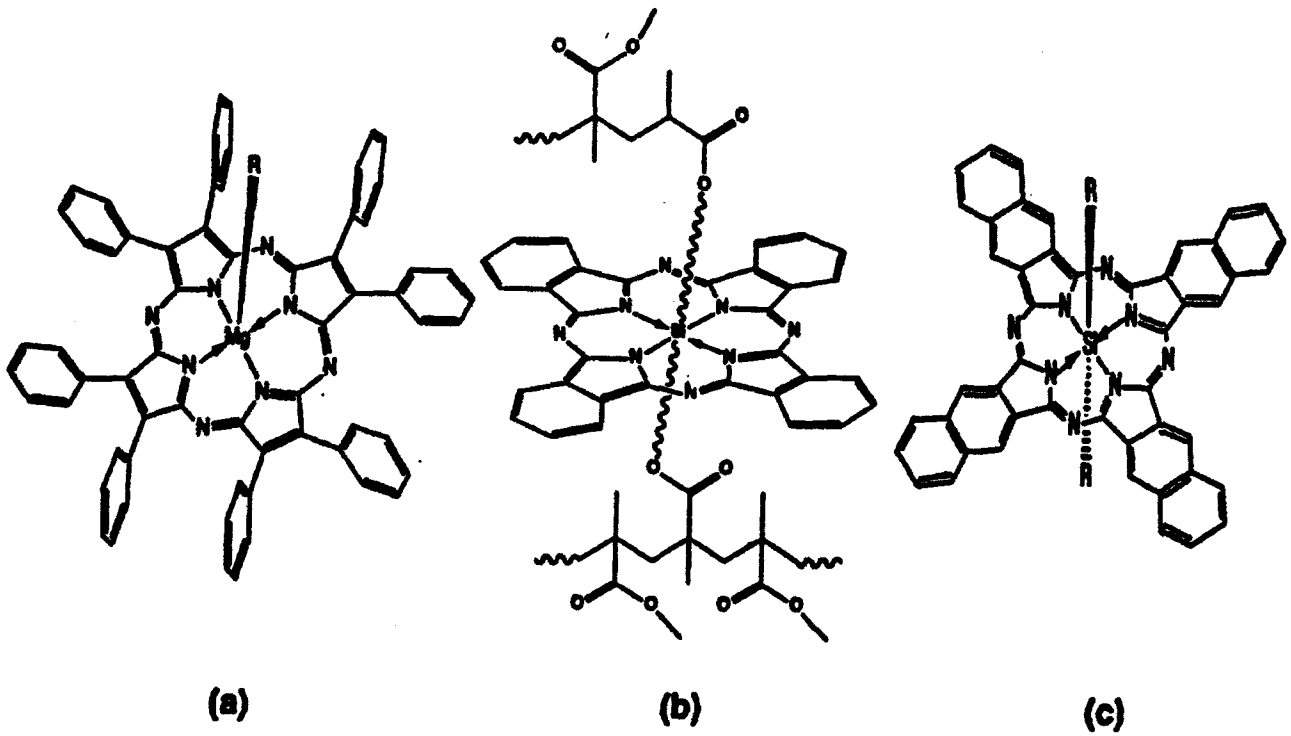

Figure 4.3 Structures of (a) magnesium octaphenyl tetraazaporphyrin, (b) silicon phthalocyanine bisacrylate copolymer and, (c) silicon naphthalocyanine.

chromophore as a cross-linking agent, and as such, at high chromophore concentrations (> 10%) thin films formed from the polymers are increasingly brittle. The films were formed by spin coating onto glass or quartz substrates, and were of high uniformity and mechanical strength. Copolymer films were of at least the same quality as guest/host films for the 10% SiPc/MMA copolymer. The UV-VIS absorption spectra of thin films of the three systems are compared in Figure 4.4, demonstrating the large shift in the Q-band absorption maximum in progressing from Mg:OPTAP to SiNc; all curves were normalized to give the same Q-band peak intensity. These absorption lines are among the narrowest and most intense to be found in organic materials, with the absorption coefficient of the 30% SiNc/PMMA guest/host being about 2×10^5 cm^{-1}.

Another attractive feature of these materials (especially 10% SiPc/MMA copolymer and 30% SiNc/PMMA) is that they have a large transparency window in the visible that may provide windows of low two-photon absorption for near infrared (1.06 μm or 1.3 μm) device operation; SiNc has already been shown to have a low absorption coefficient (< 0.2 cm^{-1} at 10% in solution at 1.3 μm). A disadvantage to highly loaded guest/host systems, such as the 30% SiNc/PMMA is their tendency toward the creation of microcrystallites of the host chromophore, as evidenced by broadening and shifting of the Q-band; covalent incorporation of the chromophore on a polymer chain reduces this tendency as shown below.

$\chi^{(3)}$ measurements were performed using DFWM in the phase conjugate geometry; both $\chi^{(3)}_{xxxx}$ and $\chi^{(3)}_{xyyx}$ components were measured. All measurements were done in the small-signal regime, although even in this regime deviation from cubic behavior was observed for the Mg:OPTAP sample, and fitting the signal to a function of the form $S = CI^b$ yielded values of b less than 2. This result comes from saturation of the nonlinearity in Mg:OPTAP at low powers, since the exciting wavelength is only 30 nm from the λ_{MAX} of the chromophore. Indices of refraction for the thin films were estimated using a Kramers-Kronig analysis, absorption coefficients were determined by UV-VIS spectrophotometry, and thicknesses were found by surface profilometry. A summary of the properties found for each of the thin film systems is given in Table 4.1, where we see that the 10% SiPc/MMA copolymer has a larger $\chi^{(3)}$ than the 30% SiNc/PMMA guest/host owing to the effects of resonance enhancement of the nonlinearity and real excitation. The fact that the ratio of the tensor components for all cases is close to three ($\chi^{(3)}_{xxxx}/\chi^{(3)}_{xyyx} = 3$) suggests that the nonlinearities are predominantly electronic, although they are not nonresonant.

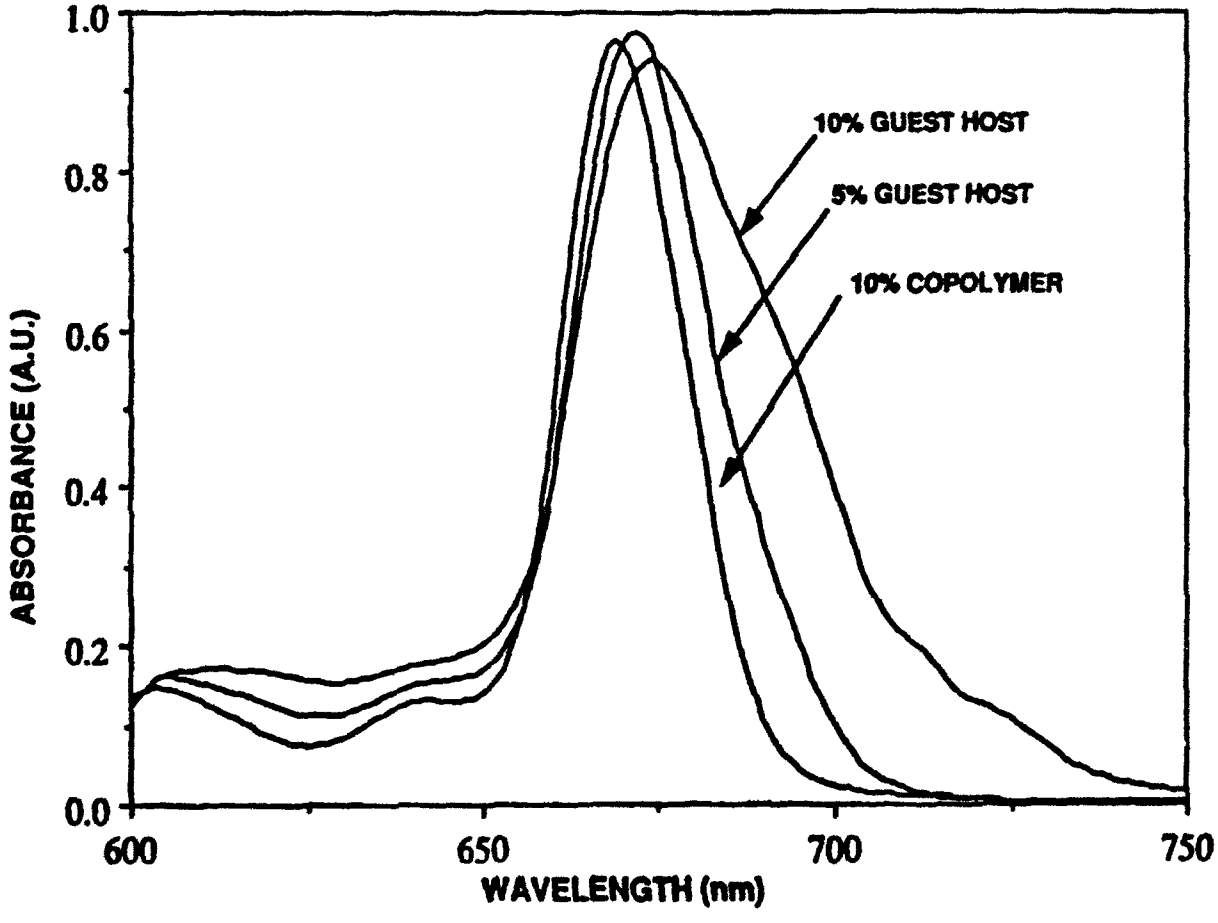

Figure 4.4 UV-Vis spectra of materials whose structures are shown in Figure 4.3.

Table 4.1 Linear and Nonlinear Optical Properties of Thin Film Samples

Material	L (μm)	n (λ = 598 nm)	αL	$\chi^{(3)}_{xxxx}$ (10^{-11} esu)	$\chi^{(3)}_{yxxy}$ (10^{-11} esu)
Mg:OPTAP 5% in PMMA	3.12 ± 0.08	1.480	0.17	1.17	0.303
SiPc/MMA 10% Copolymer	2.41 ± 0.05	1.420	1.94	9.4	3.24
SiNc 30% in PMMA	2.63 ± 0.05	1.434	0.41	2.09	0.61

Figure 4.5 demonstrates the time domain results for the three thin film samples, and these data were fit to (4.2). Table 4.2 summarizes the coefficients and response times for the three different polymer systems, and shows that the Mg:OPTAP system has a much larger non-instantaneous response than the other two systems, and can in fact be fit to a single exponential decay (A = 0 in (4.2)). The SiNc/PMMA guest/host system could not be fitted adequately by (4.2), but could be fitted if a very long-lived exponentially decaying component was added. If the lifetime of this additional portion of the response was taken to be 1 nsec, then the corresponding coefficient C was 0.435, while the other parameters are as given in Table 4.2. By contrast, the SiPc/MMA copolymer response can becompletely fit by (4.2), and the non instantaneous response time is similar to that of the fast portion of the SiNc/PMMA non-instantaneous decay.

The origin of the fast resonant response is likely to be an interaction between neighboring excited molecules, such as an exciton-exciton interaction [19]. Since the spontaneous singlet decay times of porphyrins in solution have been measured to be several nanoseconds, the long lived response in SiNc/PMMA can be attributed to the singlet lifetime that is not significantly shortened in the guest/host polymer environment, which is consistent with the exciton-exciton relaxation mechanism since the excitation density in this material is about 5 times smaller than in the SiPc/MMA copolymer at 598 nm (see Table 4.1). Similarly, the lifetime in the Mg:OPTAP guest/host is even longer because the excitation density in this case is 12 times smaller than in the SiPc/MMA, which means that the excited chromophores are much more isolated from one another.

Concerning the possible waveguide device utility of these materials, we note that the copolymer form prevents the formation of microcrystallites, which, as mentioned earlier, usually obtain in high concentration guest/hosts, and this significantly narrows the absorption band for systems with the same dye loading. Figure 4.6 shows this effect for a series of SiPc/MMA copolymer and guest/host systems, clearly demonstrating the band narrowing in the copolymer case. This band narrowing is crucial for applications of the material off resonance, since the figure of merit $n_2/\alpha\lambda$ increases with decreasing band breadth. Furthermore, the copolymer form will have less scattering than a guest/host of the same loading because of its increased homogeneity. We now proceed to a more careful investigation of a series of SiPc copolymers.

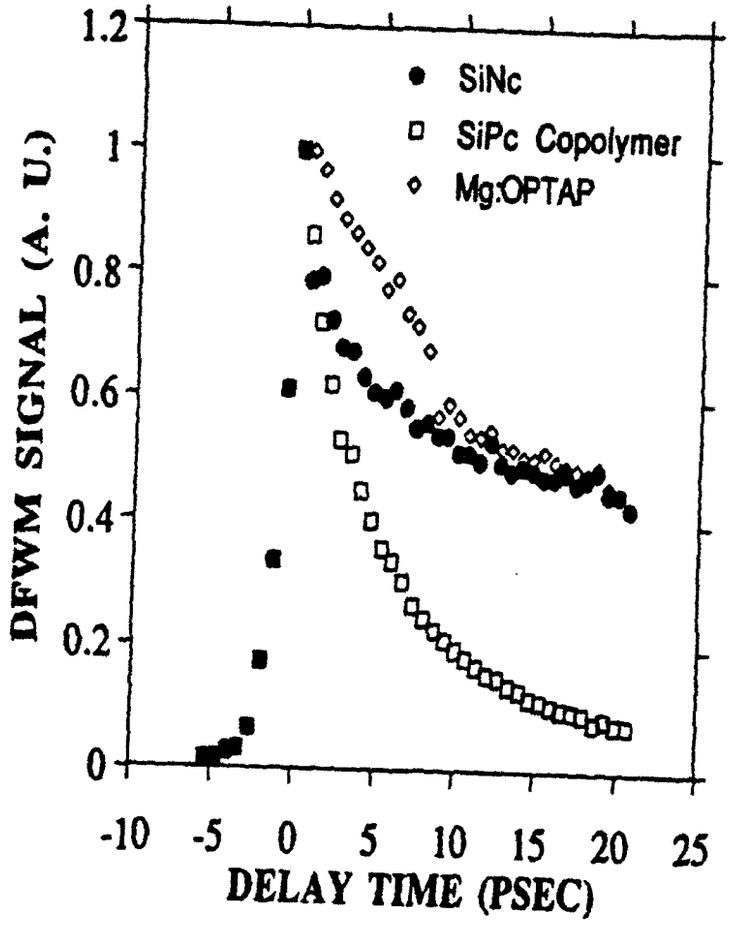

Figure 4.5 Picosecond resolved DFWM response of the thin film sample, showing rapid decay of 10 % SiPc/MMA copolymer response.

Table 4.2 Fitting Coefficients for DFWM Response

Material	A	B	C	τ_r (psec)
Mg:OPTAP 5% in PMMA	0.03 ± 0.05	0.99 ± 0.02	--	44.1 ± 2.3
SiPc/MMA 10% Copolymer	0.27 ± 0.03	0.76 ± 0.02	----	15.3 ± 0.40
SiNc 30% in PMMA	0.21 ± 0.03	0.33 ± 0.01	0.435 ± 0.02	16.2 ± 2.1

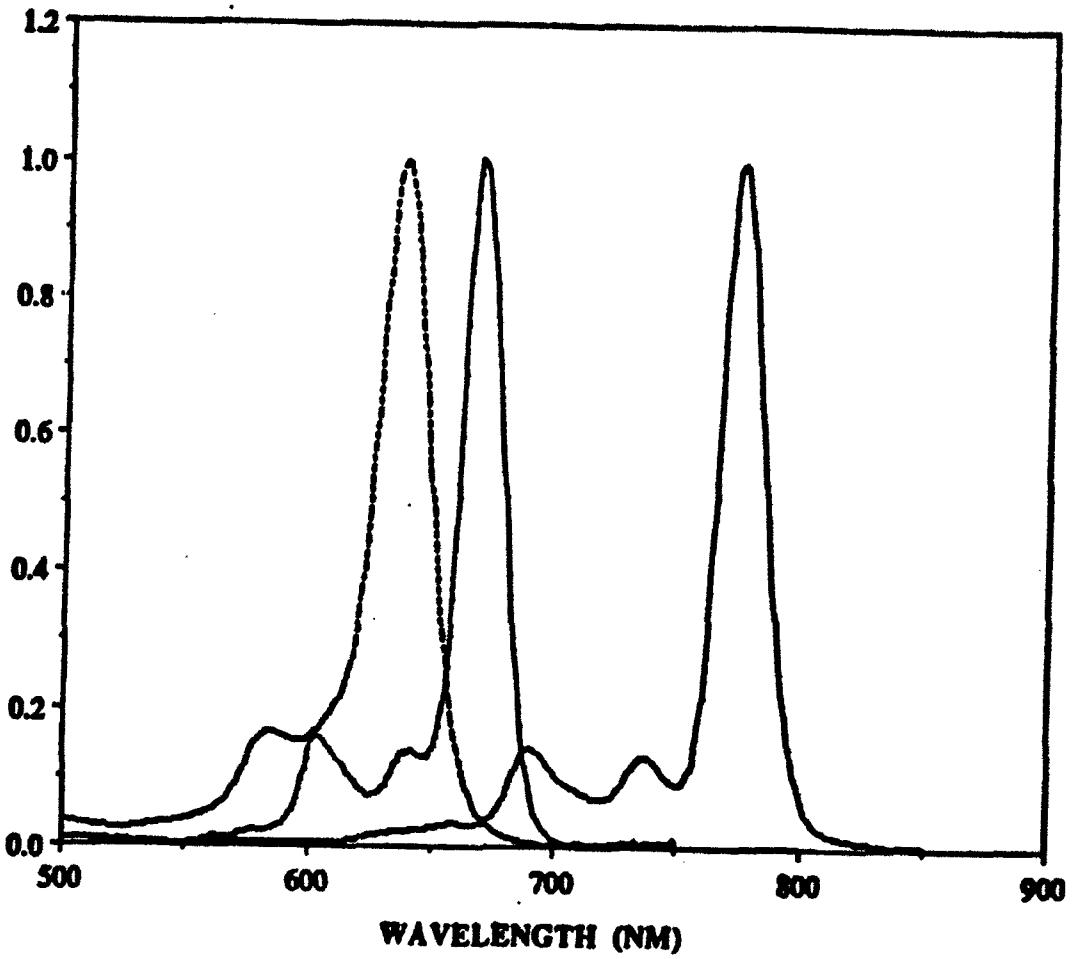

Figure 4.6 Comparison of SiPc/MMA copolymer and SiPc guest/host spectra: full width half maximum of the copolymer is 0.033 eV, that of the 10 % guest/host is 0.07 eV.

4.3.3 Silicon Phthalocyanine Coploymers

Over the past few years we have succeeded in synthesizing several new classes of porphyrin incorporated polymers, in particular mono- and bis-methacrylate copolymers of silicon phthalocyanine (SiPc). The initial investigations on one of thesecopolymers were described above. To gain further understanding into the mechanisms for the optical nonlinearity in these copolymers, a series of copolymers with different chromophore incorporations was investigated. The nonlinear optical measurements on these systems at 598 nm concentrate on the effects of excited state population on the response times of a series of copolymers of differing chromophore incorporation. At low SiPc concentrations (<1 mole percentage) the bis-methacrylate copolymers were used, while at concentrations higher than 1 mole % only the mono-methacrylate copolymers could be synthesized as tractable polymers. As shown below, measurements of 1 mole % SiPc bis- and mono-methacrylate copolymers show nearly identical nonlinear optical properties for these two systems, validating the comparison of the low and high concentration polymers.

Figure 4.7 shows the absorption coefficient of the copolymers at 598 nm as a function of mole % and a relatively good line is obtained. Deviations from linearity can come from slight band shifting and broadening that occur as the chromophore concentration is increased as was discussed in Section 3.3. These results show that interactions between SiPc chromophores in their ground state in the copolymer have only a marginal effect on the optical properties of the material.

For these polymers both $\chi^{(3)}_{1111}$ and $\chi^{(3)}_{1221}$ were measured and the results are shown in Figures 4.8 and 4.9 where we plot the measured nonlinear optical susceptibility versus SiPc mole percentage for the series of copolymers. The off-diagonal component is considerably smaller than the diagonal component in all cases, roughly by a factor of three. We mention that fitting of the data to the standard cubic intensity dependence was difficult in most cases, since the actual intensity dependence appeared to be closer to quadratic than cubic, except at low intensities, as would be expected for a resonant process near saturation. In this case the cube root of the signal was plotted versus intensity and the fitting was cutoff at that point where deviation from linearity began. An interesting feature of Figures 4.8 and 4.9 is that in both cases the increase of the nonlinearity with chromophore loading appears to begin to saturate at a loading of approximately 6% (molar) of the SiPc chromophore. As discussed further below, this result appears to be consistent with a resonant nonlinearity with a predominantly bimolecular decay mechanism.

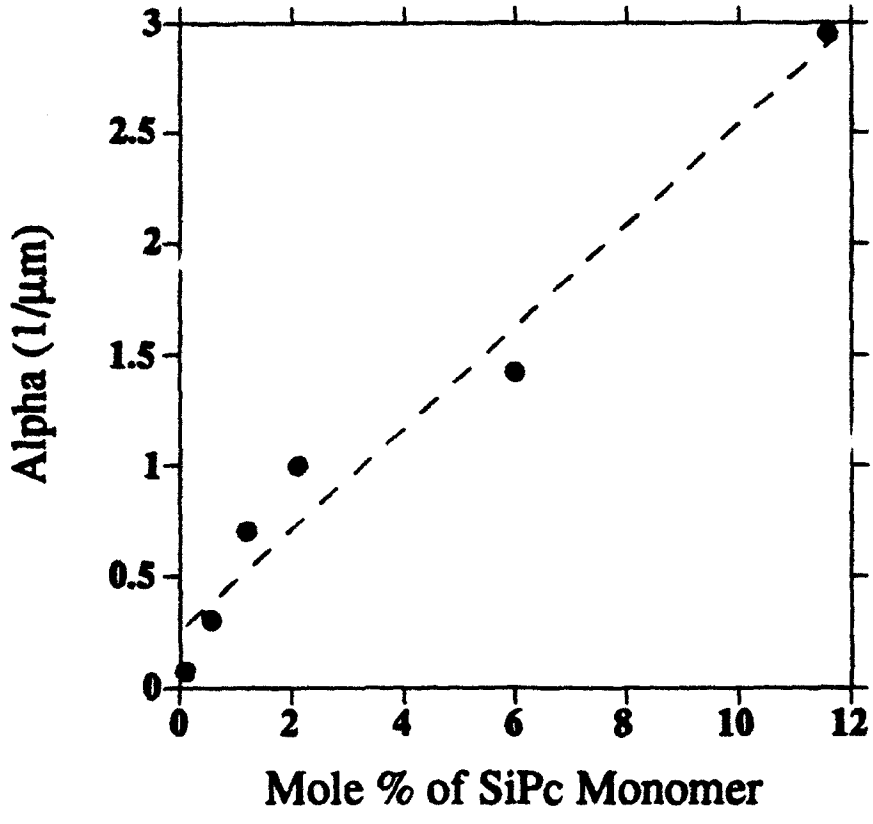

Figure 4.7 Absorption coefficient at 598 nm vs. mole % of SiPc monomer in the copolymer

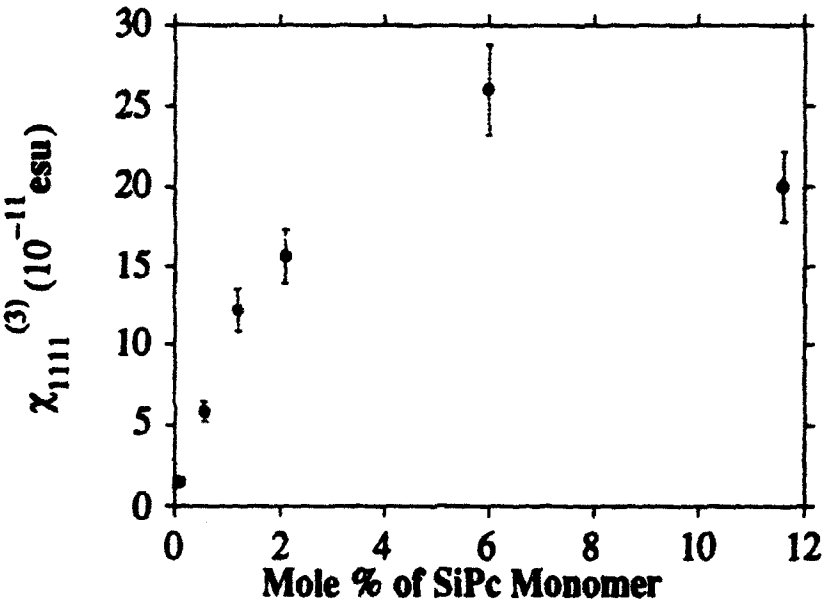

Figure 4.8 $\chi^{(3)}_{1111}$ of the SiPc copolymers vs. SiPc monomer concentration

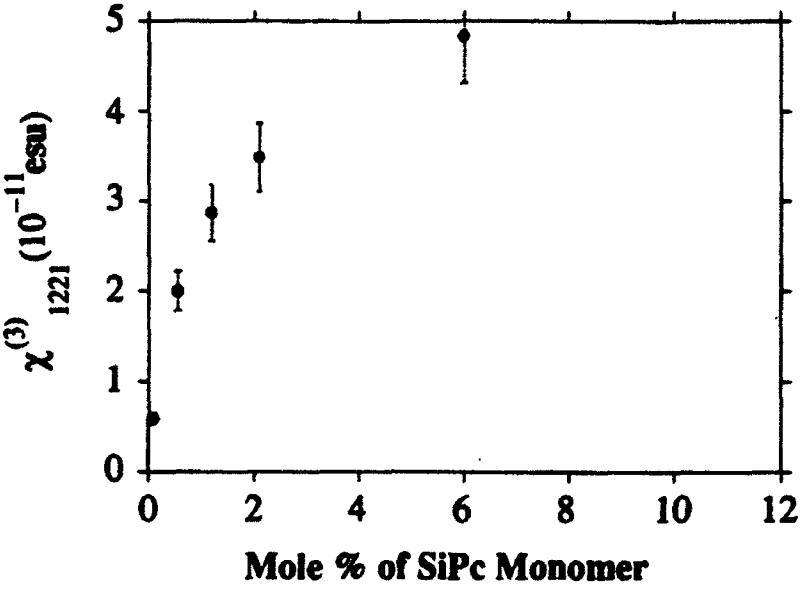

Figure 4.9 $\chi^{(3)}_{1221}$ of the SiPc copolymers vs. SiPc monomer concentration

To understand better the role of interactions between the SiPc monomers, we studied the $\chi^{(3)}$ properties of a 10% by weight guest/host SiPc/PMMA thin film, a 10% by weight (SiPc monomer) mono-methacrylate and a 10% by weight bis-methacrylate copolymer. The properties of the three samples are given in Table 4.3, where we see that the nonlinearity for the copolymer samples is more than three times that measured in the guest/host sample of the same by weight loading. Since the dominant mechanism for the nonlinearity in the SiPc chromophore at these wavelengths is excited state population, one would expect that $\chi^{(3)}$ and the linear absorption coefficient would be directly related, and this is indeed the case. Notice also that the ratio of the tensor components for the copolymers is larger than for the guest/host, presumably because the guest/host system has a larger instantaneous portion of the nonlinearity (where the ratio should be nearly three).

Dynamical DFWM data for $\chi^{(3)}_{1111}$ on the three 10% by weight systems are shown in Figure 4.10, and a considerable difference between the guest/host and the copolymers is observed. If we modify the function given in (2) so that a long-lived component of the response can be included we have

$$S(t_D) = A\exp(-t_D/0.91) + B\exp(-2t_D/\tau_r) + C\exp(-t_D/500),\ t_D > 0 \qquad (3)$$

where C is that fraction of the response that shows no measurable decay over the time scale of the measurement and the other variables are as defined above. If the data of Figure 4.10 is fit to (3) the fitting coefficients given in Table 4.4 are obtained. Here we see that the copolymer systems exhibit primarily a single exponential decay with small instantaneous and long time fractions, while the guest/host sample has a much larger fraction of its response dominated by a long time component, which is presumably due to the population of a long lived excited state either in the SiPc chromophore itself or in dimers or trimers forming when the chromophores closely associate. In one model of SiPc ring interaction, the energy level diagram completely changes between the monomer and dimer states [16]. The present data is consistent with the majority of the nonlinearity at this wavelength being due to an excited state grating. In the solution state, the excited state lifetime of phthalocyanine is greater than one nanosecond, and thus the rapid decay seen in the polymer matrix is the result of the interaction of the chromophore with the polymer matrix itself or with neighboring chromophores.

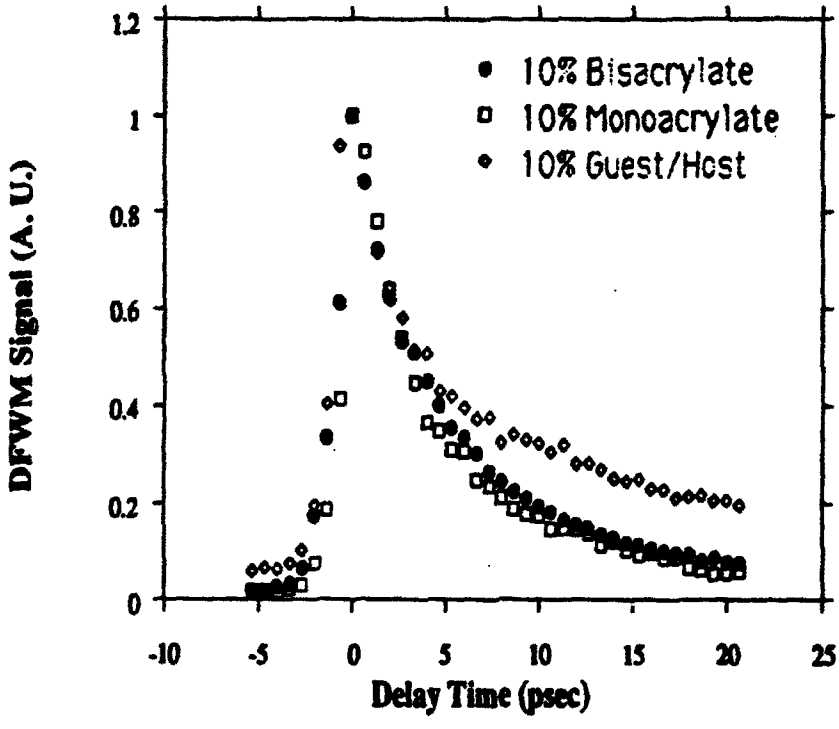

Figure 4.10 DFWM dynamics for a 10% by weight guest/host sample and the two 10% by weight polymers, evidencing the pronounced slow decay component in the guest/host.

Table 4.3

Optical and Nonlinear Optical Properties of 10% by Weight SiPc Guest/Host and Copolymer Films

Sample	α (μm^{-1})	L (μm)	$\chi^{(3)}_{1111}$ (10^{-11} esu)	$\chi^{(3)}_{1221}$ (10^{-11} esu)
10% Guest/Host SiPc/MMA	0.29	1.297 ± 0.008	2.57	1.04
10% SiPc/MMA Bis-methacrylate	0.81	2.41 ± 0.05	9.4	3.24
10% SiPc/MMA Mono-methacrylate	0.70	0.801 ± 0.016	9.51 ± 1.03	2.29 ± 0.25

Table 4.4

Fitting Coefficients for DFWM Dynamical Data on 10% by Weight SiPc Guest/Host and Copolymer Films

Sample	A	B	C	τ_r (psec)
10% SiPc/PMMA Guest/host	0.262 ± 0.023	0.563 ± 0.015	0.192 ± 0.003	12.88 ± 0.55
10% SiPc/MMA Bis-methacrylate	0.166 ± 0.018	0.782 ± 0.011	0.062 ± 0.005	11.21 ± 0.33
10% SiPc/MMA Mono-methacrylate	0.092 ± 0.004	0.887 ± 0.036	0.055 ± 0.006	9.07 ± 0.48

We can calculate the peak population density of the excited state grating using the optical density of the film and the intensity of the beams forming the excited state grating. Taking this intensity to be 500 MW/cm^2, for the 10% mono-methacrylate sample (αL = 0.56) we calculate a peak population density of approximately 5 x 10^{19}/cm^3. This gives an average separation between excited centers of approximately 27 Å, which compares with a neighbor to neighbor SiPc monomer separation that is calculated to be about 20 Å. Therefore, it is very likely that neighboring molecules are simultaneously excited, leading to possible cooperative decay mechanisms such as exciton-exciton annihilation, as has been previously suggested. This is also consistent with the larger long lived component in the SiPc guest/host case since the absorption coefficient is nearly three times less at 598 nm than in the copolymers, leading to a lower population density of excited centers and therefore a low probability for exciton-exciton decay. The origin of the lower absorption coefficient is both reduced oscillator strength and band shifting in the guest host sample, as well as agglomeration.

If the exciton-exciton annihilation model is correct, then one should see a decreased lifetime of the excited state nonlinearity as the loading of the SiPc monomer in the copolymer is increased. This is indeed observed as shown in Figure 4.11, where we plot the DFWM dynamics ($\chi^{(3)}_{1111}$) for a series of copolymers (listed by weight % loading) and include the response function of the DANS/MMA copolymer as a reference. The origin of time has been set equal in all cases for easy graphical comparison, although there were slight shifts in the time origin owing to the similar magnitudes of the laser pulse length and the excited state relaxation, which is also dependant on loading.

There is one apparent exception to the trend, which is exhibited by the 60% by weight (12 % molar) SiPc copolymer. However, detailed fitting of the data using (3) shows that the origin of the increased lifetime in this case is caused by an increased fraction of very long lived species, not by a change in the lifetime of the fast decaying component. This is shown in Figure 4.12 where we plot the fast response time τ_r versus SiPc monomer %. We see that the increase in the fast decay rate for the copolymers saturates at 1 mole %, which is consistent with the calculation we performed above that indicates that the exciton density would be close to saturated at this point. This explains why there is little difference between the decay curves for copolymers with SiPc loadings greater than 1 mole %, except for the 12 mole % case. However, it has been shown in the materials section that this copolymer begins to exhibit significant band broadening and shifting, so that the difference

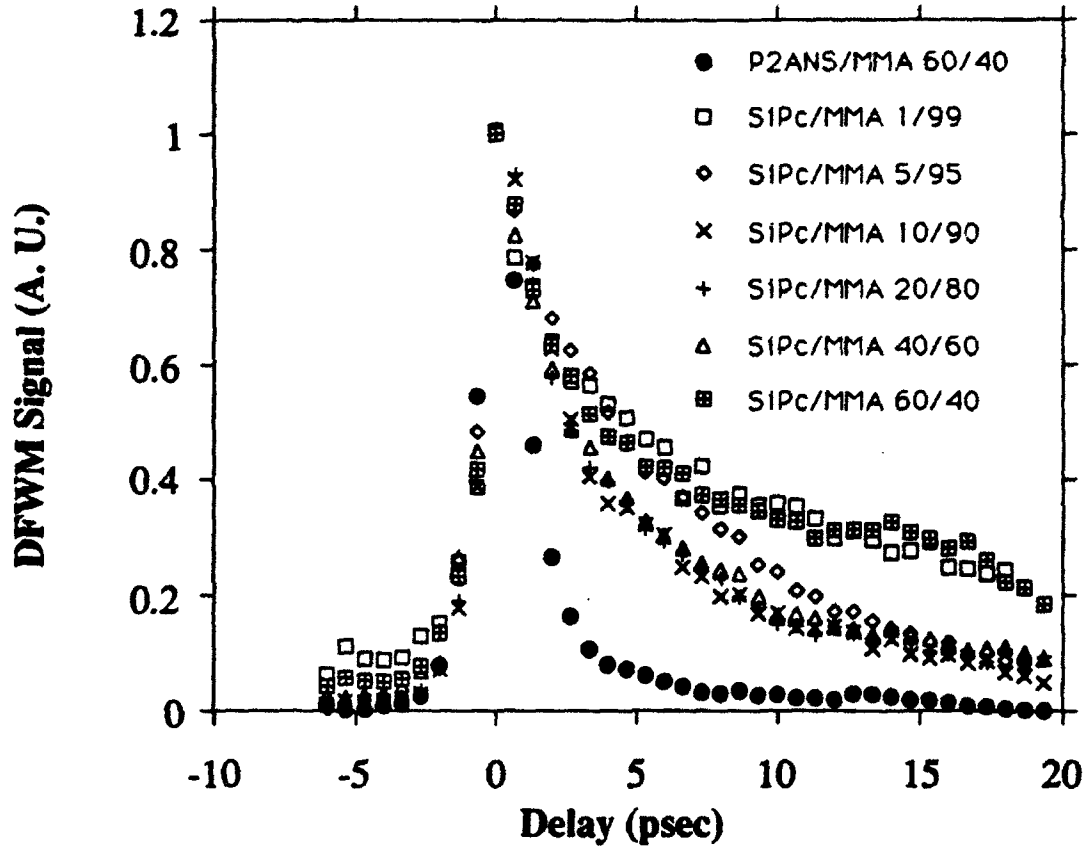

Figure 4.11 DFWM dynamics for series of SiPc/MMA copolymers; the ultrafast response of a DANS/MMA copolymer is shown for comparison.

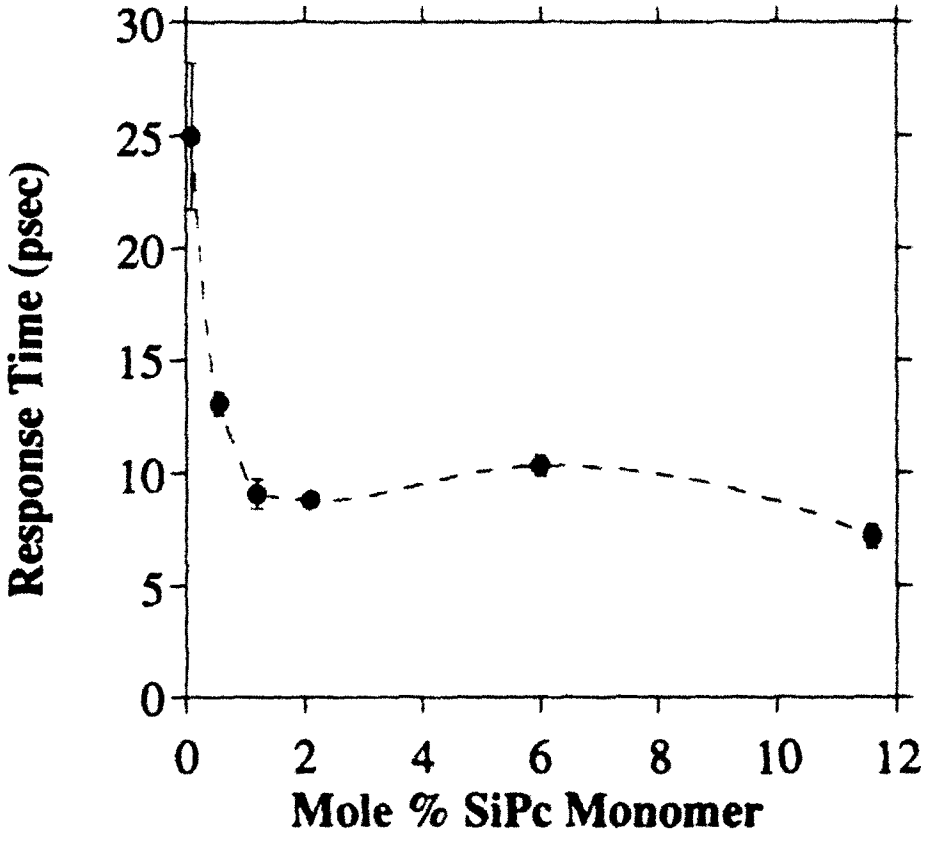

Figure 4.12 Fast response time as obtained by fitting to (3) vs. SiPc monomer mole %

may be due to spectral changes or even the emergence of a new excited state species that is at too low a concentration to decay by way of exciton-exciton annihilation.

Complete analysis of the dynamical data could be performed using a rate equation analysis for the excited state population N_{ex}. If we assume the presence of a bimolecular decay process as well as the usual monomolecular decay, we may write the following rate equation

$$\frac{\partial N_{ex}}{\partial t} = (N_0 - N_{ex})\sigma I(r,t) - k_1 N_{ex} - k_2 N_{ex}^2 \qquad (4)$$

where N_0 is the ground state population, σ the molecular absorption coefficient, $I(r,t)$ the exciting pulse intensity, k_1 the unimolecular decay rate, and $k_2 N_{ex}^{max}$ the effective bimolecular decay rate at the maximum excitation density obtained. (4) has been used by Casstevens, et al, to analyze DFWM results on Langmuir-Blodgett films of SiPc derivatives and evaporated films of metal free phthalocyanine [19]. However, in the present case one must also consider the possibility of energy transfer down the polymer coil between excited species, as is well-known in polymer photophysics [20].

This leads to the question of what the actual mechanism is for the excited state annihilation. The simplest possibility is Förster annihilation in which two proximate excited molecules E* and E* undergo the following reaction [21]

$$E^* + E^* \Rightarrow E^{**} + G \qquad (5)$$

where E** is a higher excited state of the molecule and G is the ground state. The Förster model predicts that the rate of annihilation k_{annih} is a function of the separation of the excited state pair R such that

$$k_{annih}(R) = k_E\left(\frac{R_0}{R}\right)^6 \qquad (6)$$

where k_E is the unimolecular decay rate ($= 1/\tau_E$) and R_0 is the spectral overlap integral given by

$$R_0 = \left(\left(\frac{9000\kappa^2\Phi_{D^*}}{128\pi^5 n^4}\right)\int \varepsilon_A(\nu) I_{D^*}(\nu)\nu^{-4}d\nu\right)^{1/6} \qquad (7)$$

where $\varepsilon_A(\nu)$ is the extinction coefficient of the "acceptor", ν the energy in wavenumbers, $I_{D^*}(\nu)$ the corrected emission spectrum of the "donor", Φ_{D^*} the fluorescence quantum yield of D^*, n the refractive index (ignoring dispersion), and κ^2 is an orientational factor. R_0 is typically about 15-30 Å, depending on the molecule. In the present case we would identify $E^* \Rightarrow G$ with the emission ($I_{D^*}(\nu)$) and $E^* \Rightarrow E^{**}$ with the absorption ($\varepsilon_A(\nu)$). We note that for the polymer case we do not have a good estimate of R unless some details of the microstructure can be elucidated. Furthermore to estimate R_0 we need to know the fluorescence spectrum of an isolated SiPc molecule in a polymer matrix, as well as the excited state absorption spectrum of the molecule. Qualitatively, we can say that phthalocyanines are poor fluorescers so that Φ_{D^*} is expected to be small, but that the overlap integral itself may be large since

(1) phthalocyanines exhibit very small Stokes shifts in their fluorescence spectra and;
(2) the next excited state of SiPc, the Soret band, has nearly twice the energy of the Q-band, into which we are exciting the molecule.

In conclusion, a Förster-type annihilation mechanism may be responsible for the observed bimolecular decay, but detailed photophysical measurements would be required to determine the size of R_0. As mentioned above, excited species energy transfer along the polymer chain (as opposed to directly between chromophores) is also a possible mechanism. The latter would presumably be more sensitive to the particular polymer environment; in the data presented here this is not observed as evidenced by the similarity between the data for the bis-methacrylate and mono-methacrylate copolymers.

4.4 3 AND 5 RING SMALL MOLECULES AND COPOLYMERS

A number of polymer films provided by Professor L. Dalton at the University of Southern California were examined for the third order nonlinear optical response. The structures of the compounds investigated are given in Table 4.5, where we see that a series of pendant copolymers and main chain polyenic polymers were synthesized. Films were cast on glass slides and usually had large nonuniformities. The refractive index of the reference carbon disulphide is $n_R = 1.6246$; for more colored samples (red) n_S was assumed to be 1.63 (same as the reference), while for less colored samples (yellow) it was assumed to be 1.55. We have recently purchased a rapid index measurement machine (Metricon prism coupler) that should allow us to improve upon such approximations in the future. The sample length was measured by averaging values determined with a surface profilometer at several points near where the DFWM measurement was made. Most of the films were uniform to within 20%, but one was only uniform to 50%, leading to a large uncertainty in the nonlinearity. The absorption coefficient α_S was measured with a Perkin-Elmer UV-VIS spectrophotometer, where the spectra were referenced to a blank glass slide.

An example of the intensity dependant phase conjugate signal for the 3 ring system on PVP is shown in Figure 4.13. The fit is to a function with cubic and linear dependence on the laser intensity; the linear portion is to account for scattering which was quite large in this sample. Notice that no evidence for saturation of the nonlinearity is seen, suggesting that the response in this case is primarily nonresonant, as is born out by time domain measurements of $\chi^{(3)}_{1111}$ on the 3-ring and 5-ring samples as shown in Figure 4.14. This Figure shows that the 5-ring sample has a slightly large "long-time" component than the 3-ring, which suggests an increased excited state population for the 5-ring.

Table 4.6 gives the values of $\chi^{(3)}_{1111}$, α and $\chi^{(3)}_{1111}/\alpha$ for the samples. As mentioned above, the values for α were determined by UV-VIS spectroscopy, referenced to a blank glass slide; any changes in transmission were attributed solely to absorption, so any changes in reflection were not taken into account. This is a small correction as long as the sample's index is close to that of glass and the absorption coefficient is appreciable (larger than 100-200 cm^{-1}). The error bars are due mainly to errors in thickness, which result from poor film uniformity, and from systematic errors in the DFWM experiment, estimated to be about 15-20%. As can be seen from the table, the most promising material in terms

Table 4.5
Structures of Compounds Obtained from USC

Sample	Structure
3 ring on PVP	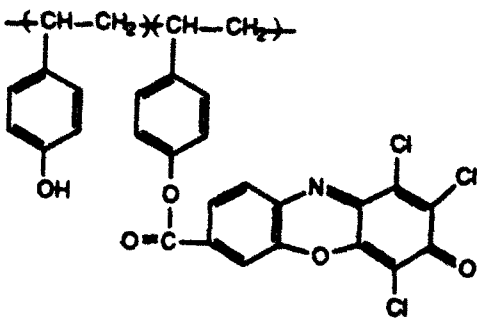
5 - ring on PVP	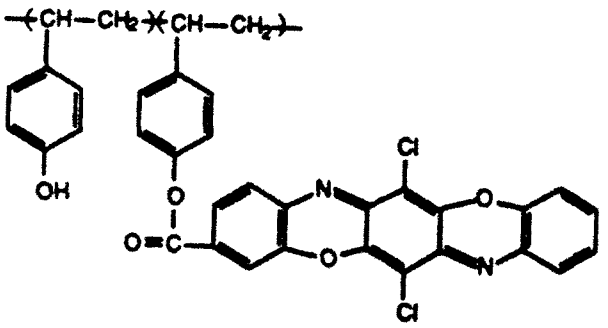
Me_2N - 30%	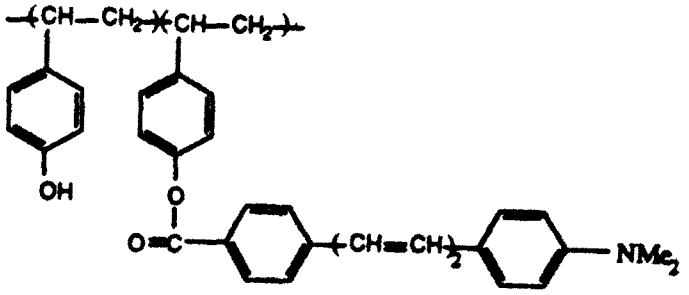
$Thio_2$	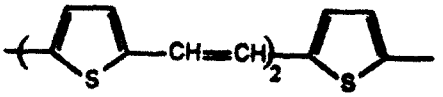
$Poly_n$	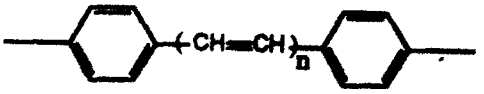

Copolyamide general structure

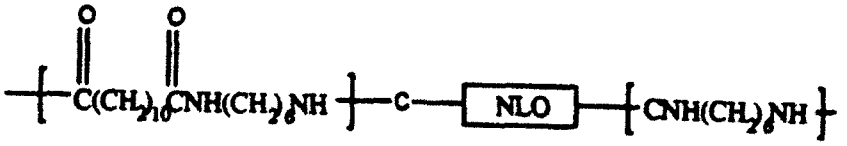

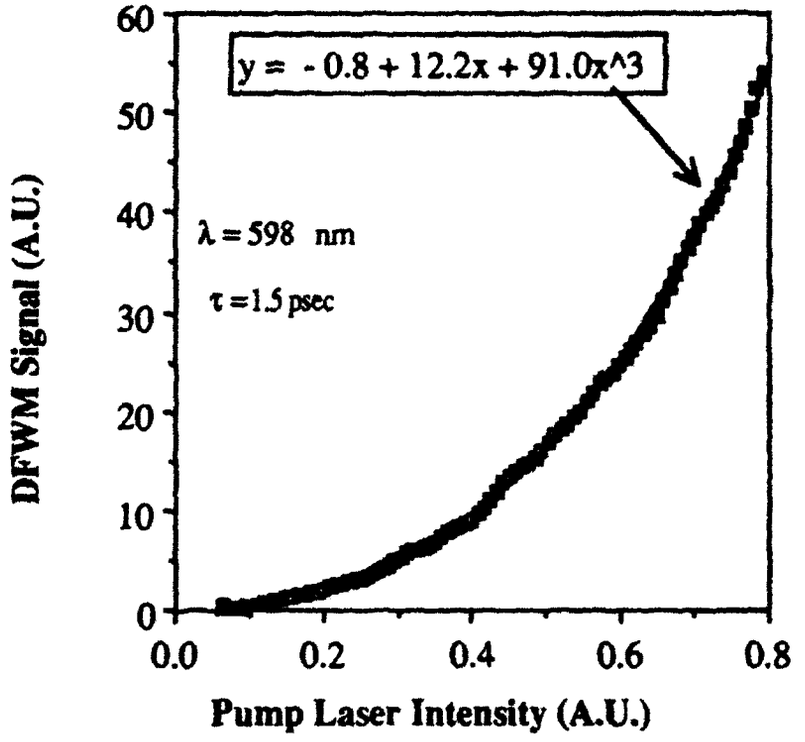

Figure 4.13 Phase conjugate intensity as a function of pump laser intensity for 3-ring on PVP sample

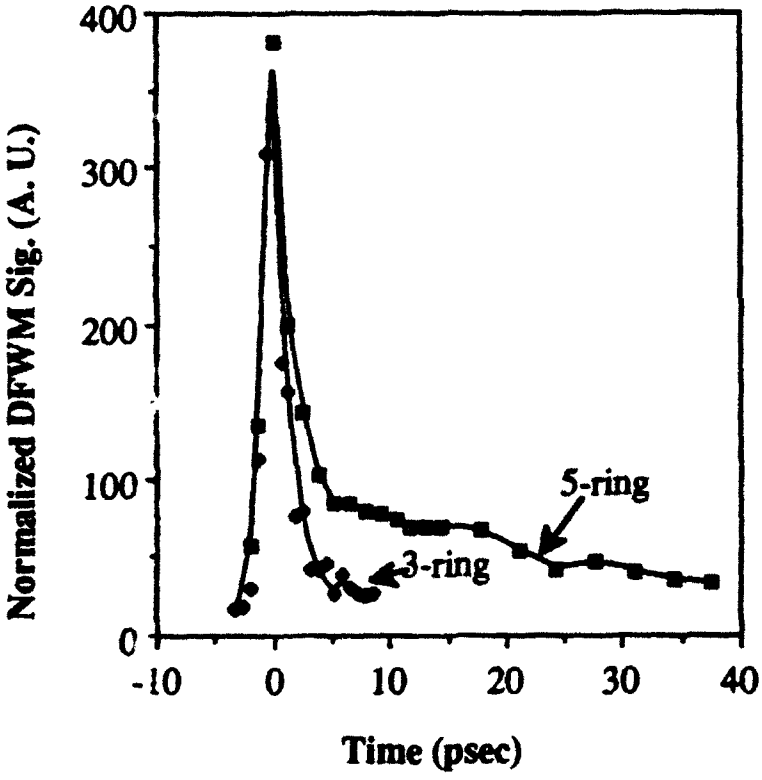

Figure 4.14 DFWM dynamics of 5-ring and 3-ring pendant copolymer systems

of $\chi^{(3)}/\alpha$ at 598 nm is the 5-ring side chain polymer with a $\chi^{(3)}/\alpha$ approaching 10^{-14} esu-cm. Also notable is the fact that this material has a $\chi^{(3)}$ twice as large as that of the 3-ring side-chain polymer, while having practically the same α, suggesting that increased "tailing" of the absorption is not occurring.

Table 4.6

Nonlinear Optical Properties of Several Ladder Polymers and Incorporated Polyene Polymer Systems

Sample	α (cm^{-1})	$\chi^{(3)}_{1111}$ (10^{-11} esu)	$\chi^{(3)}_{1111}/\alpha$ (10^{-15} esu-cm)
3-Ring 20% on PVP	3600±900	1.2±0.3	3.3±1.1
3-Ring 30% on PVP	4300±1100	1.4±0.2	3.3±1.1
5-Ring 20% on PVP	3700±1000	2.6±0.9	7.1±2.0
20% Incorpor. 5- ring polyamide	230 ± 20	0.15±0.01	6.5±0.7
Copolyamide with 10% $Thio_2$	320±80	0.20±0.03	6.3±1.8
Copolyamide with 10% $Poly_3$	<100	Unmeasurable	-
Copolyamide with 10% $Poly_4$	1040±20	0.23±0.08	2.2±0.8
Copolyamide with 10% $Poly_5$	640±20	0.054±0.02	0.85±3.0
Me_2N - 30%	430±40	0.16±0.03	3.8±0.70

Note - some of the values in the table are the result of averages of several different samples of the same material - in particular 3-ring/20% is the result of an average of three different samples

4.5 HCC SIDE CHAIN NLO COPOLYMERS

HCC side-chain electro-optic polymers, while developed for electro-optics, may have promise as all-optical materials as discussed in a number of recent papers [15-16]. Therefore, we measured the third order nonlinear optical response of two representative electro-optic polymers. Figure 4.15 shows the structures of the side-chain copolymers of 4-amino-4'-nitrostilbene (DANS) and 4-oxy-4'-nitrostilbene (ONS) with methylmethacrylate, both of which have been used extensively as electro-optic materials when in the poled state.

The synthesis and polymer properties of these materials have been described elsewhere [2-4]; in the current work the DANS and ONS copolymers had 60 mole percentage and 50 mole percentage incorporation of the chromophore monomer, respectively. At 598 nm, the DANS copolymer has n = 1.68 and α = 540 cm^{-1}, while the ONS copolymer has n = 1.62 and α = 40 cm^{-1}. The results of DFWM measurements of the magnitude of the third order nonlinear susceptibility on DANS and ONS copolymer films spun onto glass slides are given in Table 4.7. Table 4.3 also lists the results of third harmonic generation measurements on these systems by us and others. The DANS system exhibits a nonlinearity about 3 times as large as the ONS system, as might be expected from dispersion effects. A simple two level model picture of DFWM predicts that the $\chi^{(3)}_{1111}$ of the DANS polymer should be 2-3 times that of the ONS polymer, as is observed. Because of the limits of experimental sensitivity, the $\chi^{(3)}_{1221}$ component could only be measured for the DANS copolymer, and is approximately 1/3 as large as the $\chi^{(3)}_{1111}$ component, as would be expected for an electronic process in an isotropic material.

Figure 4.16 shows picosecond time-resolved DFWM data on the DANS copolymer, and the response is seen to be pulse length limited and was used to determine the "instantaneous" response of the system. The additional pulse at approximately 15 psec from the zero delay is a satellite pulse that results from the saturable absorber in the synchronously pumped dye laser being at too low a concentration. In the present instance this satellite explicitly exhibits the ultrafast response and recovery of the DANS copolymer. Although these copolymers have been developed for electro-optics and exhibit only modest third order susceptibilities, they may have utility as third order materials because of their excellent processability, amenability to various waveguide fabrication techniques (RIE, photobleaching), low-loss at 1.3 μm and expected low two-photon absorption at 1.3 μm.

ONS/MMA 50/50

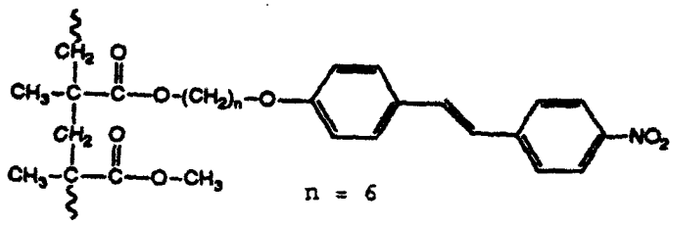

DANS/MMA 60/40

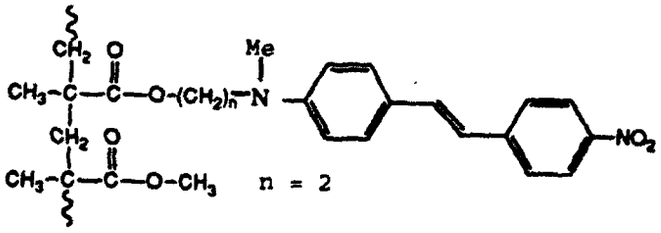

Figure 4.15 Structures of side chain polymers with ONS and DANS

Table 4.7

Third Order Nonlinear Properties of DANS/MMA and ONS/MMA Copolymers

Polymer	λ_{max} (nm)	$\chi^{(3)}_{1111}$ (DFWM 10^{-12} esu)	$\chi^{(3)}_{1111}$ (THG 10^{-12}esu)	$\chi^{(3)}_{1221}$ (DFWM 10^{-12} esu)
DANS/MMA 60/40	438	6.9 ± 1.0	5.0 ± 0.5 (1.9 μm)	2.2 ± 0.5
ONS/MMA 50/50	370	2.0 ± 0.5	2.0 ± 0.5 (1.9 μm)	-

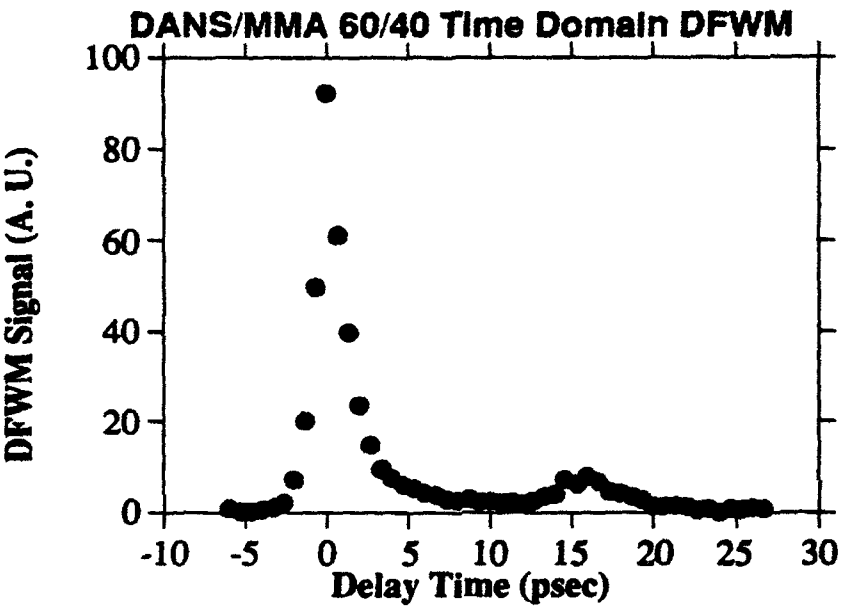

Figure 4.16 DFWM dynamics of DANS/MMA copolymer film; the additional pulse is a satellite pulse that is formed with the synchronously pumped dye laser

4.6 CONCLUSIONS

Picosecond degenerate four wave mixing at 598 nm was used to study the third order nonlinear optical properties of thin film polymer samples. A series of main chain and pendant copolymers synthesized by L. Dalton's group at the University of Southern California were measured, with a 5-ring pendant copolymer having both the highest nonlinearity ($\chi^{(3)}_{1111} = 3 \times 10^{-11}$ esu) and also the highest value of $\chi^{(3)}_{1111}/\alpha$ for this group. Electro-optic polymers previously synthesized at HCC were investigated and a DANS/MMA 60/40 copolymer was found to have $\chi^{(3)}_{1111} = 7 \times 10^{-12}$ esu, while an ONS/MMA 50/50 copolymer had a nonlinearity only one third that of DANS/MMA 60/40. Dynamical studies indicated that the response of DANS/MMA 60/40 is ultrafast (subpicosecond). This property, coupled with the availability of high quality DANS/MMA waveguides, may make this material an interesting candidate for all-optical switching at 1.3 μm.

We have performed DFWM measurements on three thin film polymer systems incorporating several different two-dimensional π-conjugated chromophores. The narrow absorption bands of the chromophores in the visible and near infrared lead to relatively large $\chi^{(3)}$'s (10^{-10} esu) at 598 nm. Time-resolved DFWM measurements explictly demonstrated the role that one-photon excitation plays in the nonlinear optical response of these porphyrin derivatives. Furthermore we have shown that copolymerization of silicon phthalocyanine chromophores is an effective technique for obtaining high loadings that result in decreasing material recovery time for resonant nonlinearities and increasing transparency for nonresonant applications.

A detailed study of a series of copolymers of SiPc with MMA was undertaken, to determine the size and dynamics of the resonant nonlinearities in these materials. Resonant $\chi^{(3)}_{1111}$ values as large as 2.6×10^{-10} esu were observed for copolymers with 6 mole % SiPc. Mono-methacrylate and bis-methacrylate versions of the copolymers were studied and high quality thin films could be spun from all of the synthesized materials. A saturation of $\chi^{(3)}_{1111}$ with increased chromophore loading was observed to set in between 2 and 6 mole % loading. This effect could result from band shifting owing to chromophore interaction or from the onset of another nonlinear mechanism that has opposite sign to the nonlinearity present at low loadings. As the loading of the SiPc chromophore was increased from 0.1 to 6 mole %, fairly dramatic changes were observed in the picosecond dynamics of the resonant nonlinearity. A significant decrease in the response time (from 25

psec to 9 psec) was observed at higher loadings, which appears to be consistent with a model in which bimolecular interactions of molecules in the excited state lead to rapid decay (exciton-exciton annihilation). The actual mechanism may be some form of Förster annihilation, commonly seen in fluorescence spectroscopy.

V. DEVICE FABRICATION

5.1 INTRODUCTION

The fabrication of useful electro-optic devices using organic polymers requires techniques for depositing many polymer and metal layers onto a substrate and ways for defining linear waveguiding structures in a multi-layer film. Thin film layers of polymer will be produced by spin-coating, a standard fabrication technique used in electronics industries. However, more detailed studies on the effects of spinning speed, solution viscosity, and solvent nature on film thickness, film quality, and adhesion are necessary in order to fabricate defect-free polymeric electo-optical devices.

A typical waveguide device is consisted of multilayers of polymers and metals. Thin polymer films are deposited upon one another so that optical cladding and core structure can be easily developed for waveguiding. The index of refraction of cladding and core layers can be precisely controlled by varying monomer compositions in NLO copolymers. This structure is built on top of a silicon substrate and bottom metal electrode which is vacuum deposited gold. The cladding and guiding NLO polymer layers are spin coated upon this gold layer and then a waveguide pattern is defined by the various methods. After a top cladding polymer layer is coated on this structure, the upper electrode pattern is established by gold evaporation using lithographically defined patterns.

Two separate routes have been pursued for demonstration of the device utility of the third order material developed under the contract. One area that is promising for all-optical materials is ultra-high speed switching in nonlinear optical fiber devices. These have been demonstrated in fused silica fibers, but the nonlinearity in this case is so low that extremely high power lasers and long lengths of fiber must be used. The latter is impractical from a high speed switching point of view, since large delay lines will have to be tolerated by the system. However, if more nonlinear fiber could be made with relatively low loss, these devices could be only a meter or so in length, significantly reducing the clocking problem. To demonstrate highly nonlinear single mode fiber an external research program was initiated with Prof. M. G. Kuzyk at the Washington State University who has produced nonlinear optical fibers using guest/host doping of various dyes in PMMA. Monomer samples of silicon phthalocyanine have been supplied to Prof. Kuzyk in order to incorporate these monomers into a methacrylate polymer in situ. Some of the results on

this investigation are attached to this report as an appendix.

The other device effort we have studied is a nonlinear directional coupler made with a silicon phthalocyanine/MMA copolymer. A vertically integrated approach was adopted to take advantage of the excellent thin film forming properties of the polymers. The directional couplers, in their channel waveguide version, could function as ultrafast switches for telecommunications or datacom. 1.06 μm was chosen as the design wavelength, since this choice simultaneously resonantly enhances the nonlinearity of the material while hopefully avoiding two-photon absorption, which has deleterious effects on nonlinear directional coupler performance. Silicon phthalocyanine and similar compounds have a transparency window in the visible which could correspond to a two-photon transparency in the near-infrared. A number of planar waveguide devices, whose structure can be readily turned into channel waveguide directional couplers by photobleaching or selective etching, have been fabricated and demonstrate waveguiding in both active layers as well as evidence of coupling between layers.

5.2 FABRICATION TECHNIQUES

5.2.1 Spin Coating

The spin coating process is used extensively in producing thin solid polymeric films for use in microelectronics. The process is relatively simple and convenient, and it usually produces uniform films which are quite reproducible. Typical applications include photoresists, inter-metal dielectrics, and passivation layers. This process can be described as consisting of three stages: solution deposition, spin, and solvent evaporation. In order to get defect-free films from this technique, the effects of solvent nature, spinning parameters, and drying conditions on film quality have to be understood. Since the final film thickness is largely dependent on the solution viscosity and spinning speed and time, a desired film thickness can be obtained by changing one of the above parameters. This technique allows us to make reproducible and uniform polymer films with thicknesses ranging from 0.1 to a few microns.

One of important property of solvents used in spin coating is their boiling point. The lower boiling solvents (60 - 120 ^{o}C) create uneven surface due to rapid drying while higher boiling solvents (170 - 250 ^{o}C) lead to a problem in drying. The best results in the film forming process were achieved with solvents in the middle boiling point range (120 - 170 ^{o}C). When a hygroscopic solvent were used, a clouding phenomenon was observed in the film. This can be attributed to an absorption of moisture by the solvent during the drying process. As the solvent evaporates, the amount of non-solvent (water) increases in the solution due to the moisture absorption. This results in phase separation in the spin-coated solution. After most of solvents evaporate, then the solvent rich phase in the polymer solution becomes a void in the film which scatters visible light.

Various types of surface defects are observed when polymer solutions are spun on a substrate such as silicon wafer. One of the most common defects is orange peel which is a textured appearance resembling the skin of an orange. This defect results when the polymer solution is not fluid enough to flow together evenly on the surface during spin-coating. Fisheye is the appearance of circular depression in the polymer film due to repulsion of the polymer solution by some surface contaminants, such as oils and greases. Pinholing and cratering arise when solvent is lost rapidly by heating from the polymer film while it is still wet.

When N-methylpyrrolridone (NMP) is used as a solvent for the NLO polymers, a defect such as creeping or crawling is found after spin-coating on a silicon wafer. Crawling is a tendency of a wet polymer film to recede from certain areas of a coated surface. This type of defect is caused by poor wetting of the NMP solution on the silicon substrate since it has a higher surface tension compared to the usual cyclohexanone solution which does not show crawling. A similar defect was observed when the spin-coating solvent was changed to poor wetting solvents such as butyrolactone or benzaldehyde.

In order to overcome above problems and get a smooth and uniform film, the surface tension of the polymer solution should be lower than the surface energy of the substrate or contaminants. One of the way to solve such problems is an addition of surfactants which can reduce surface tension of solutions. Some of non-ionic surfactants (FC-430 and FC-431 from 3M Co.) have been tested and found to be an excellent solution for the problems in the spin coating procedure. These coating additives are fluoroaliphatic polyesters and are soluble and compatible with most NLO polymers studied. Since very small amount of the surfactants (0.2 wt% of polymer) was added, no adverse effects due to the addition of surfactants on optical waveguiding property has been observed. It even reduces the scattering loss in waveguide by eliminating the leveling problem caused by surface tension gradients formed during the film drying stage.

5.2.2 Multi-layer Structure Fabrication

The premature crack formation in polymers at stresses considerably below the nominal yield stress, while in contact with aggressive environments, is called environmental stress cracking. This problem is observed in the fabrication process of multilayer structures of NLO polymer films. After the first layer of the polymer film is spun and dried on a silicon substrate, the polymer solution is again applied on the top of this film in order to make second layer of a film. This process inevitably leads to the contact of the dried first layer film with a solvent in the applied polymer solution. The solvent acts upon the polymer, especially at a flaw located at the film surface, and causes localized plasticization and swelling. This brings about the onset of crack formation in the film which is already under the influence of residual stresses induced during a drying procedure. Upon application of another solution on top of these films, the surface of the second layer again shows cracks. This brings about considerable problems in designing

multilayer structure waveguide devices if mechanical strength of the NLO polymers is not strong enough to withstand environmental stresses..

In order to solve such a solvent cracking problem in the spin-coating process, a few hundred angstrom thick plasma polymer layer is employed as a barrier layer between two polymer film layers. This barrier layer is dense enough not to allow penetration of solvent molecules to the next layer yet thin enough not to interfere with guided waves in the NLO polymer film. As a preliminary experiment, a 300 Å thick plasma polymer from CH_4 was coated on the HCC NLO copolymer film which was spin-coated and dried on a silicon wafer. When a solvent is spread over the surface of the film to see if the solvent stress cracking occurs, only the portion of the film not covered with the plasma polymer layer exhibits many cracks due to direct solvent contact to polymer surface. Even the plasma polymer as thin as 100 Å thick seems to be effective as a solvent barrier. Hexamethyldisiloxane has also been used to form a plasma layer on the NLO film and been found to be a good barrier layer although it shows different surface property due to its hydrophobic nature. This plasma technique seems to be suitable for the device fabrication process since it takes only a few minute for the whole procedure and does not result in ıy adverse effects on optical waveguiding property of NLO polymers.

5.2.3 Linear Waveguide Fabrication

Lateral confinement of light in the films can be achieved by three different ways: lithographic methods, laser ablation, and photobleaching techniques [22]. In the lithographic methods, gold is evaporated on top of the substrate to form a ground plate. The cladding polymer is spin coated on this gold layer and a channel is lithographically defined. Using gold as the masking layer, the linear waveguide pattern on the cladding layer can be etched by a reactive ion etcher. NLO active core material is spin coated to fill the channel, followed by the deposition of a third upper cladding layer. The upper electrode pattern is established by evaporation of gold using lithographically defined patterns.

The laser ablation technique provides a much simpler way to form a linear waveguide. After cladding and guiding layers are spin coated, a linear waveguide structure can be formed by ablation of polymer layers. Radiation from a excimer laser is passed

through a mask and the waveguide structure is imaged onto the surface of the polymer film. The laser light can ablate materials which are not covered by the mask resulting in a rib waveguide structure. Another cladding material is then overcoated on the rib structure. The photobleaching method utilizes the photochemical properties of the NLO chromophores in the polymer. When the NLO chromophores are irradiated with light near their electronic absorption bands, photochemical reactions may occur. This can alter the chemical structure in such a way as to reduce the polarizability of the chromophore. From the Sellmeier equation, the theory predicts that either a reduction of oscillator strength of the chromophore or a hypsochromic shift of its absorption maximum wavelength will cause a lowering in the refractive index. In order to make a channel waveguide, the NLO polymer is exposed to radiation through a mask which contains a pattern of the optical waveguide structure.

5.3 VERTICALLY INTEGRATED DIRECTIONAL COUPLER

5.3.1 Device Design

One area of application has been pursued for demonstration of the device utility of the primary third order materials developed under this contract, the silicon phthalocyanine copolymers. Here we report on the device development work of a vertically integrated directional coupler. A vertically integrated approach was adopted to take advantage of the excellent thin film forming properties of these polymers. These directional couplers, in their channel waveguide version, could function as ultrafast switches for telecommunications or datacom.

Figure 5.1 shows the vertical structure which consists of five layers: (1) lower cladding layer (PMMA), (2) lower waveguide layer (SiPc/MMA), (3) separation layer (PMMA), (4) upper waveguide layer (SiPC/MMA), and (5) upper cladding layer (PMMA). Coupling will occur between the two waveguide layers once light is launched into one of the layers. If the waveguides are identical so that their propagation constants match ($\Delta\beta = 0$) complete coupling of energy from one waveguide to the other will occur after a distance called the coupling length. If the waveguiding material has an index of refraction that is a function of light intensity, this coupling length can be changed by changing the incident light intensity, thereby changing how much light emerges from the two waveguides at the end of the device.

In the present design this switching could be achieved in at least three ways. In one case the incident light beam would act on itself, and as its own intensity increased or decreased the coupling between the two waveguides would change. Another approach would be to have a low intensity probe beam propagating through the waveguide structure whose coupling ratio would be controlled by the imposition of an intense pumping beam. This pump beam could be at nearly the same wavelength as the probe and copropagating with the probe, being wavelength filtered out of the network at the end of the device. On the other hand, the pump could be imposed from above the waveguide and could change the coupling between the waveguides if its wavelength were such that the majority of the pump light was absorbed in the upper waveguide.

Since the proposed device is all-optical, isolation of the coupling region through the use of waveguide bends is not critical. However, for the electro-optic case this problem

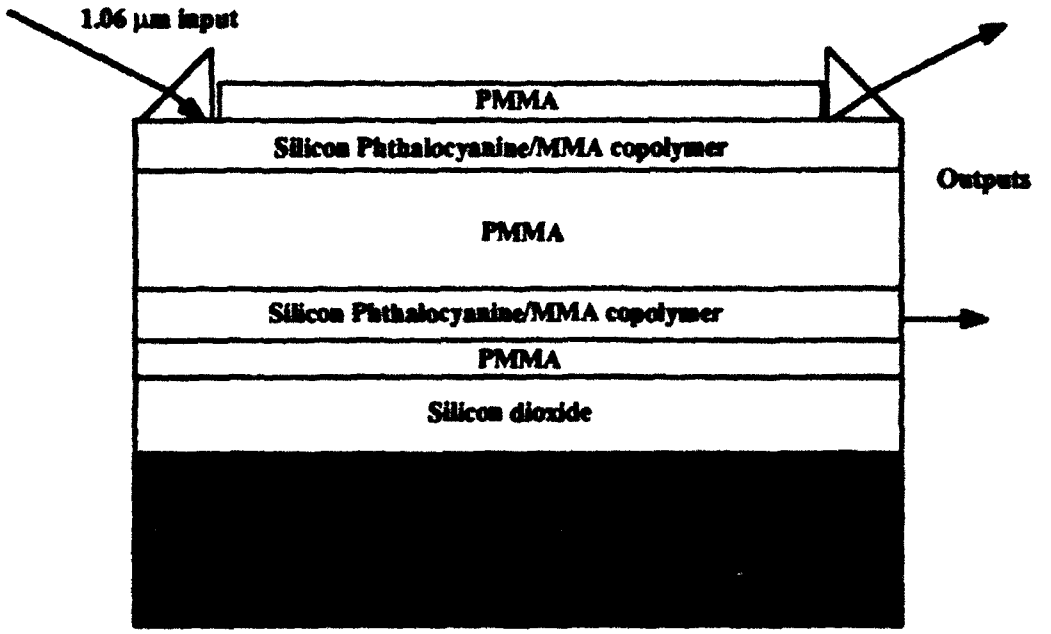

Figure 5.1 Slab directional coupler design using Silicon phthalocyanine/MMA copolymer; active layer - 1.3 μm, center PMMA - 2.5 μm; top and bottom PMMA layer - 2.0 μm

could be solved if, for example, a photobleachable material were used for the center layer, in which case a graded index structure could be formed that would act like a bend, since it would allow the adjustment of the waveguide coupling. Furthermore, a structure such as that in Figure 5.1 could be readily turned into a channel waveguide device by direct photolithography or by photobleaching.

A directional coupler's characteristics depend critically on the wavelength of light used, the refractive indices of the materials, the dimensions of the waveguides and their separation. In the present case, the layer thicknesses were determined by considering three basic principles.

a) According to coupled mode theory [23] the single mode cutoff condition (for TE modes)

$$\Delta n = \frac{\lambda_0^2}{4t_g^2(n_1 + n_0)} \qquad (1)$$

depends on the active layer thickness t_g, λ_0 the wavelength of light, and the refractive indices of the active layer n_1 and the cladding layer n_0; $\Delta n = n_1 - n_0$. The Metricon prism coupler was used to measure the refractive indices of the active layer silicon phthalocyanine/MMA 2/98 (1.520 @ 1.289 μm) and that of the cladding layer PMMA (1.483 @ 1.289 μm). The actual operating wavelength for the directional coupler in a single beam configuration was then designed for 1.064 μm radiation to avoid the presence of two photon absorption, which has been measured to be very large in the silicon phthalocyanine/MMA copolymer at 1.3 μm. The above information suggests that the thickness of silicon phthalocyanine should be approximately 1.3 μm to be below multimode cutoff and therefore single mode for 1.064 μm light. This calculation ignores the effect of refractive index dispersion from 1.3 μm to 1.064 μm which will be small for the PMMA layer, but may be appreciable for the silicon phthalocyanine layer.

b) The cladding (passive) layers should be thick enough to prevent light from reaching the substrate. For TE light the attenuation of the exponentially decaying wave in the cladding layer is given by

$$I = I_0 e^{-2px} \qquad (2)$$

where

$$p = (N_{eff}^2 - n_{PMMA}^2)^{1/2}(\frac{2\pi}{\lambda_0}) \quad (3)$$

N_{eff} is the effective index of the waveguide, and x is the cladding layer thickness. Application of (2) and (3) suggests that x should be much larger than 2/2p (x >>2/2p) and for the present materials determines an upper and lower cladding PMMA layer thickness of approximately 2 μm.

c) The coupling length is related to the thickness of the middle PMMA layer by

$$L = \frac{\pi}{2k_{12}} \quad (4)$$

where L is the coupling length, and k_{12} the amplitude coupling coefficient. For the designed device operating at 1.06 μm, k_{12} may be expressed as $k_{12} = k_0 e^{-3.46d}$ where 2d is the center to center guide separation and $k_0 = 0.590\ \mu m^{-1}$. Therefore $L = \frac{p}{2k_0} e^{3.46d} = 2.67\ e^{3.46d}\ \mu m$. To obtain a coupling length of a few millimeters at 1.06 μm we need a central PMMA layer thickness of approximately 2.5 μm. The coupling length is exponentially varying with the waveguide parameters so that small changes in thickness, wavelength, or refractive index give large changes in the coupling length. As demonstrated below, this was manifested by a significantly shorter coupling length than the design length being observed at 1.29 μm.

5.3.2 Waveguide and Coupling Experiments

A number of five layer devices were made for investigation of waveguide loss, coupling and reproducibility of the fabrication techniques. Also, since the coupling characteristics are highly dependent on the center layer thickness and optical wavelength, a number of devices with differing center layer thicknesses were fabricated. The center to center waveguide separation and resulting coupling lengths calculated are given in Table 5.1 for 1.289 μm and 1.064 μm wavelengths; dispersion in the copolymer refractive index was taken into account with a two level-model.

Table 5.1

Coupling Length as a Function of Guide Separation for 1.289 μm and 1.064 μm Wavelengths

Center to center guide separation (μm)	Coupling length (@ 1.289 μm) (mm)	Coupling length (@ 1.064 μm) (mm)
3.80	0.548	1.908
3.54	0.409	1.217
3.30	0.304	0.804
3.04	0.227	0.513

Since there are no electronic absorptions in silicon phthalocyanine in the near-infrared, the loss of the material should be only weakly dependent on wavelength. Although the design wavelength was 1.06 μm for reasons of increasing $\chi^{(3)}$ and avoiding two-photon absorption, it is reasonable to use 1.289 μm light for assessing waveguide loss. This was done using a standard setup based on the detection of light scattering from the guiding layer for light launched by prism coupling (made possible by the lift-off technique) into the guidelayer. Figure 5.2 shows the loss of a three layer waveguide (PMMA/SiPc:MMA/PMMA) as measured with the 1.289 μm loss apparatus for the TE mode. The loss is estimated to be 5-7 dB/cm, which is not prohibitively large if the device is only a few millimeters long. The origin of loss may be absorption but could also be scattering caused by partial alignment of the silicon phthalocyanine copolymers. Figure 5.3 demonstrates evidence for a modulation with a 1 mm periodicity in the loss of a 5 layer device. This represents coupling between the two waveguides since the top guide will scatter considerably more than the bottom guide. This modulation should have a periodicity of twice the coupling length, which is consistent with the calculated coupling length of 500 μm for this 5 layer device at 1.289 μm (see Table 5.1). The "extinction ratio" cannot be accurately determined from this data since the bottom guide will still exhibit some scattering.

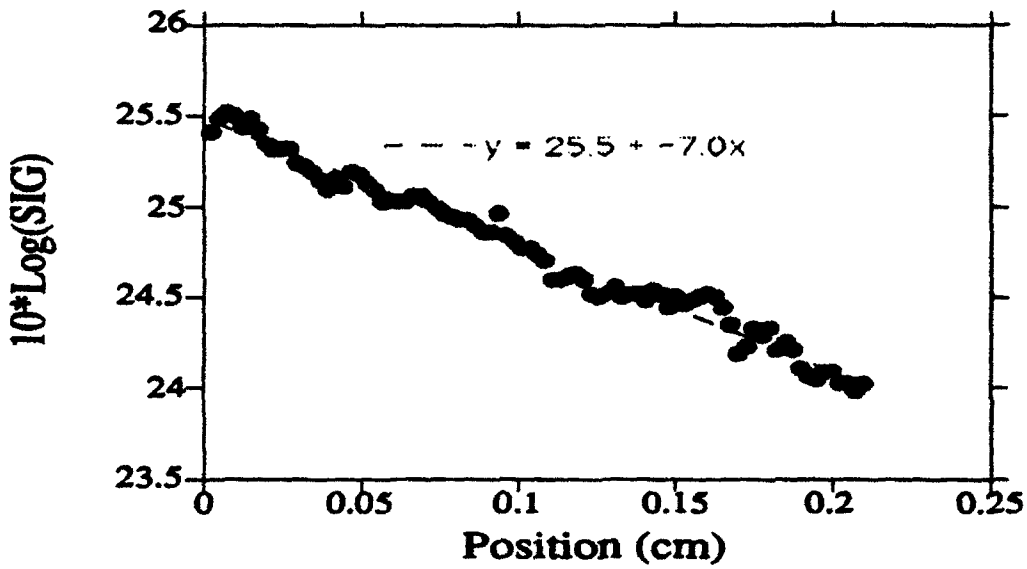

Figure 5.2 Loss of a three layer waveguide as measured by the scattering technique at 1.289 μm.

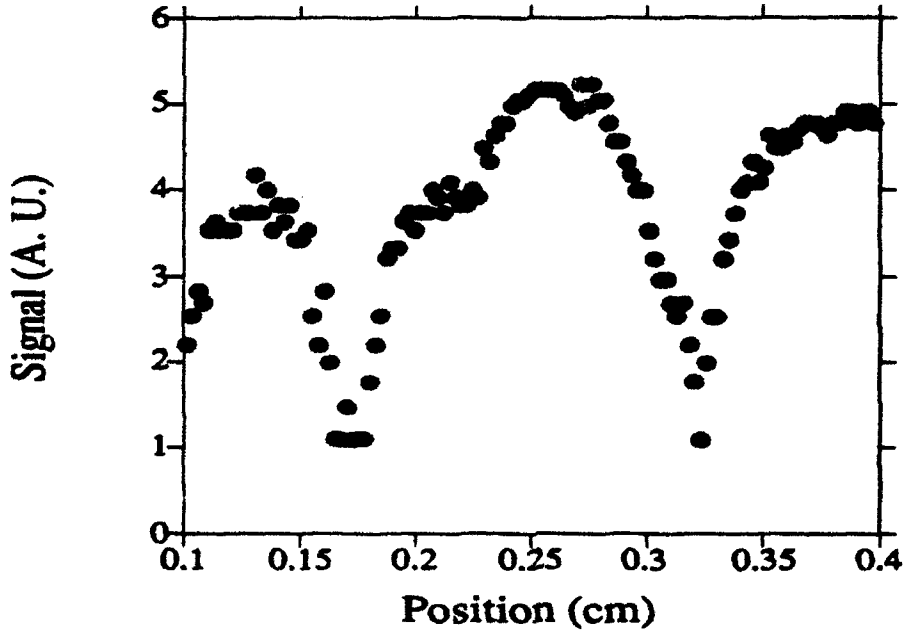

Figure 5.3 Coupling between Silicon phthalocyanine/MMA waveguides as measured with the scattering technique.

Waveguiding was also observed using endfire optical fiber coupling into the waveguides and an infrared camera and beam scanning system to image the output. A 1.06 μm diode pumped Nd:YAG laser was used, and slab waveguiding in both waveguides was clearly observed as shown in Figure 5.4. The beam scanning system which was used to quantify the waveguiding shows that the top waveguide confines light more strongly than the bottom. This comes from the inherent asymmetry in the structure shown in Figure 5.1, since the top waveguide sees an air "substrate" while the bottom sees an Si/SiO_2 substrate. These experiments demonstrate that relatively low loss waveguiding can be achieved at 1.06 μm and that both silicon phthalocyanine layers can simultaneously support waveguiding modes. Future work will concentrate on demonstrating switching between the two waveguides, either through the imposition of a resonant optical pump incident perpendicular to the plane of the slab waveguide or a nonresonant optical pump along the waveguide.

Figure 5.4 Photograph (computer generated) of both waveguides waveguiding in a five layer sample at 1.06 μm as obtained with an infrared camera.

5.4 CONCLUSIONS

The spin coating process is used extensively in producing thin solid polymeric films because this process is relatively simple and convenient, and it usually produces uniform films which are quite reproducible. In order to get defect-free films from this technique, the effects of solvent nature, spinning parameters, and drying conditions on film quality have to be understood. The best final film property is obtained when non-hygroscopic solvents with a medium boiling point (120 - 170 °C) are used in the spin coating process. Various types of surface defects, such as orange peel, fisheye, pinholing, and crawling, are observed when polymer solutions are spun on a substrate such as silicon wafer. These defects results in poor film properties and many problems when the film is further processed in drying or poling stages. It was found that addition of nonionic surfactants could eliminate most of the coating problems by reducing surface tension of the polymer solutions.

When multilayer structure devices are fabricated, it is inevitable to experience the problem of solvent stress cracking. A plasma polymer layer which is dense enough not to allow penetration of solvent molecules to the bottom layer yet thin enough not to interfere with guided waves has been successfully employed to prevent the solvent stress cracking. This plasma technique seems to be suitable for the device fabrication process since it takes only a few minute for the whole procedure and does not result in any adverse effects on optical waveguiding property of NLO polymers.

We have demonstrated that the third order NLO polymer, silicon phthalocyanine /methymethacrylate copolymer, can be used as an active material in the slab waveguide directional coupler. The optical loss of the three layer waveguide was measured at 1.289 μm and found to be 5 - 7 dB/cm. The evidence for a modulation with a 1 mm periodicity in the loss of the five layer waveguide device was shown. This represents coupling between the two waveguides since the top waveguide will scatter considerably more than the bottom guide.

VI. CONCLUSIONS

A series of new side chain polymers was synthesized and characterized for the second and third order NLO applications. Linear copolymers containing maleic anhydride as an active functional group on the main chain were prepared in this work. The maleic anhydride group reacts, by ring opening esterification with an appropriate alcohol containing an NLO functionality, to form an acid ester. These copolymers were also found to be suitable for branching or crosslinking reactions with α,ω-diols. On esterification of the anhydride unit, the backbone became inherently more flexible, resulting in a lower glass transition. In all cases, polymerization of maleic anhydride and comonomers such as butyl vinyl ether and styrene resulted in high molecular weight polymer. Introduction of a slight excess of the anhydride in the feed ratio ensured synthesis of an alternating copolymer. The electrooptic property measurements resulted in rather low activities. The electrooptic coefficient found from the styrene/maleic anhydride copolymers is about 1 pm/V when poled in a field of 50 volts/μm at 140 °C.

New NLO molecules based on the metallated macrocycle family are synthesized. A series of substituted silicon and aluminum phthalocyanines were prepared to study their third order nonlinear responses. A nitro/amino substituted aluminum phthalocyanine was also made along with mixtures of benzo substituted silicon phthalocyanines. A synthetic route was investigated to directly produce donor acceptor phthalocyanines which may show promise for macrocyclic second order materials. A series of monomethacrylate and dimethacrylate silicon phthalocyanines and naphthalocyanines have been synthesized and characterized. Average molecular weights range from 20,000 to 307,000 with glass transition temperatures of 73 °C to 129 °C. The highest concentration achieved so far of the active chromophore in a copolymer is 12 mole percent (60 percent by weight). All of these copolymers show excellent film forming characteristics and can be made into tough micron thick films.

A number of NLO molecules and polymers have been characterized for third order responses by the technique of degenerate four wave mixing. A series of main chain and pendant copolymers synthesized by L. Dalton's group at the University of Southern California were measured, with a 5-ring pendant copolymer having both the highest nonlinearity ($\chi^{(3)}_{1111} = 3 \times 10^{-11}$ esu) and also the highest value of $\chi^{(3)}_{1111}/\alpha$ for this group. Electro-optic polymers previously synthesized at HCC were investigated and a

DANS/MMA 60/40 copolymer was found to have $\chi^{(3)}_{1111} = 7 \times 10^{-12}$ esu, while an ONS/MMA 50/50 copolymer had a nonlinearity only one third that of DANS/MMA 60/40. Dynamical studies indicated that the response of DANS/MMA 60/40 is ultrafast (subpicosecond). This property, coupled with the availability of high quality DANS/MMA waveguides, may make this material an interesting candidate for all-optical switching at 1.3 μm. Resonant $\chi^{(3)}_{1111}$ values as large as 2.6×10^{-10} esu were observed for silicon phthalocyanine copolymers with 6 mole percent active chromophore. Device designs based on the silicon phthalocyanine copolymers in both waveguide and single mode fiber forms have been presented which may yield ultrafast all optical switching devices.

The fabrication of useful electro-optic devices using organic polymers requires techniques for depositing many polymer and metal layers onto a substrate and ways for defining linear waveguiding structures in a multi-layer film. The spin coating process is used extensively in producing thin solid polymeric films because this process is relatively simple and convenient, and it usually produces uniform films which are quite reproducible. In order to obtain defect-free films through this technique, the effects of solvent nature, spinning parameters, and drying conditions on film quality need to be understood. The best final film property is obtained when non-hygroscopic solvents with a medium boiling point (120 - 170 °C) are used in the spin coating process. Various types of surface defects, such as orange peel, fisheye, pinholing, and crawling, are observed when polymer solutions are spun on a substrate such as silicon wafer. These defects results in poor film properties and many problems when the film is further processed in drying or poling stages. It was found that addition of nonionic surfactants could eliminate most of the coating problems by reducing surface tension of the polymer solutions.

When multilayer structure devices are fabricated, it is inevitable to experience the problem of solvent stress cracking. A plasma polymer layer which is dense enough not to allow penetration of solvent molecules to the bottom layer yet thin enough not to interfere with guided waves has been successfully employed to prevent the solvent stress cracking. This plasma technique seems to be suitable for the device fabrication process since it takes only a few minute for the whole procedure and does not result in any adverse effects on optical waveguiding property of NLO polymers.

We have demonstrated that the third order NLO polymer, silicon phthalocyanine /methylmethacrylate copolymer, can be used as an active material in the slab waveguide directional coupler. The optical loss of the three layer waveguide was measured at 1.289

μm and found to be 5 - 7 dB/cm. The evidence for a modulation with a 1 mm periodicity in the loss of the five layer waveguide device was shown. This represents the structure proposed couples light from the upper waveguide to the bottom waveguide. Further work will be needed to demonstrate the light intensity dependence for the observed coupling.

VII. REFERENCES

1) R. DeMartino, R. Keosian, I. McCulloch, R. Norwood, J. Sounik, "AFOSR contract:F49620-89-C-0097, First Interim Report, July 1990.

2) L. Charbonneau, R. DeMartino, I. McCulloch, R. Norwood, J. Sounik, J. Popolo, "AFOSR contract:F49620-89-C-0097, Second Interim Report, July 1991.

3) J. Stamatoff, R. DeMartino, D. Haas, G. Khanarian, H. Man, R. Norwood, H. Yoon, *Ange. Makro. Chem.*, 1990,183, 151.

4) R. DeMartino, "Polymers for Nonlinear and Electro-optic Applications", in Fine Chemicals for the Electronics Industry II: Chemical Applications for the 1990s", edited by D.J. Ando and M.G. Pellatt, Royal Society Special Publication, 1991, **88**, 223.

5) J. Wu, J. Heflin, R. Norwood, K. Wong, O. Zamani-Khamiri, A. Garito, P. Kalyanaraman and J. Sounik, *J. Opt. Soc. Am. B*, 1989, 6(4), 709.

6) J. Shirk, J. Lindle, F. Bartoli, C. Hoffman, Z. Kafafi and A. Snow, *Appl. Phys. Lett.*, 1989, **55**(13), 1287.

7) D. Rao, F. Aranda, J. Roach and D. Remy, *Appl. Phys. Lett.*, 1991, **58**(12), 1241.

8) M. Cassetevens, M. Samoc, J. Pfleger and P. Prasad, *J. Chem. Phys.*, 1990, **92**(3), 2019.

9) Z. Z. Ho, C. Y. Ju and W. Hetherington, *J. Appl. Phys.* 1987, **62**(2), 716.

10) A. Kaltbeitzel, D. Neher, C. Bubeck, T. Sauer, G. Wegner and W. Caseri, "Electronic Properties of Conjugated Polymers III", Springer-Verlag, 220, (1989)

11) T. Sauer, W. Caseri and G. Wegner, *Mol. Cryst. Liq. Cryst.*, 198

12) C. Bubeck, D. Neher, A. Kaltbeitzel, G. Duda, T. Arndt, T. Sauer and G. Wegner, "Nonlinear Optical Effects in Organic Polymers", Kluwer Academic, 162,185, (1989).

13) B. Wheeler, G. Nagasubramanian, A. Bard, L. Schectman, D. Dinniny, M. Kenney, *J. Am. Chem. Soc.*, 1984, **106**, 7404.

14) D. Batzel, PhD. Thesis, Case Western Reserve University, 1990.

15) W. E. Torruellas, R. Zanoni, M. B. Marques, G. I. Stegeman, G. R. Möhlmann, E. W. P. Erdhuisen, and W. H. G. Horsthuis, *Chem. Phys. Lett.* **175**, 267 (1990).

16) W. E. Torruellas, R. Zanoni, G. I. Stegeman, G. R. Möhlmann, E. W. P. Erdhuisen, and W. H. G. Horsthuis, *J. Chem. Phys.* **94**, 6851 (1991).

17) D. V. G. L. N. Rao, F. J. Aranda, J. F. Roach, and D. E. Remy, *Appl. Phys. Lett.* **58**, 1241 (1991).

18) T. Sauer, W. Caseri, and G. Wegner, presentation at the *Unconventional Photoactive Solids Symposium*, San Jose, California, October 16-18, 1989.

19) M. K. Casstevens, M. Samoc, J. Pfleger, and P. N. Prasad, *J. Chem. Phys.* **92**, 2019 (1990).

20) S. E. Webber, *Chem. Rev.* **90**, 1469 (1990).

21) K. Kamioka and S. E. Webber, *Chem. Phys. Lett.* **133**, 353 (1987).

22) K. Song, R. Norwood, J. Stamatoff, P. Landi, H. Goldberg, B. Feuer, "Optical Interconnect Technology", Proposal for AFOSR Contract, June 1991.

23) R. G.Hunsperger,"Integrated Optics: Theory and Technology," (Springer-Verlag, Berlin, 1984).

VIII. INTERACTIONS AND PUBLICATIONS

8.1 EXTERNAL INTERACTIONS

The NLO research team has had a variety of interactions which have benefitted the program. During the contract period, the research team has interactively consulted with the following Air Force and DOD laboratories:

Individual	DOD Agency
D. Ulrich	AFOSR
C. Lee	AFOSR
P. Land	AFML
A. Yang/L. Durvasula	DARPA
E. Sharp	CNVEOL

Hoechst Celanese has also supported a number of university related research programs in the NLO area which including the following:

Individual	University	Program Focus
Prof. L. Dalton	USC	Polymer Synthesis
Prof. A. Griffin	USM	Side Chain Polymers
Prof. M. Kenney	CWRU	Organometallic Chemistry
Prof. M. Kuzyk	WSU	Fiber Devices
Prof. G. Stegeman	U. Arizona	Waveguide Devices
Prof. A. Tanguay	USC	Electro-optic Devices

8.2 PATENT ACTIVITY

1. RFPA 30871 G, J. Sounik, J. Popolo, "Acrylate based phthalocyanine and naphthalocyanine copolymers".
2. RFPA 30881 G, J. Sounik, "Styrene copolymers and homopolymers modified with phthalocyanines and naphthalocyanines".

3. RFPA 30882 G, J. Sounik, J. Popolo, "Liquid crystal side chain phthalocyanine and naphthalocyanine acrylate copolymers".

4. RFPA 30883 G, J. Sounik, T. Leslie "Styryl maleic anhydride copolymers modified with phthalocyanine and naphthalocyanine".

5. RFPA 30976 C, K. Song, "Plasma polymer as a barrier layer for solvent stress cracking".

8.3 PUBLICATIONS

1. C. W. Spangler, M. L. Saindon, E. G. Nickel, L. S. Sapochak, D. W. Polis, L. R. Dalton, and R. A. Norwood, "Synthesis and incorporation of ladder polymer subunits in copolyamides, pendant polymers and composites for enhanced nonlinear optical response", *Proc. SPIE* **1240** (1991).

2. R. A. Norwood, J. R. Sounik, J. Popolo and D. R. Holcomb, "Third order nonlinear optical characterization of side-chain copolymers", *Proc. SPIE* **1560** (1991).

3. R. A. Norwood, T. K. Findakly, H. A. Goldberg, G. Khanarian, J. B. Stamatoff, and H. N. Yoon, "Optical polymers and multifunctional materials" chapter for *Polymers for Lightwave and Integrated Optics: Technology and Applications* ed. by L. A. Hornak (Marcel Dekker, in press).

4. R. A. Norwood and J. R. Sounik, "Third order nonlinear optical response in polymer thin films incorporating porphyrin derivatives", *Appl. Phys. Lett.*, **60** (3), 295, 1992.

5. J. R. Sounik, R. A. Norwood, J. Popolo, and D. R. Holcomb, "Side-chain copolymers for third order nonlinear optical applications," presented at 202nd American Chemical Society National Meeting, New York, August 25-29, 1991.

6. J. Sounik, R. Norwood, J. Popolo, D. Holcomb, "Side-chain copolymers for third order nonlinear optical applications," *Poly. Preprints*, 1991, **32** (3), 158.

Appendix

Annual Report

to

Hoechst Celanese
Summit, NJ 07901

on the

SYNTHESIS OF LARGE-LOOP AND POLAR PHTHALOCYANINES FOR USE IN NONLINEAR OPTICAL DEVICES

by

Vance O. Kennedy and Malcolm E. Kenney

Department of Chemistry
Case Western Reserve University
Cleveland, OH 44106

July 2, 1991

ABSTRACT

An account of work on the synthesis of macrocycles for use in the fabrication of nonlinear optical devices is given. Work directed towards the synthesis of fused-ring phthalocyanines is described. Also described is work on the synthesis of phthalocyanines having electron withdrawing or donating groups on three arms of the macrocycle and groups of the opposite kind on the fourth arm. Further work to be done in both these areas is outlined.

INTRODUCTION

A major objective of this work is the preparation of aromatic ring systems that have large conjugated loops. These compounds are being sought because it has been concluded that the non resonant macroscopic third order nonlinear optical susceptibilities of such systems should be unusually large,[1] and because such systems often have good material properties. This makes selected members of this group good candidates for use in the fabrication of nonlinear optical devices.

Initially two types of systems were considered, expanded porphyrins[2-4] such as the one shown in Figure 1, and fused-ring phthalocyanines[5] such as those shown in Figures 2 and 3.

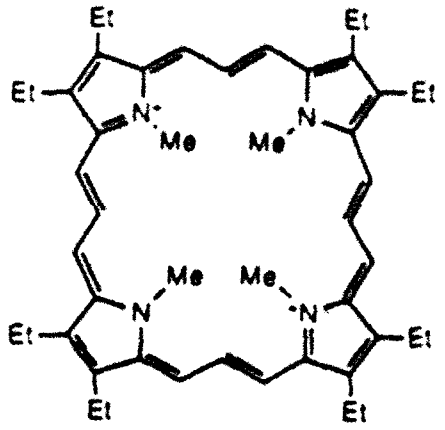

Figure 1. An expanded porphyrin

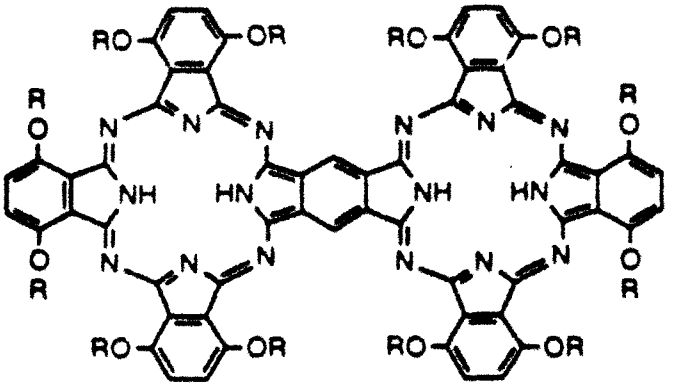

Figure 2. A fused-ring phthalocyanine

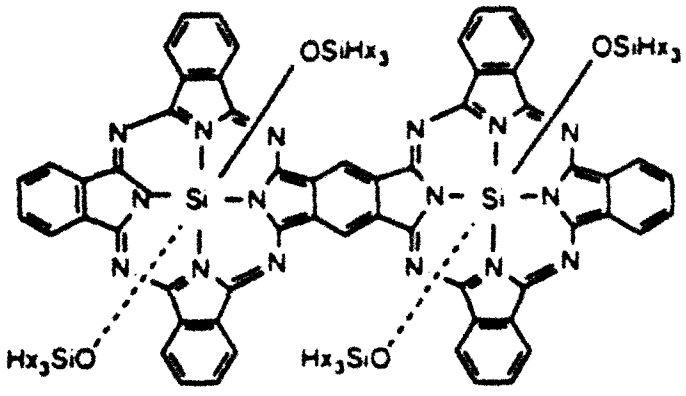

Figure 3. Another fused-ring phthalocyanine

Both types of systems were evaluated carefully and ultimately it was decided to start work on the fused-ring phthalocyanines.

WORK ACCOMPLISHED

Synthesis of Fused-Ring Phthalocyanines by Ring Closure. In the first efforts made on the synthesis of fused-ring phthalocyanines, a set of experiments was carried out in which nitriles or diiminoisoindolines were used as precursors. This work was predicated on the fact that nitriles and diiminoisoindolines are often used for the synthesis of phthalocyanines.

In one group of experiments, the following reaction sequence was carried out with three ratios of the two nitriles.

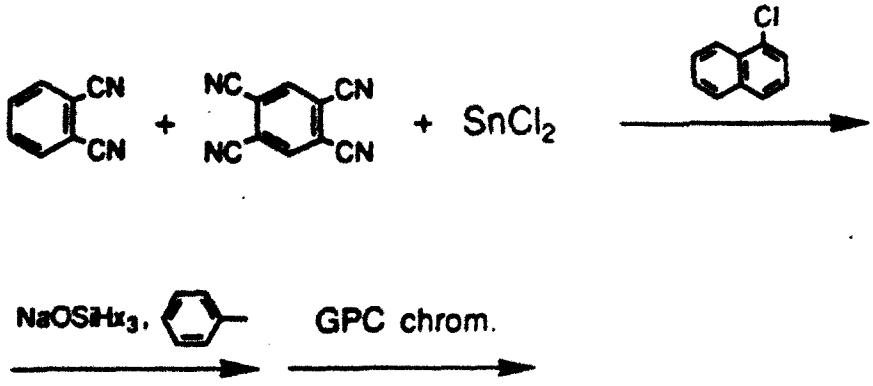

(1)

In a second group, the reaction sequence

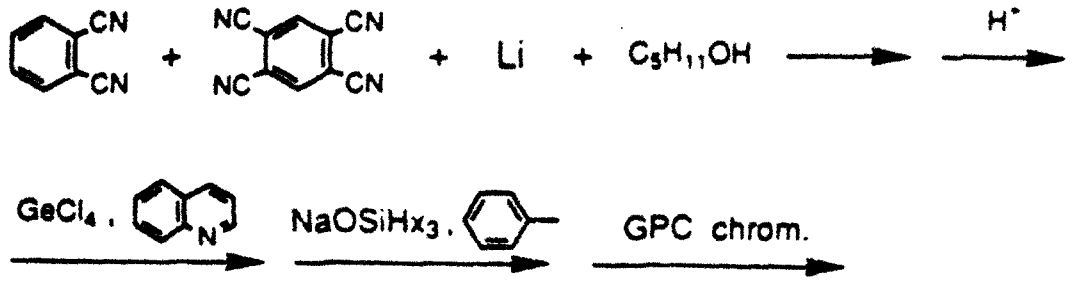

(2)

was carried out with two ratios of the nitriles. In a third group, the sequence

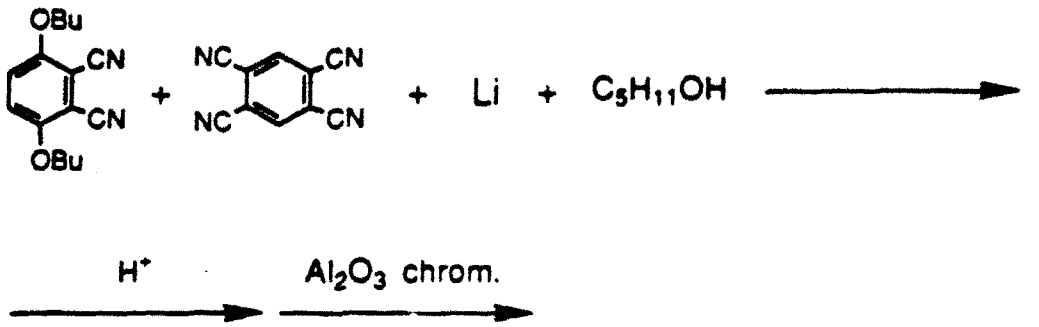

(3)

was carried out with two ratios of the nitriles. Finally in a fourth group, the sequence

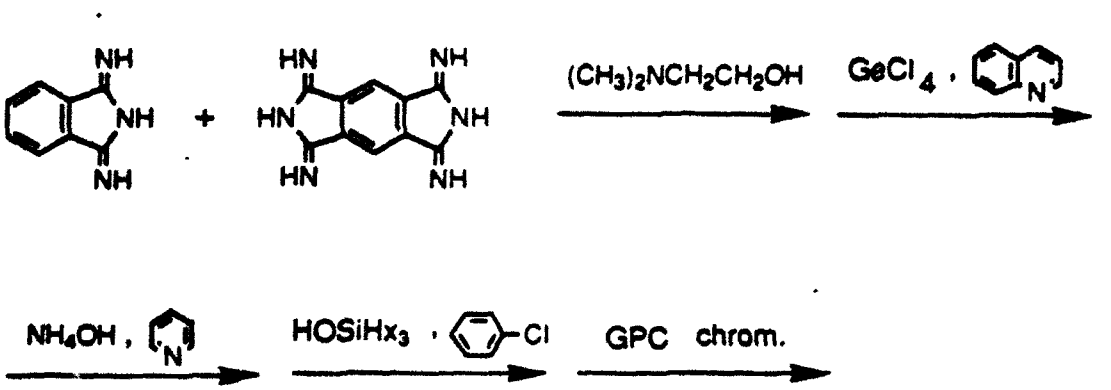

(4)

was carried out with four ratios of the diiminoisoindolines. In none of these experiments was evidence obtained that was recognized as showing that

a fused-ring phthalocyanine had been formed.

Also early in the studies, work was done on Sequence 5.

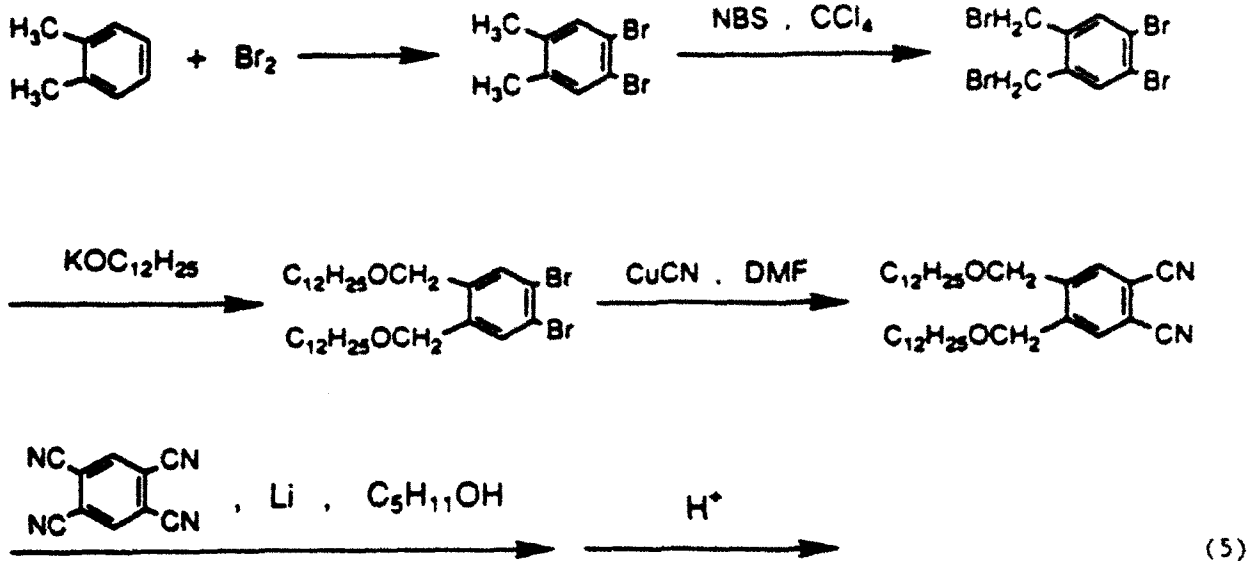

(5)

This sequence is based, as is seen, on the same type of ring formation step as Sequence 3. However, the dinitrile in this sequence has the advantage of being less hindered.

A derivative of this sequence in which diiminoisoindolines are used is also possible.

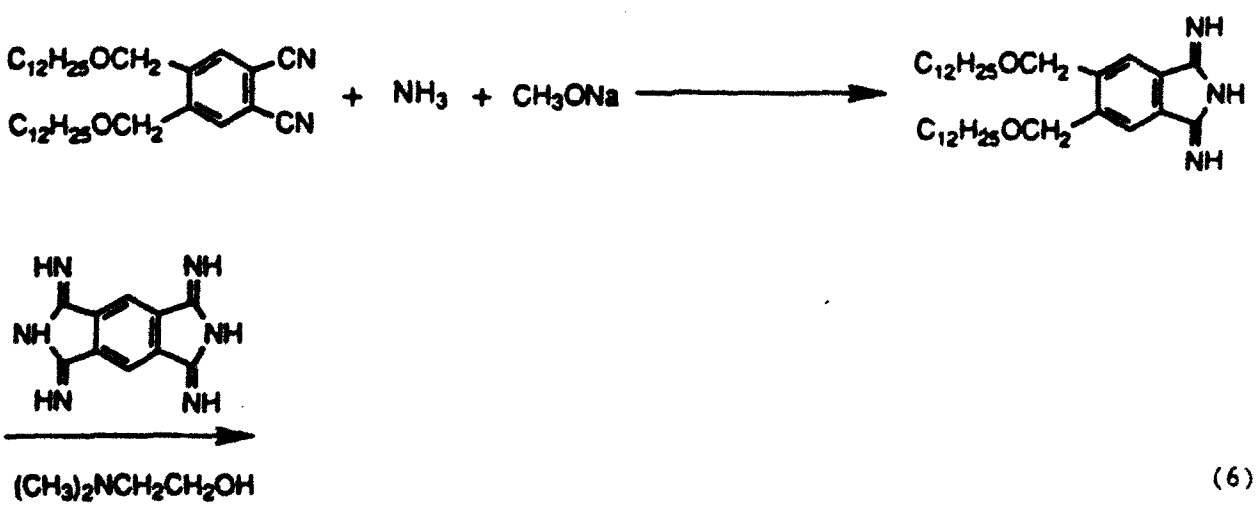

(6)

This sequence is based, as is apparent, on the same type of ring formation step as Sequence 4. It, however, is more advantageous since the diiminoisoindoline used can be assumed to be soluble in organic solvents. Work on Sequences 5 and 6 was carried as far as the synthesis of a small amount of the dinitrile.

Subphthalocyanines and Ring-Expansion Routes to Fused-Ring Phthalocyanines. While this work was in progress, a paper by Kobayashi and coworkers[6] on the formation of phthalocyanines by a new and very interesting method appeared. In this new method phthalocyanines are formed by a ring expansion. One of the reactions reported is:

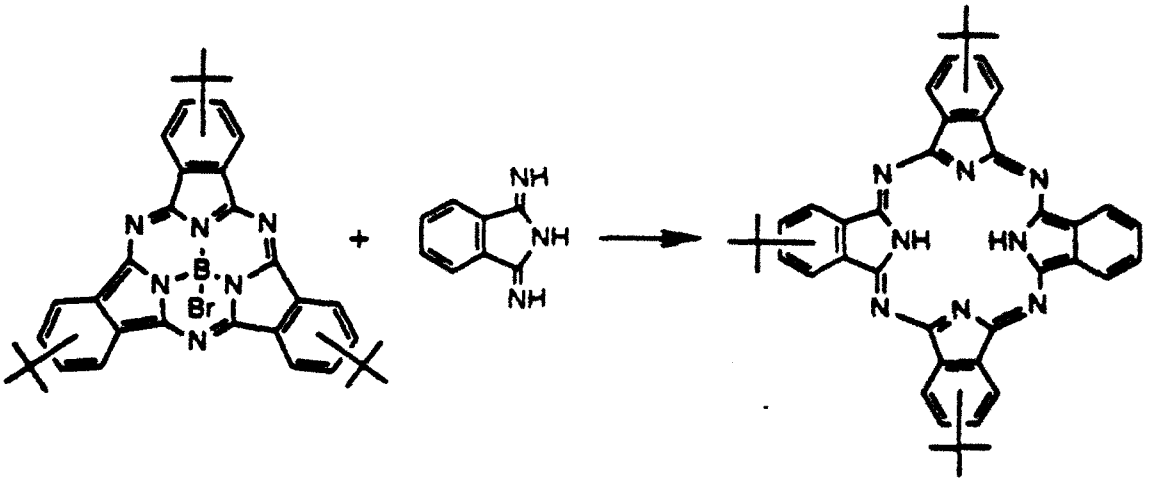

(7)

The phthalocyanine-related macrocycle in this reaction is called a subphthalocyanine and is abbreviated as subPc. Thus, the particular compound in this reaction is abbreviated as BsubPc(*t*-Bu)$_3$Br.

This new chemistry offers at least two attractive potential routes to fused-ring phthalocyanines. An illustration of one of these routes using BsubPcCl as the subphthalocyanine precursor is:

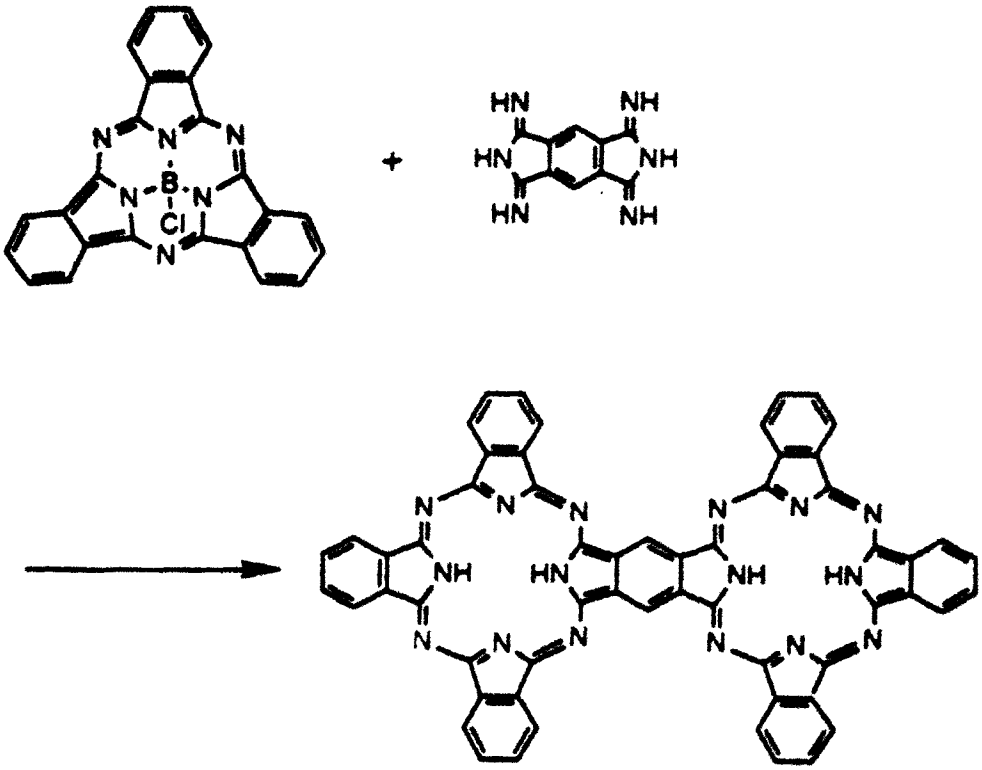

(8)

An illustration of a second route, again using BsubPcCl as the subphthalocyanine precursor is:

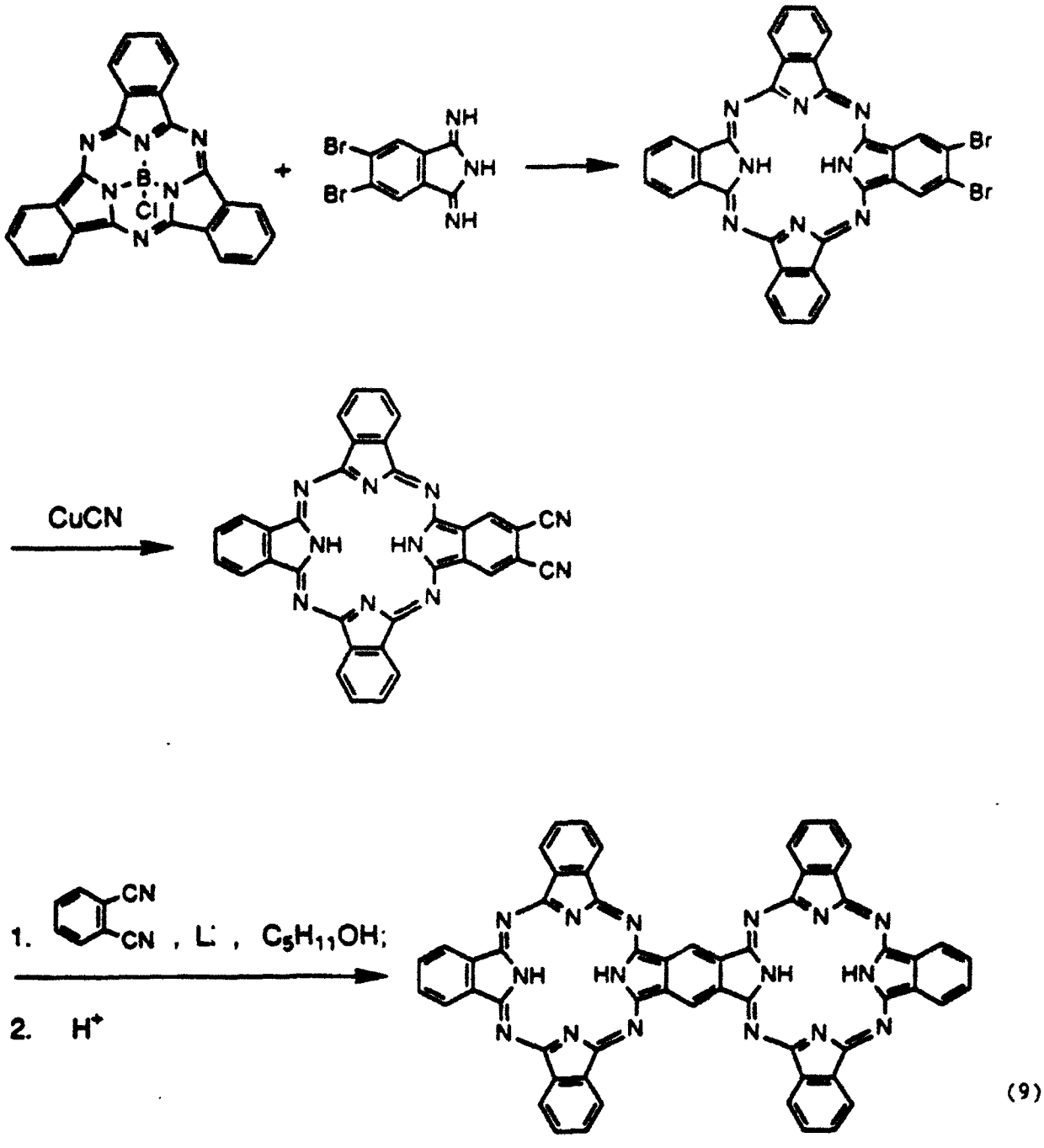

(9)

This second route is longer but is quite promising because reasonably close precedents exist for each of the steps used.

Ring-Expansion Routes to Polar Phthalocyanines and Benzophthalocyanines. In addition to offering attractive potential routes to fused-ring phthalocyanines, the subphthalocyanines also open practical

routes to phthalocyanines and benzophthalocyanines with electron donating or withdrawing groups on three arms of the macrocycle and groups of the opposite type on the fourth arm. Such compounds are of interest because they can be expected to have high dipole moments and thus high macroscopic second order nonlinear optical susceptibilities. This makes selected members of this group good candidates for the fabrication of nonlinear optical devices.

Synthesis of Subphthalocyanines. Because subphthalocyanines offer attractive routes to a wide variety of compounds of potential use for the fabrication of NLO devices, work was started on subphthalocyanines soon after Kobayashi's paper appeared. In this new phase of the work, attention was initially given to BsubPcCl. The synthesis[7] of this compound[8] on a gram scale by the route

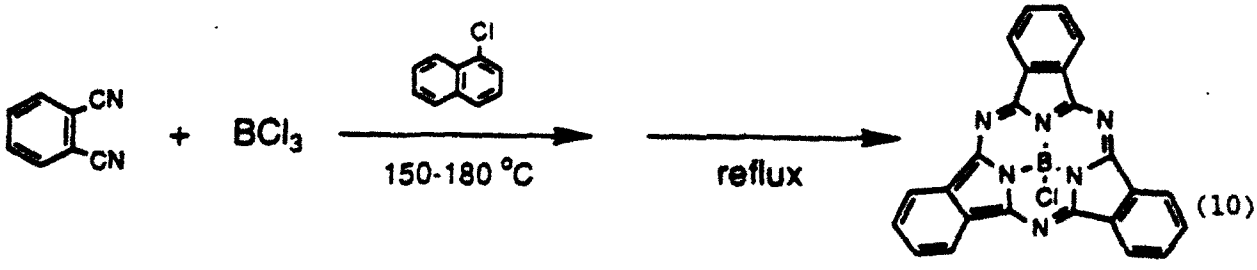

(10)

was mastered. The purification of it by sublimation was also mastered. In addition, work was done on the subphthalocyanine BsubPc(t-Bu)3Cl. The synthesis of this compound by a route parallel to that used for BsubPcCl on a half gram scale and the purification of it by gel permeation chromatography were also mastered. This latter subphthalocyanine is particularly attractive for use because it is easily soluble in organic solvents and because the phthalocyanines made from it can thus be expected to be easily soluble in such solvents.

Synthesis of Polar Phthalocyanines and Polar Benzophthalocyanines by Ring Expansion. In addition to this work on the preparation of BsubPcCl and BsubPc(*t*-Bu)$_3$Cl, work was done on the preparation of a series of phthalocyanines and benzophthalocyanines having various patterns of ring substitution. This work was carried out in order to gain facility in the preparation of phthalocyanines and benzophthalocyanines from subphthalocyanines, and in order to get small amounts of representative compounds from these two groups. The compounds made are shown in Table I.

Table 1

Phthalocyanines Synthesized from Subphthalocyanines

Subphthalocyanine	Diiminoisoindoline	Product	Yield (%)
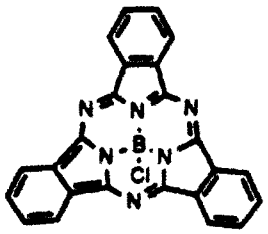	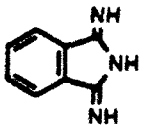	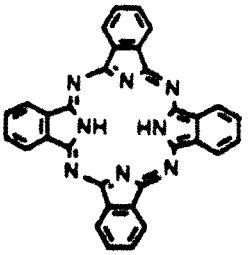 **1**	4
	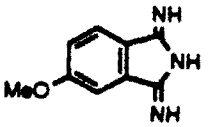	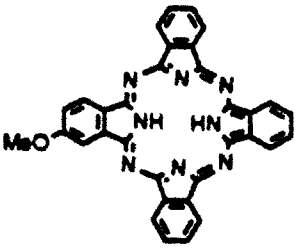 **2**	2
	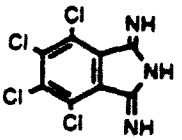	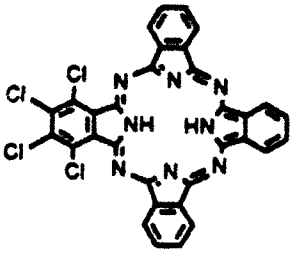 **3**	–

Phthalocyanines Synthesized from Subphthalocyanines

Subphthalocyanine	Diiminoisoindoline	Product	Yield (%)
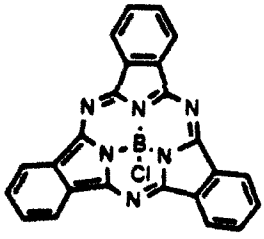	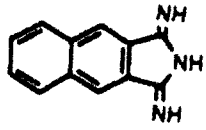	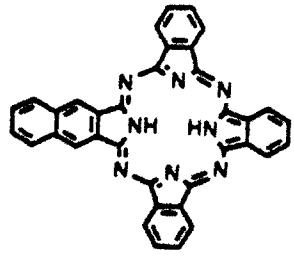 **4**	6
	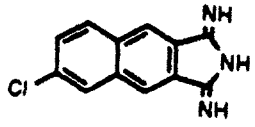	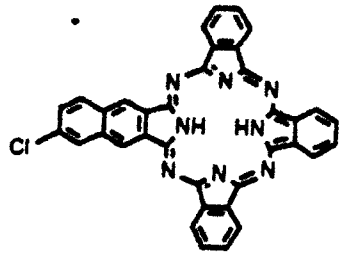 **5**	10
	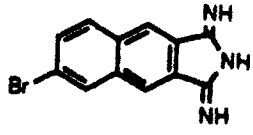	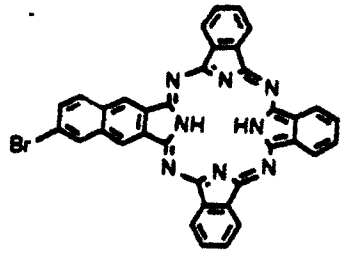 **6**	3
	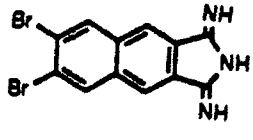	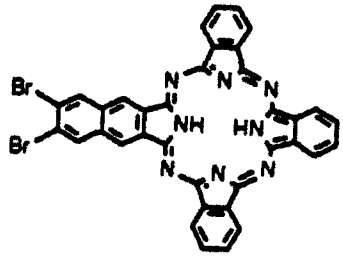 **7**	–

Table 1 (cont.)

Phthalocyanines Synthesized from Subphthalocyanines

Subphthalocyanine	Diiminoisoindoline	Product	Yield (%)
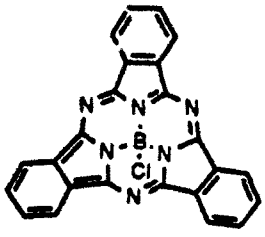	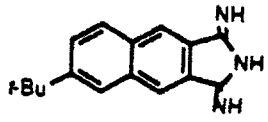	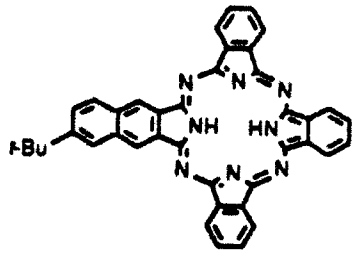 **8**	16
	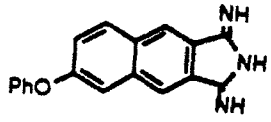	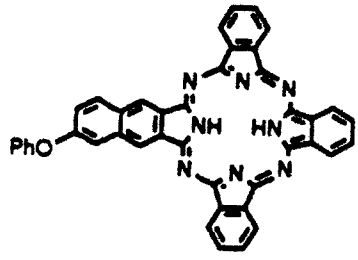 **9**	4
	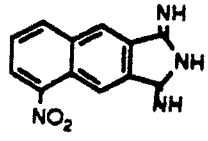	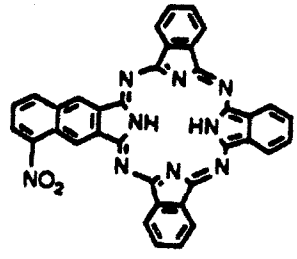 **10**	2

Table I (con't.)

Phthalocyanines Synthesized from Subphthalocyanines

Subphthalocyanine	Diiminoisoindoline	Product	Yield (%)
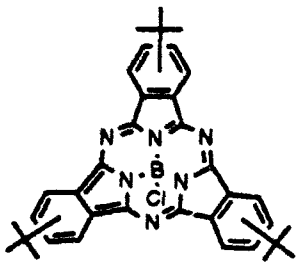	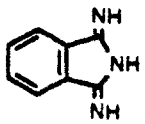	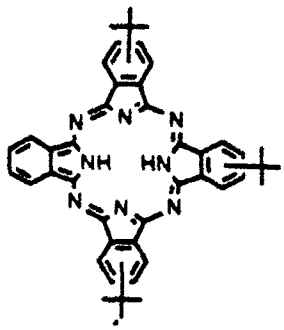 **11**	–
	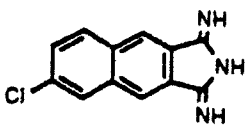	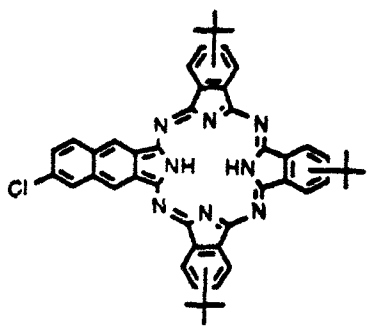 **12**	6

These compounds were made on a small scale and were not purified extensively. While the yields of the compounds obtained were low, they were high enough to show that gram quantities of the compounds can be synthesized in the future if needed. Spectra of compounds 1-10 in 1,2-dichlorobenzene are shown in Figures 4-13. These spectra show the band patterns expected on the basis of Kobayashi's work.[6] As anticipated, the phthalocyanine having three *t*-butyl groups, compound 11 in Table I, is easily soluble in organic solvents.

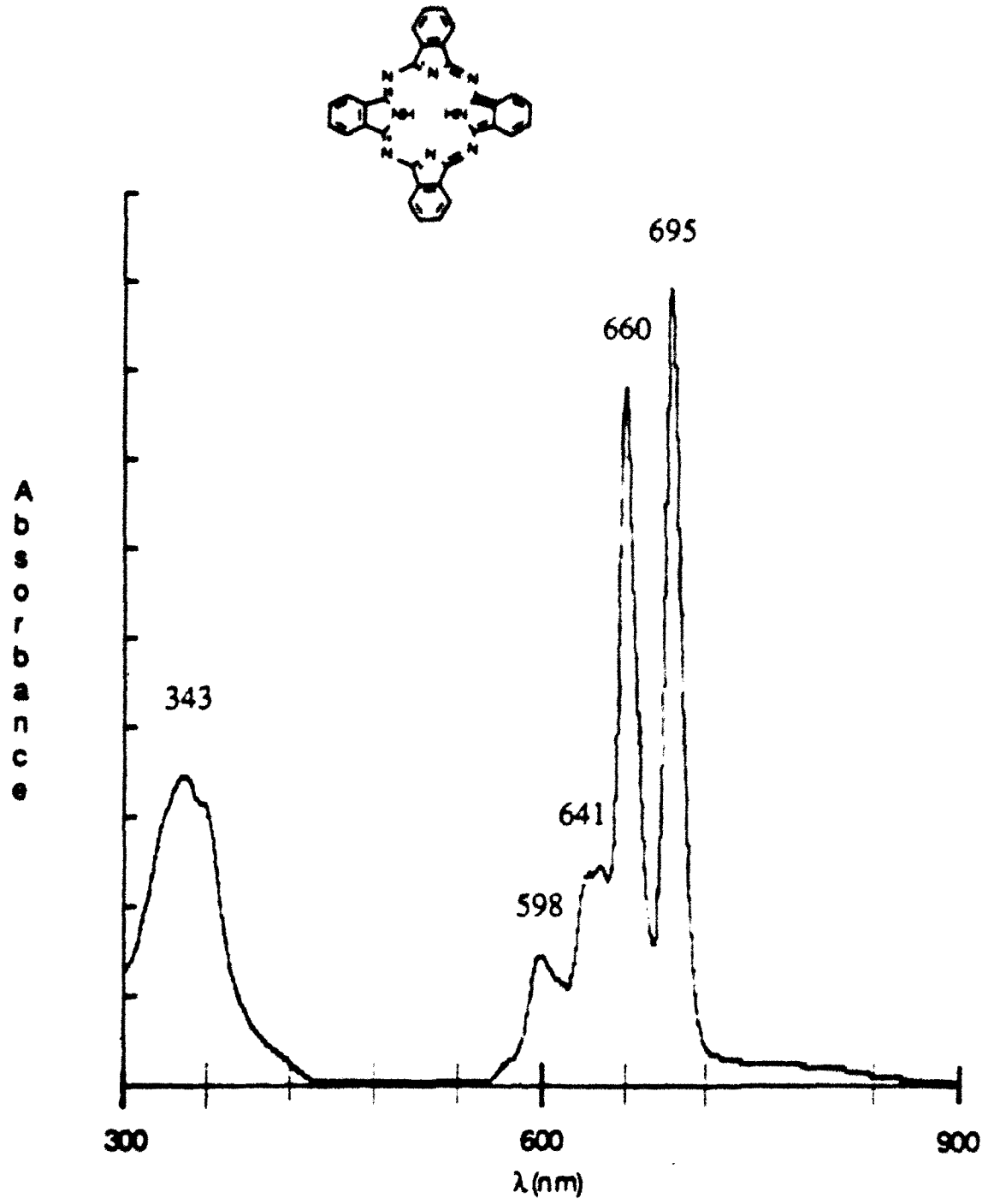

Figure 4. UV-Vis spectrum of phthalocyanine in 1,2-dichlorobenzene.

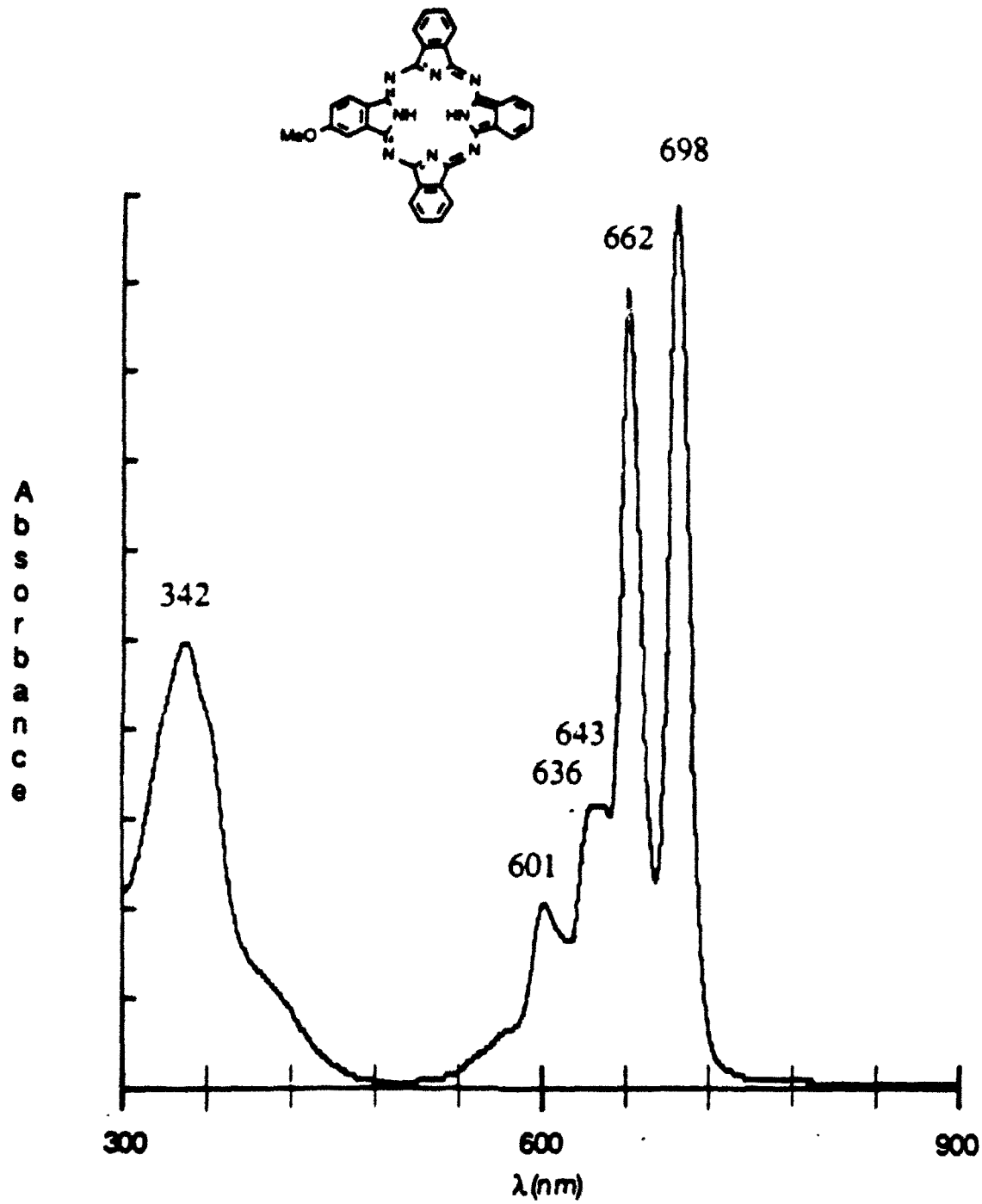

Figure 5. UV-Vis spectrum of 4-methoxyphthalocyanine in 1,2-dichlorobenzene.

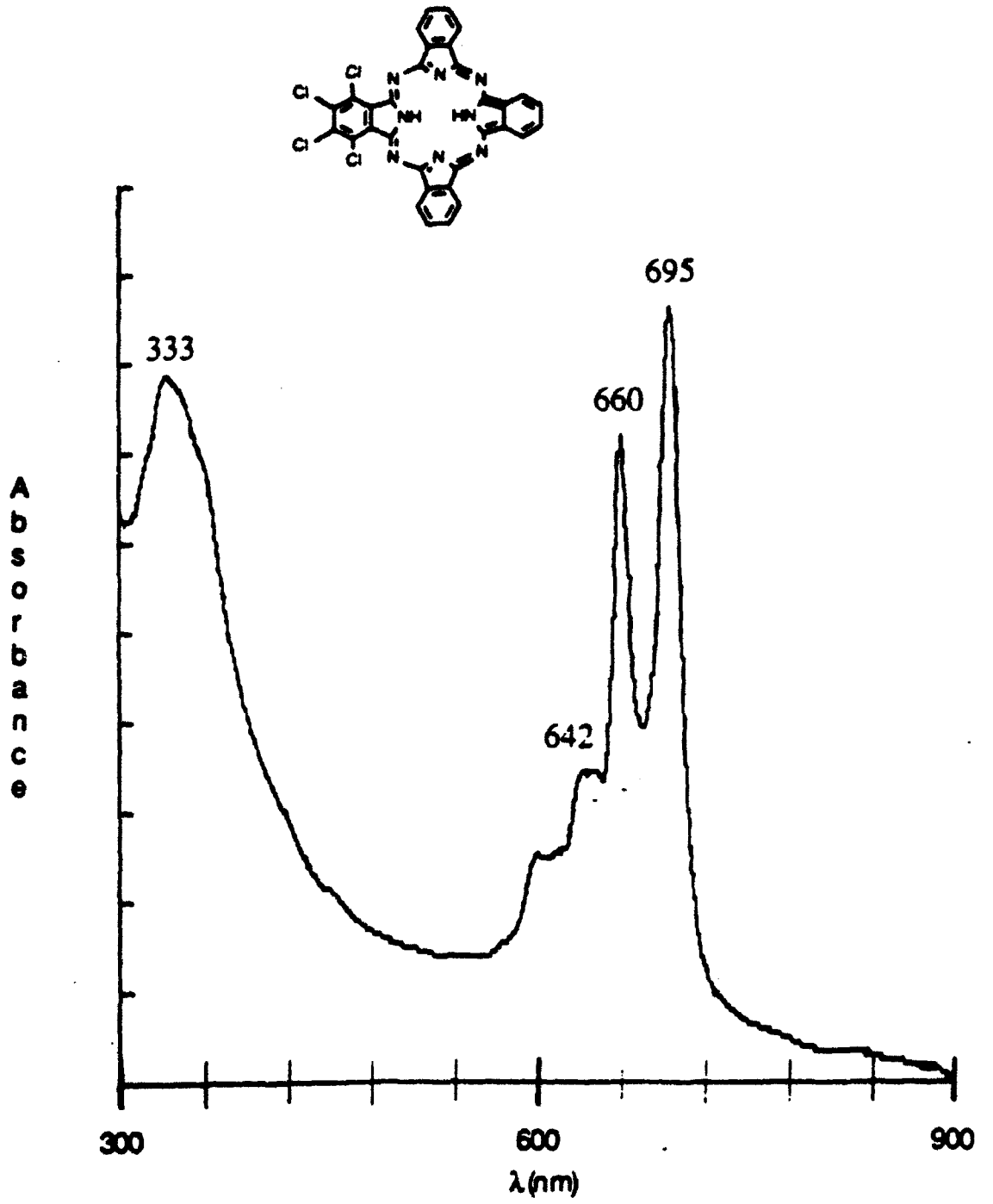

Figure 6. UV-Vis spectrum of 3,4,5,6-tetrachlorophthalocyanine in 1,2-dichlorobenzene.

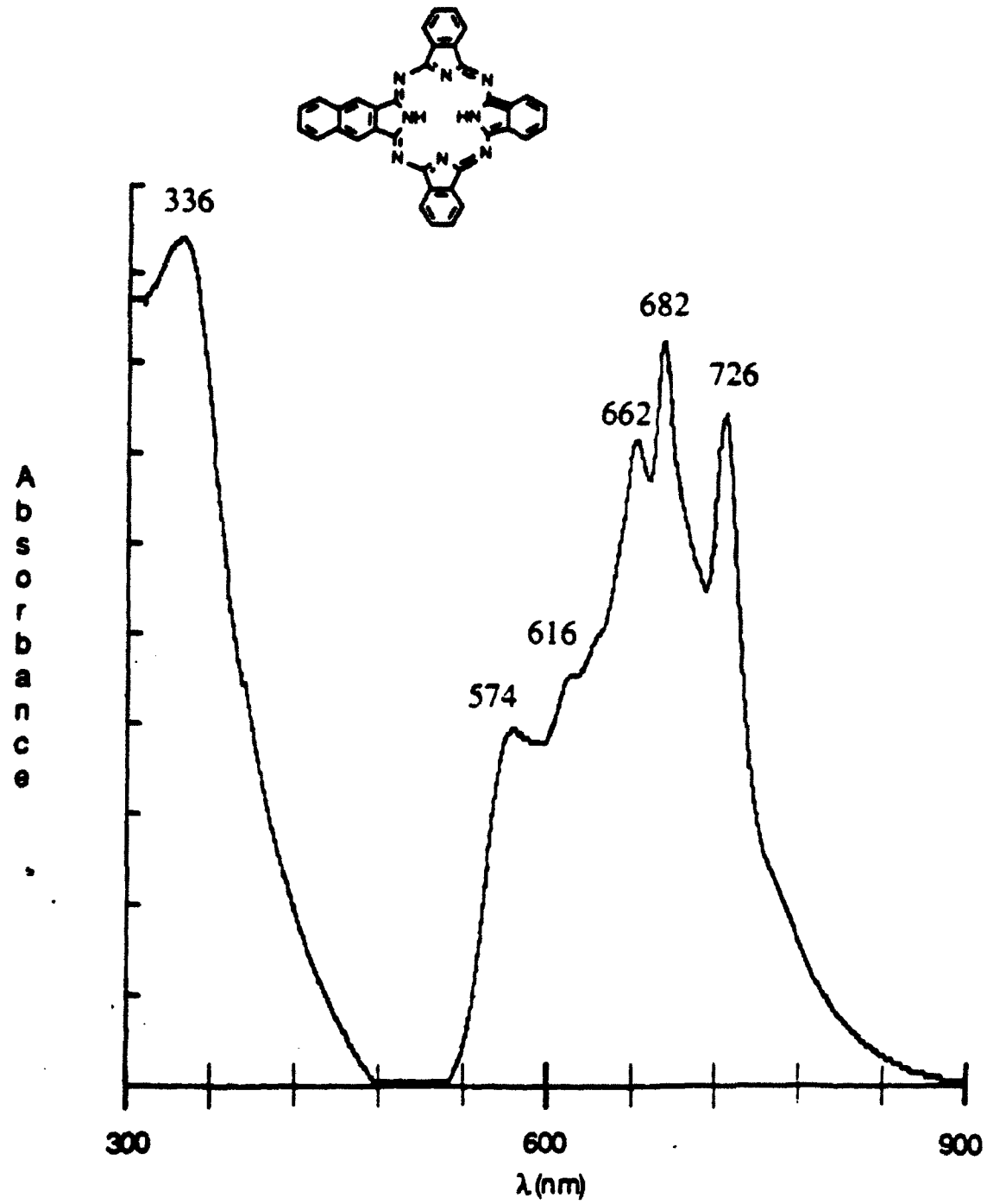

Figure 7. UV-Vis spectrum of benzo phthalocyanine in 1,2-dichlorobenzene.

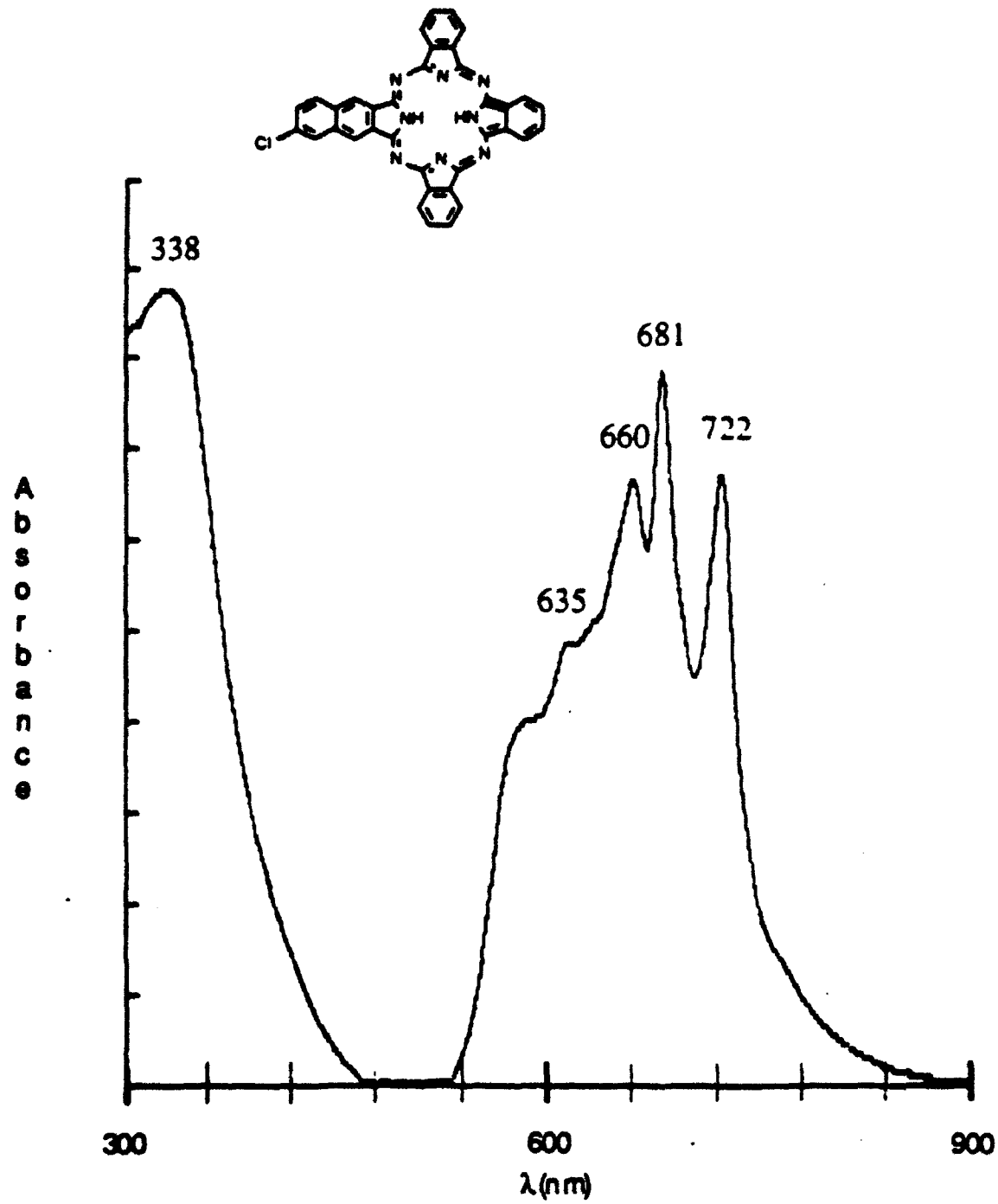

Figure 8. UV-Vis spectrum of compound **5** in 1,2-dichlorobenzene.

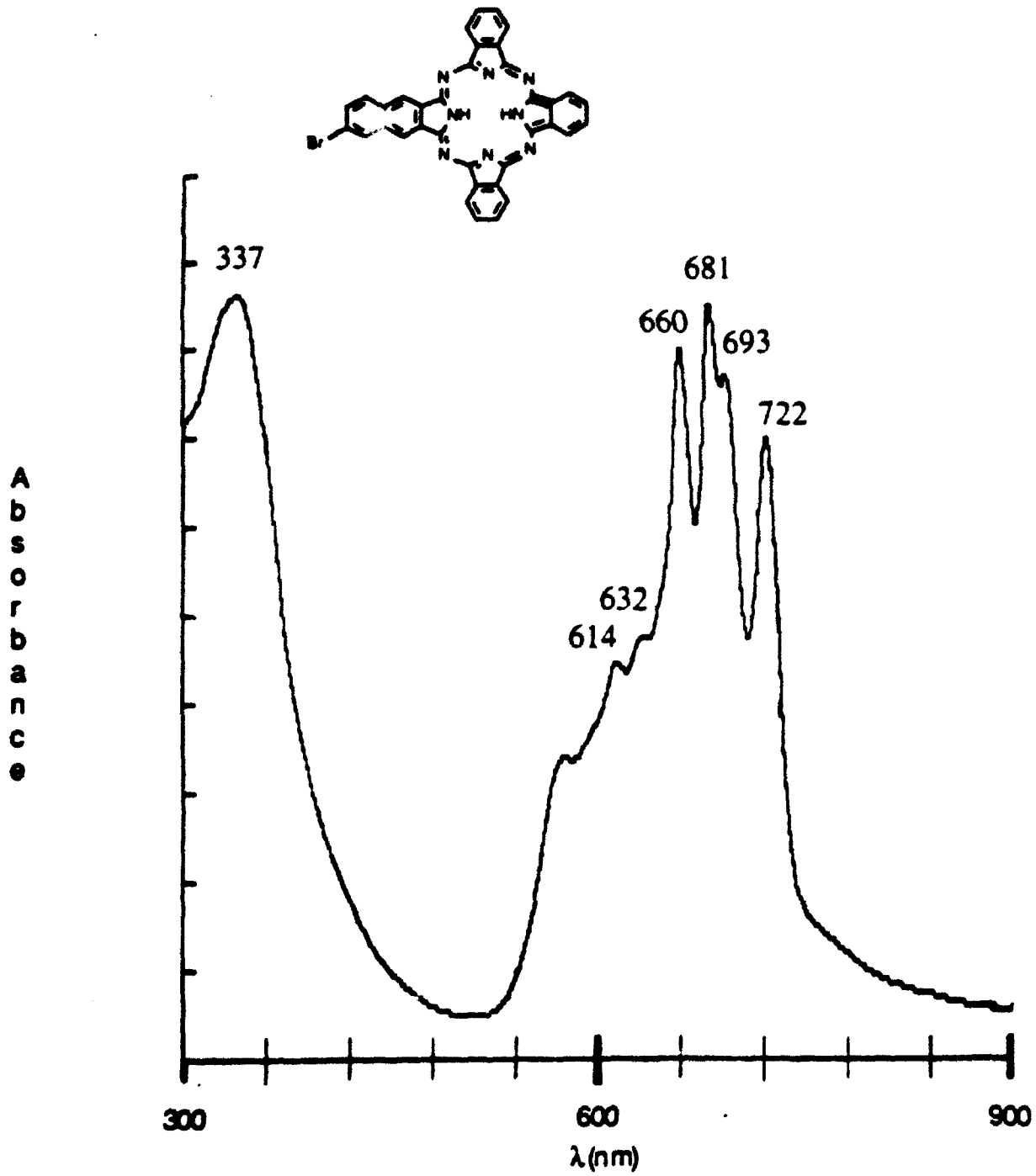

Figure 9. UV-Vis spectrum of compound **6** in 1,2-dichlorobenzene.

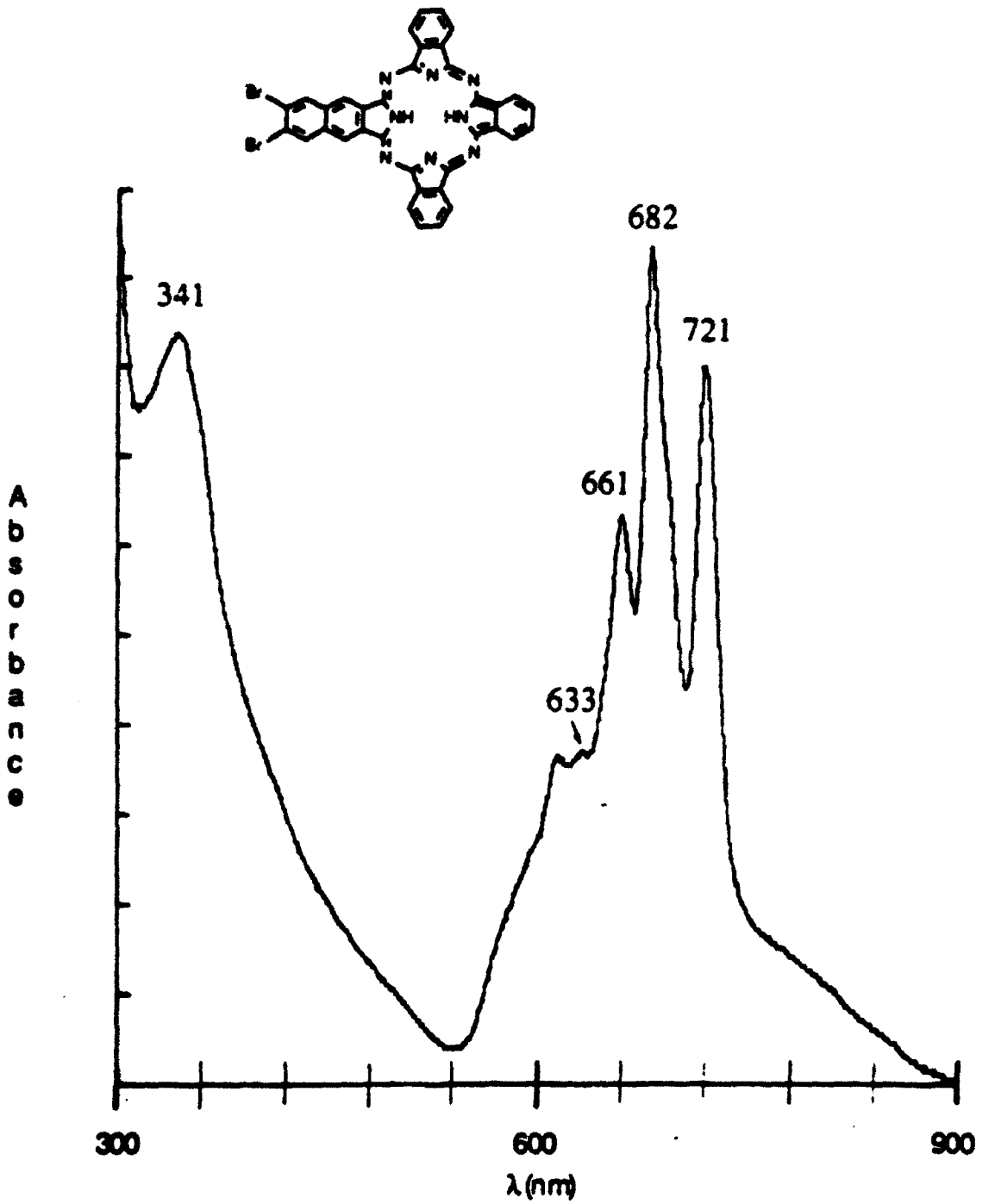

Figure 10. UV-Vis spectrum of compound 7 in 1,2-dichlorobenzene.

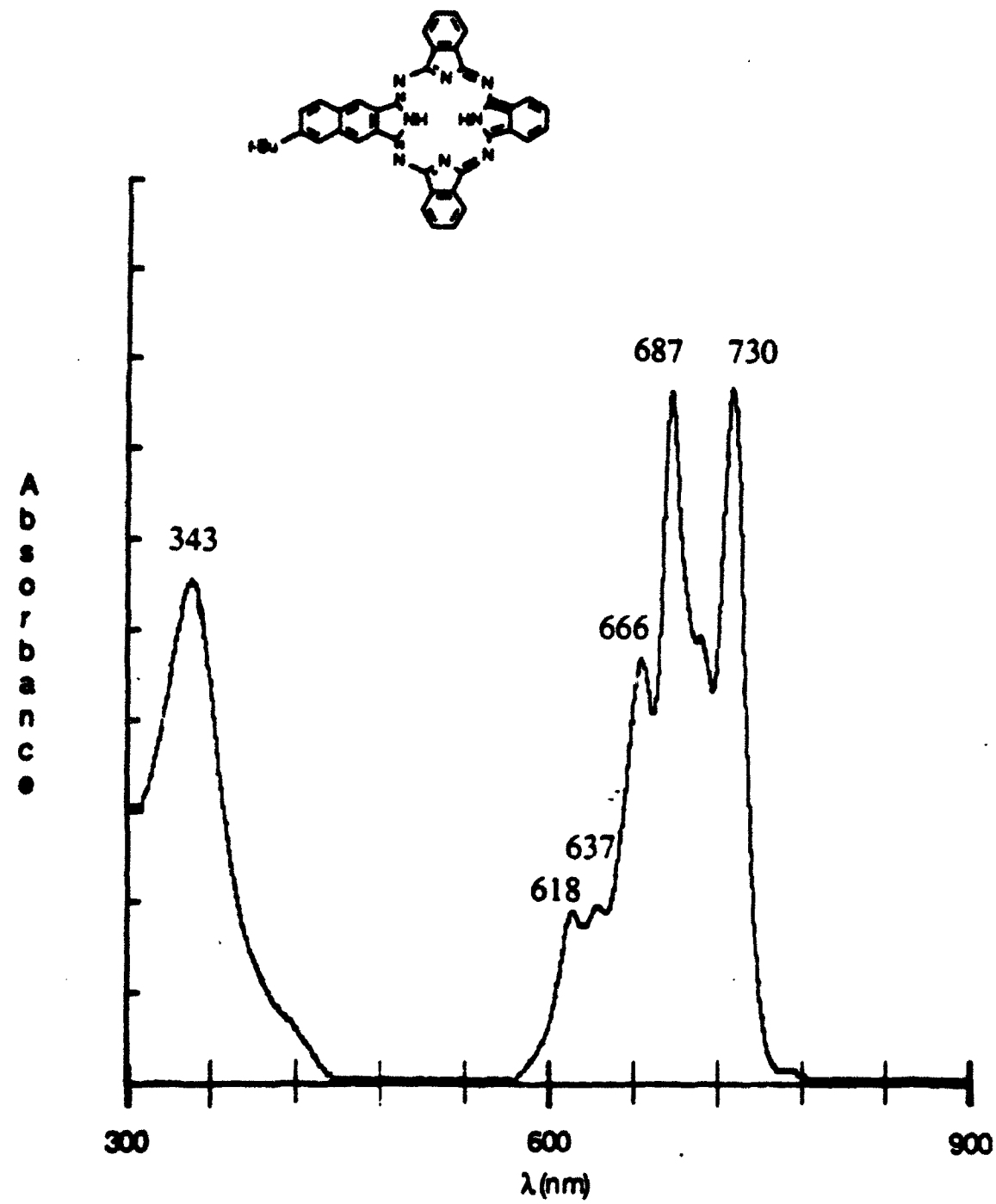

Figure 11. UV-Vis spectrum of compound 8 in 1,2-dichlorobenzene.

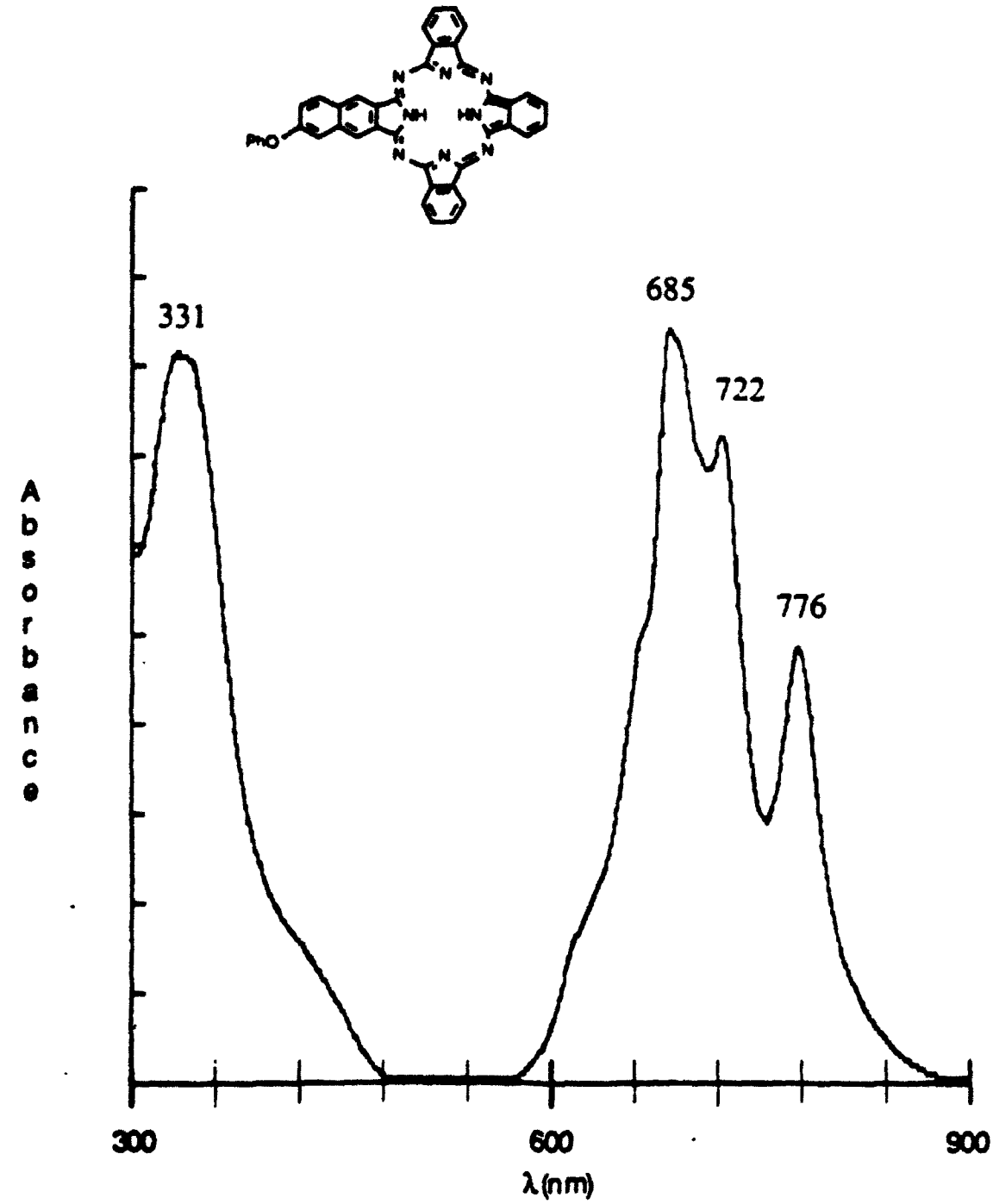

Figure 12. UV-Vis spectrum of compound **9** in 1,2-dichlorobenzene.

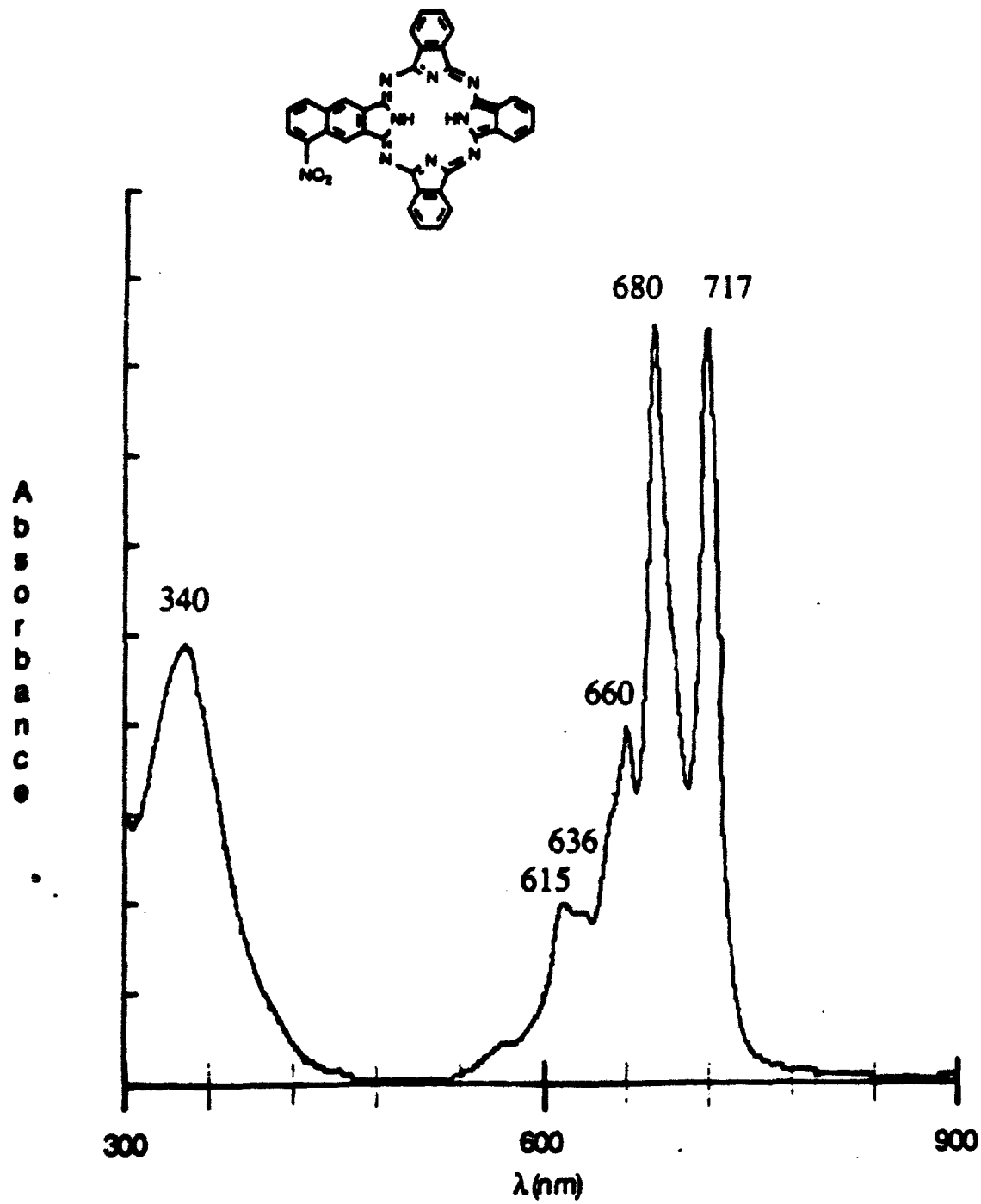

Figure 13. UV-Vis spectrum of compound **10** in 1,2-dichlorobenzene.

Synthesis of Fused-Ring Phthalocyanines by Ring Expansion. Work was also started on the use of BsubPc(*t*-Bu)$_3$Cl for the synthesis of a fused-ring phthalocyanine. The reaction initially tried is of the type illustrated by Sequence 8. The actual reaction is:

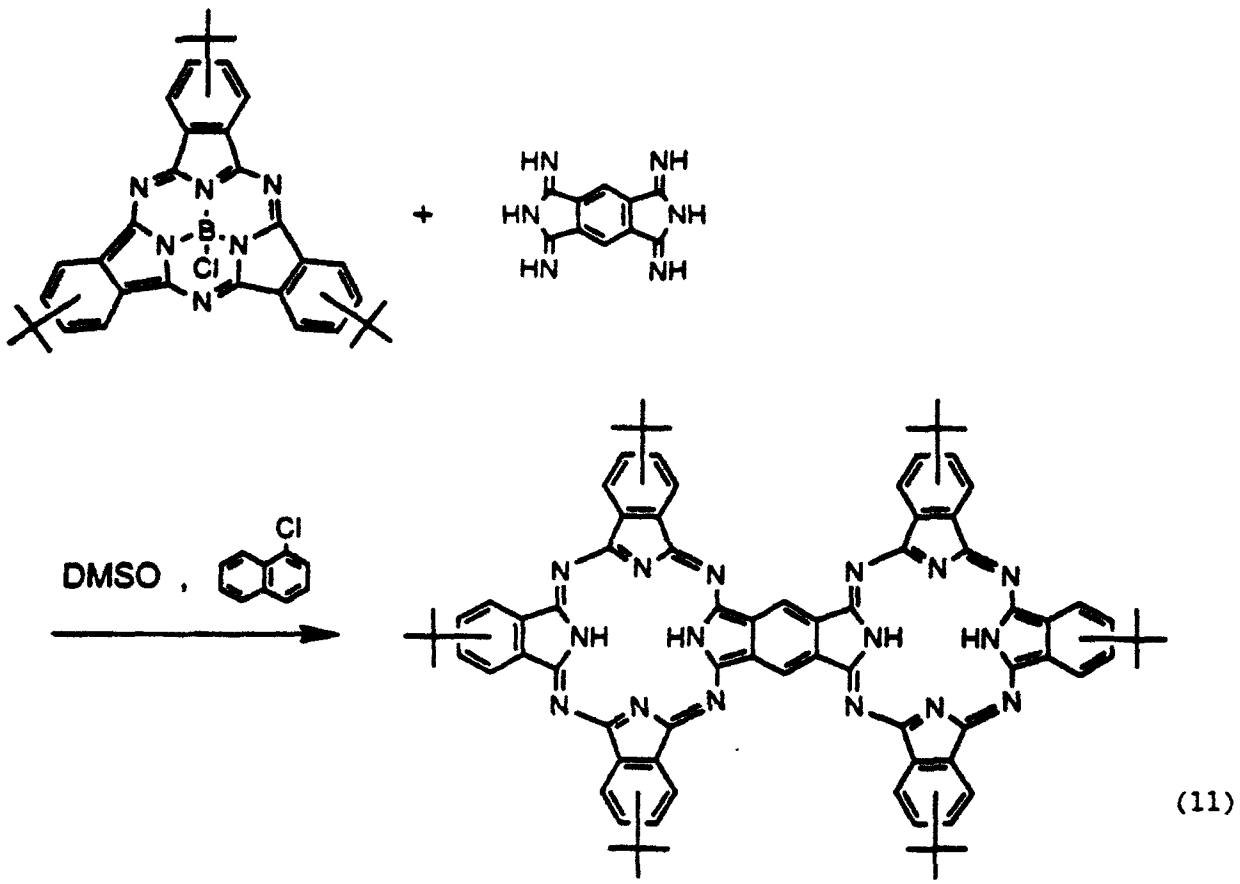

(11)

So far no fused-ring phthalocyanine has been obtained from this reaction.

The benzophthalocyanine with two bromo groups, compound 7 in Table I, is of particular interest because it opens the possibility of making a fused-ring phthalocyanine of a different type, that is, of the type shown in Figure 14.

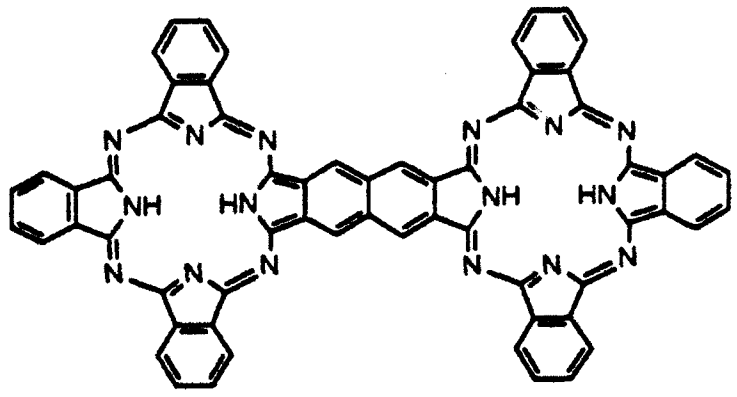

Figure 14. A fused-ring phthalocyanine with a naphtho bridge

Here the bridge between the two great rings is a naphtho group rather than a benzo group. The route opened is:

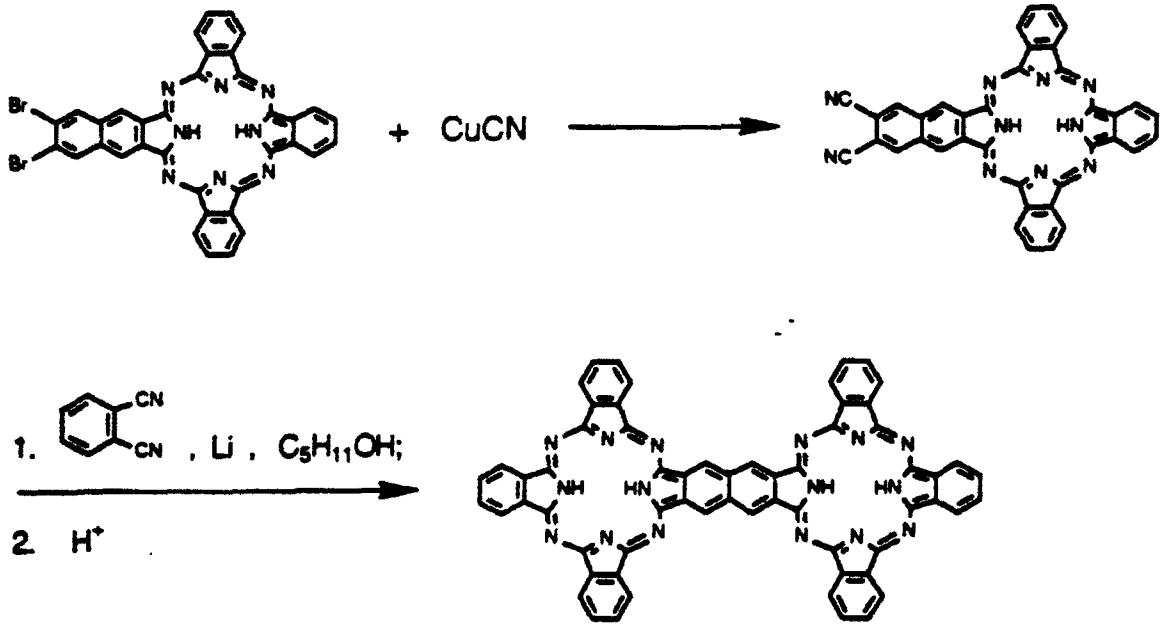

(12)

Synthesis of Metallated Polar Benzophthalocyanine. Finally, work on the metallation of two of the benzophthalocyanines was done. The mono-*t*-butylbenzophthalocyanine, compound 8 in Table I, was converted into its zinc analogue by the reaction

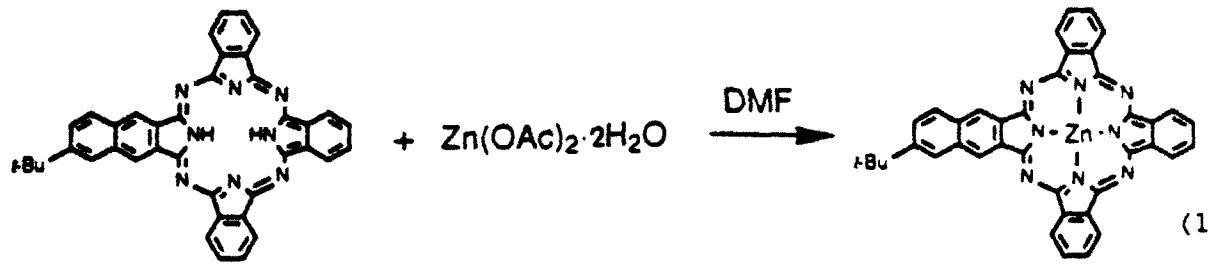

(13)

and the monochlorobenzophthalocyanine, compound 5 in Table I, was converted to its dichlorotin analogue by the reaction

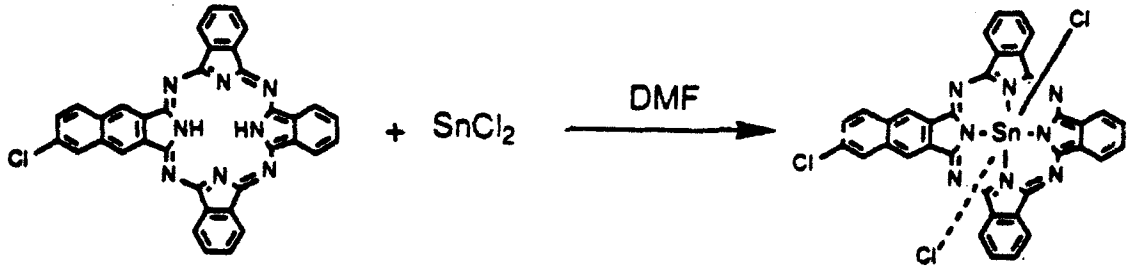

(14)

This work shows that metallated analogues of the macrocycles produced by ring expansion from subphthalocyanines can be prepared (as expected), and makes it clear that the properties of the rings in these macrocycles can be modulated by metal insertion and by axial ligand exchange when needed.

Summary. From the above it is apparent that the use of subphthalocyanines opens up practical routes to fused ring phthalocyanines that have the potential to have high $\chi^{(3)}$. In addition, it opens routes to polar phthalocyanines and benzophthalocyanines that have the potential to have high $\chi^{(2)}$.

PROPOSED WORK

Synthesis of Fused-Ring Phthalocyanines. In the coming period the synthesis of a fused-ring phthalocyanine will be vigorously pursued. In this work extensive use will be made of the knowledge developed in the past year. A series of routes will be investigated until one is found that

gives a fused-ring phthalocyanine.

The routes that will be evaluated include the sequence given above as Sequence 11, that is:

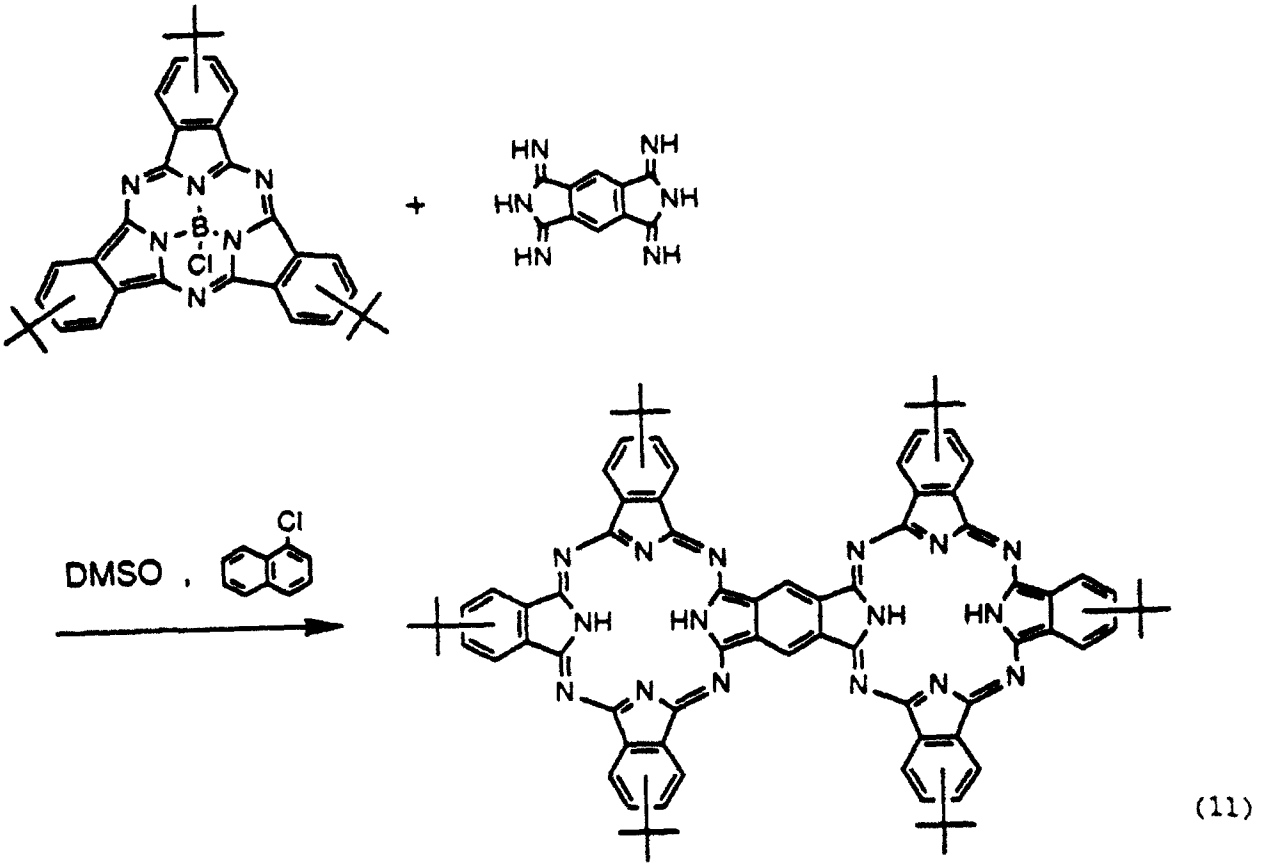

(11)

Also included is a sequence of the same type as Sequence 9.

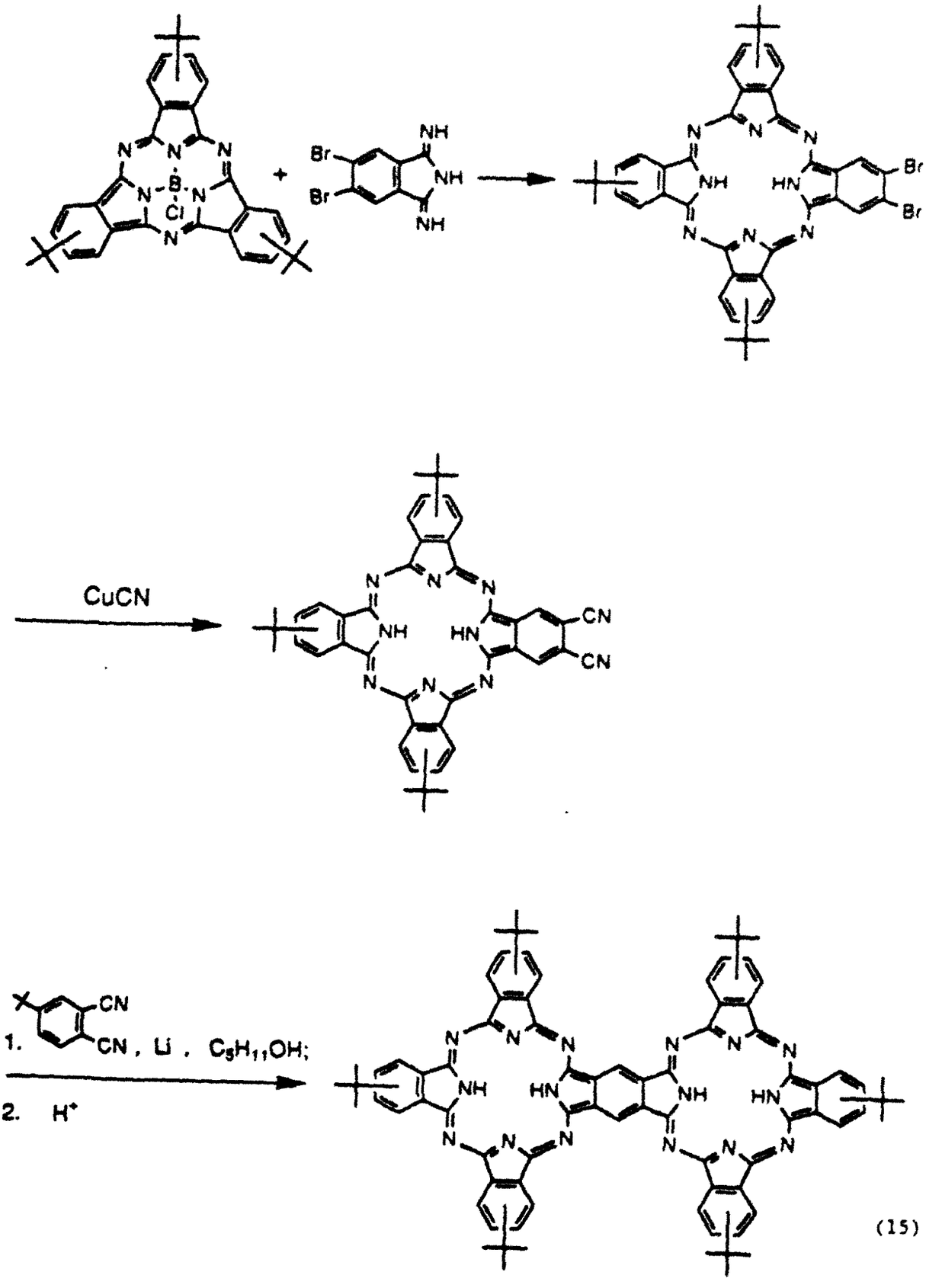

(15)

Sequence 11 will be studied first because it is shorter. However, if it

does not give the desired results, attention will be given to Sequence 15.

Since the work done on BsubPc(*t*-Bu)$_3$Cl has led to the preparation of 4-*t*-butylphthalonitrile, the possibility of using routes like parts of Sequence 5 or like Sequence 6 for making fused-ring phthalocyanines is now open. Routes of these types will also be included in the work directed to the synthesis of a fused-ring phthalocyanine. One that will be included is similar to part of Sequence 5.

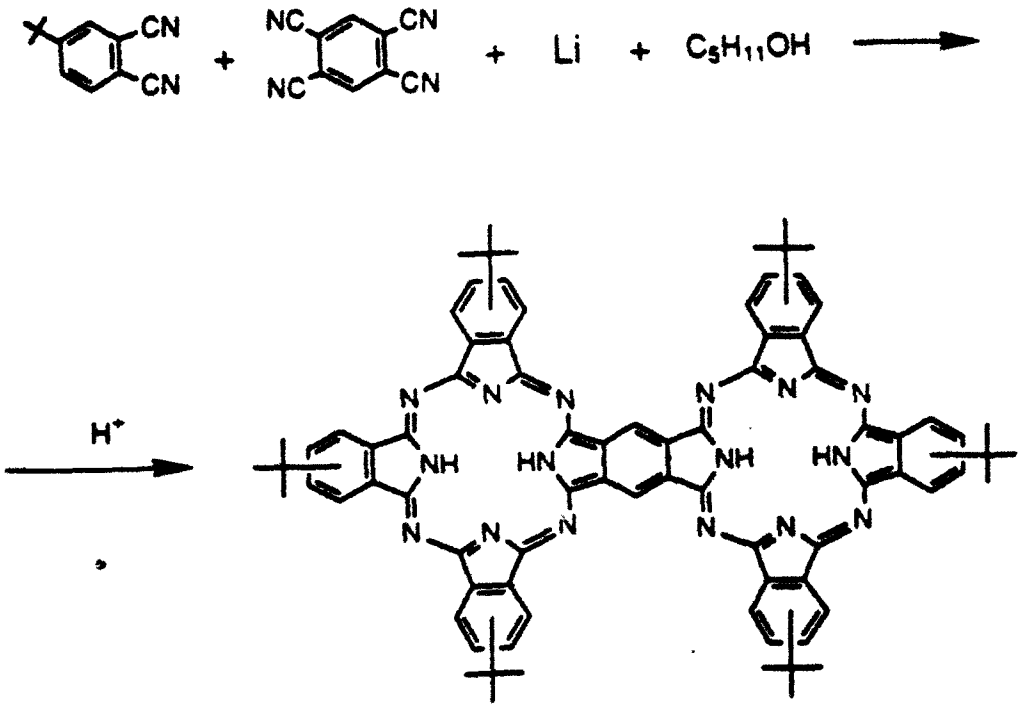

(16)

A second is similar except that $SnCl_2$ is used in place of Li.

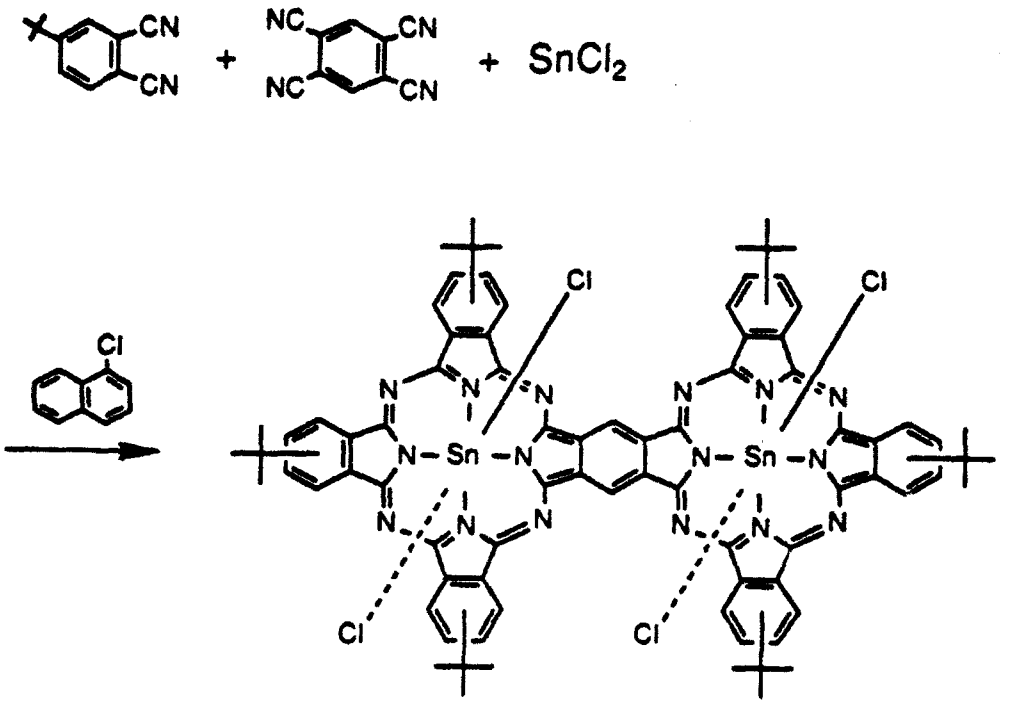

(17)

A third is like Sequence 6.

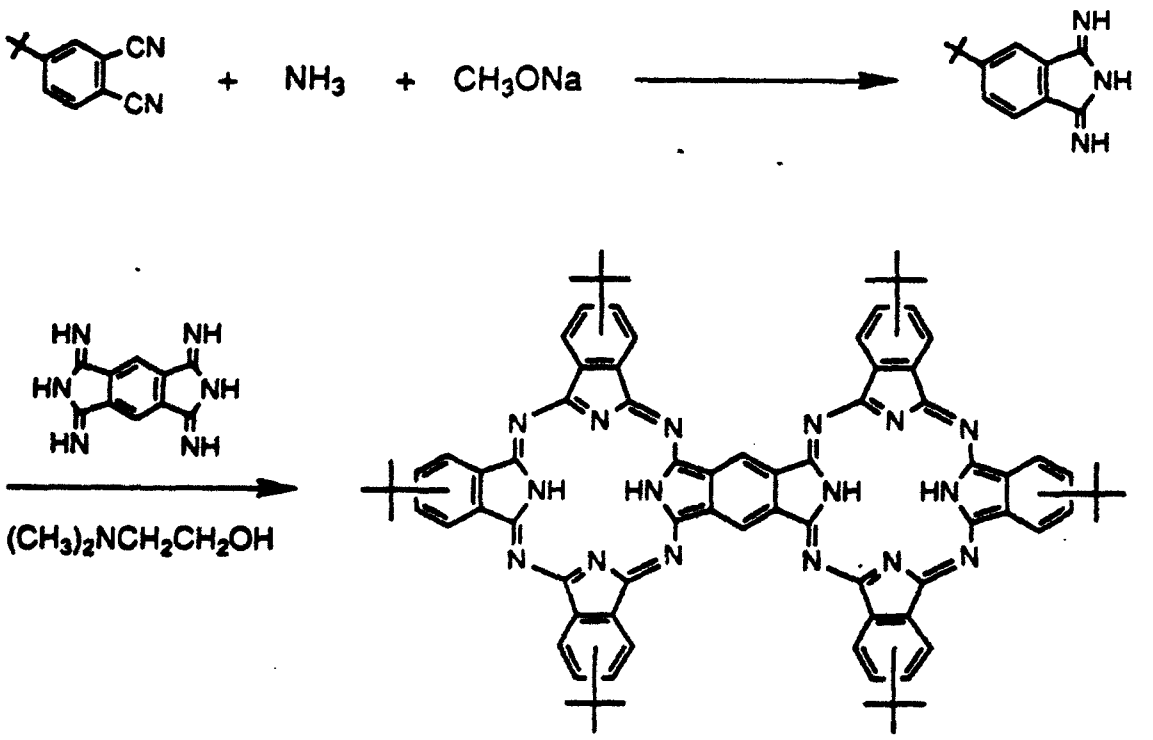

(18)

These sequences are attractive since they are simpler than the

subphthalocyanine sequences. Because of this at least some work will be done with them early in the year. Emphasis will be given to Sequences 16 and 17 first because they are shorter than Sequence 18.

Synthesis of Polar Phthalocyanines and Benzophthalocyanines. Work will also be done on the synthesis of polar phthalocyanines and benzophthalocyanines. Here for example the tri-*t*-butylnitrophthalocyanine shown in Figure 15 may be made.

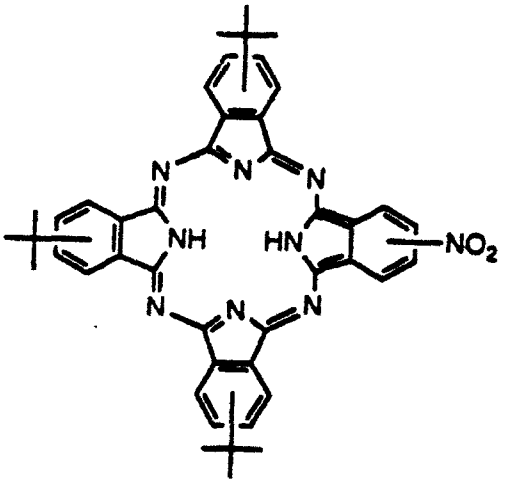

Figure 15. Tri-*t*-butylnitrophthalocyanine

The particular compounds to be made will be decided upon after detailed discussions with Hoechst Celanese personnel since a wide variety of compounds can be made and thus the particular needs of Hoechst Celanese personnel can be taken into immediate and detailed account.

Communication with Hoechst Celanese Personnel. In all the work to be done Hoechst Celanese personnel will be kept informed as to progress. Their advice as to which avenues of research should be emphasized will be actively sought. Supplies of the compounds made will be given to Hoechst Celanese personnel when requests are made. In general, an effort will be made to supply amounts in the half to one gram range initially. If larger amounts are needed later, efforts will be made to supply them.

EXPERIMENTAL

BsubPcCl. A slurry of phthalonitrile (1.01 g) and 1-chloronaphthalene (2.5 mL) was stirred under Ar for 20 min. A solution of BCl_3 in heptane (1M, 4.8 mL) was added to this slurry and the heptane was distilled off. The remainder was heated to 150-180° for 1 h, refluxed for 10 min, cooled, and filtered. The solid was washed with heptane and air dried (0.87 g, 78%).

A portion of the product was sublimed (0.1 torr, 280°, 2 h): UV-Vis (1,2-dichlorobenzene) λ_{max} 567 mm (lit. 565 nm); IR (Nujol) 952 (s, B-Cl) cm^{-1} (lit 950 cm^{-1}). MS-HR exact mass *m/z* calcd for $C_{24}H_{12}N_6BCl$ $(M)^+$: 430.0905. Found 430.0932.

The compound is bronze colored. Thin films of it are purple by transmitted light. The compound is moderately soluble in hot 1-chloronaphthalene. The unsublimed compound is satisfactory for use as a synthetic intermediate.

BsubPc(*t*-Bu)$_3$Cl. A solution of 4-*t*-butylphthalonitrile[9] (1.01 g) and 1-chloronaphthalene (2.5 mL) was stirred under Ar for 30 min. A solution of BCl_3 in heptane was added to the solution and the heptane was distilled off. The resultant was heated at 150-180° for 1 hr, refluxed for 10 min, cooled and evaporated to dryness (1 torr, 140°, 2 h) (1.98 g).

A portion of the product was subjected to gel permeation chromatography (S-X4 Bio-Beads, 4.5 x 50 cm, toluene) and vacuum dried (60 torr, 70°, 1 h): UV-Vis (toluene) λ_{max} 569 nm; NMR (200 MHz, $CDCl_3$) δ 8.91 (d, Ar); 8.81 (dd, Ar), 8.01 (dd, Ar), 1.55 (d, *t*-Bu).

The compound is a bronze colored solid. Thin films and solutions of it are purple by transmitted light. The compound is soluble in $CHCl_3$, toluene, acetone, and hexane.

Representative Synthesis of a Benzophthalocyanine, Synthesis of Compound 8. A slurry of 6-*t*-butyl-1,3-diiminobenz(*f*)isoindoline (127 mg),

BsubPcCl (52 mg), 1-chloronaphthalene (3 mL) and Me_2SO (3 mL) was stirred under Ar for 23 h while being held at 80°-90°. The resultant was vaccum concentrated (0.1 torr, 70°, ~3 mL), diluted with MeOH (40 mL) and filtered. The solid was washed with MeOH and vaccum dried (60 torr, 70°, 1 h) (12 mg, 16%): UV-Vis (1,2-dichlorobenzene) λ_{max} 730 nm.

The compound is blue-green. Thin films and solutions of it are green by transmitted light. The compound is sparingly soluble in $CHCl_3$, 1,2-dichlorobenzene, and 1-chloronaphthalene.

REFERENCES

1. Wu, J. W.; Heflin, J. R.; Norwood, R. A.; Wong, K. Y.; Zamani-Khamiri, O.; Garito, A. F.; Kalyanaraman, P.; Sounik, J. *J. Opt. Soc. Am.* **1989**, *B6*, 707.
2. Gosmann, M.; Franck, B. *Angew. Chem. Int. Ed. Engl.* **1986**, *25*, 1100.
3. Knübel, G.; Franck, B. *Angew. Chem. Int. Ed. Engl.* **1988**, *27*, 1170.
4. Schermann, G.; Schmidt, R.; Völcker, A.; Brauer, H.-D.; Mertes, H.; Franck, B. *Photochem. Photobiol.* **1990**, *52*, 741.
5. Leznoff, C. C.; Lam, H.; Marcuccio, S. M.; Nevin, W. A.; Janda, P.; Kobayashi, N.; Lever, A. B. P. *J. Chem. Soc., Chem. Commun.* **1987**, 699.
6. Kobayashi, N.; Kondo, R.; Nakajima, S.; Osa, T. *J. Am. Chem. Soc.* **1990**, *112*, 9640.
7. Miller, A.; Ossko, A. *Monatsh. Chem.* **1972**, *103*, 150.
8. Kietaibl, H. *Monatsh. Chem.* **1974**, *105*, 405.
9. Hanack, M.; Metz, J.; Pawlowski, G. *Chem. Ber.* **1982**, *115*, 2836.

DEVELOPMENT OF NON-LINEAR OPTICAL MATERIALS

Subcontract Agreement

CWRU-91-HCC-001

M. E. Kenney and V. O. Kennedy

Case Western Reserve University

Cleveland, OH 44106-7078

(216) 368-3739

Final Report

Reporting Period

12-1-91 to 7-31-92

Abstract

Work on the synthesis of materials for use in $\chi^{(2)}$ and $\chi^{(3)}$ studies is described. Attempts directed towards the synthesis of a fused-ring tetrabenzoporphyrin are outlined. In addition, work yielding several boron subphthalocyanines and a phthalocyanine with both donor and acceptor groups is described.

In this study, work directed towards the synthesis of compounds for use as $\chi^{(2)}$ and $\chi^{(3)}$ materials was carried out.

Fused-Ring Tetrabenzoporphyrins. The work on the $\chi^{(3)}$ materials was focused on the synthesis of a fused-ring tetrabenzoporphyrin of the type shown in Figure 1. This work was a continuation of earlier work in which attempts were made to make a fused-ring phthalocyanine of the type shown in Figure 2.

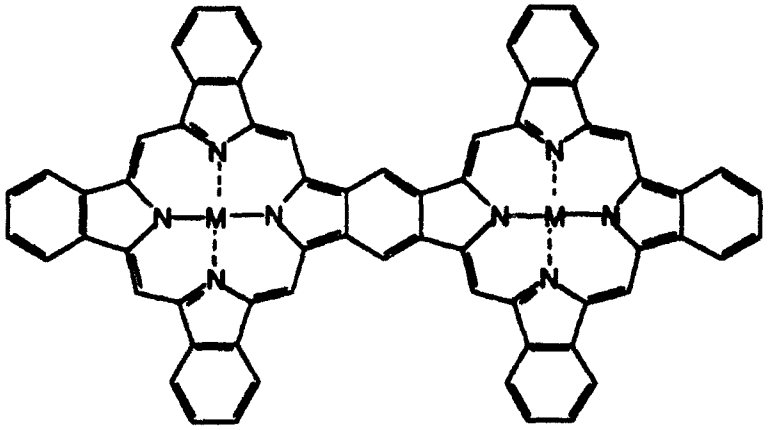

Figure 1. A fused-ring tetrabenzoporphyrin.

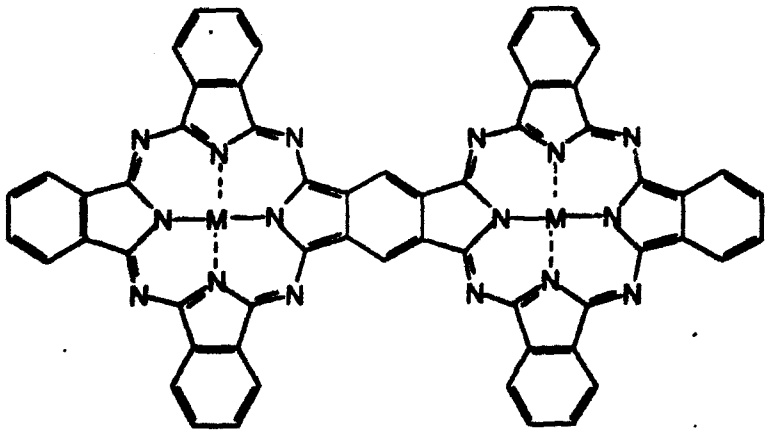

Figure 2. A fused-ring phthalocyanine.

A recent report of Kobayashi's[1] on the synthesis of a fused-ring tetrabenzoporphyrin formed the basis of the work carried out on fused-ring tetrabenzoporphyrins. In this work, attention was first devoted to the synthesis of the model compound zinc tetrabenzoporphyrin, ZnTBP, Figure 3. This compound was synthesized according to the procedure of Luk'yanets.[2,3] The equation for this synthesis is:

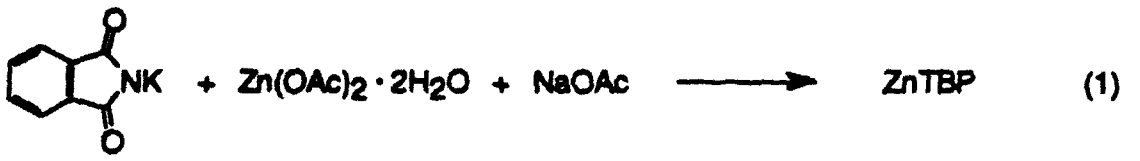

The product obtained was purified by adsorption chromatography. It was shown to be the desired compound by UV-Vis spectroscopy.

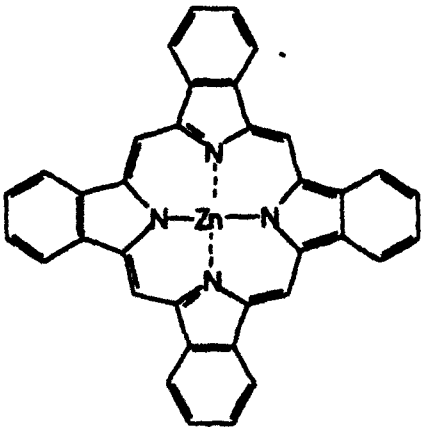

Figure 3. Zinc tetrabenzoporphyrin, ZnTBP.

After this compound had been made, attention was given to the synthesis of zinc fused-ring tetrabenzoporphyrin, Zn_2FRTBP, Figure 4. The route tried was parallel to that of Kobayashi.[1]

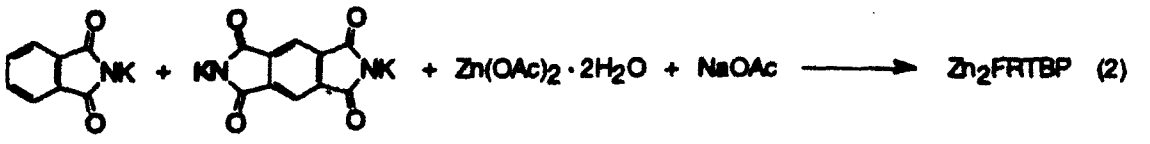

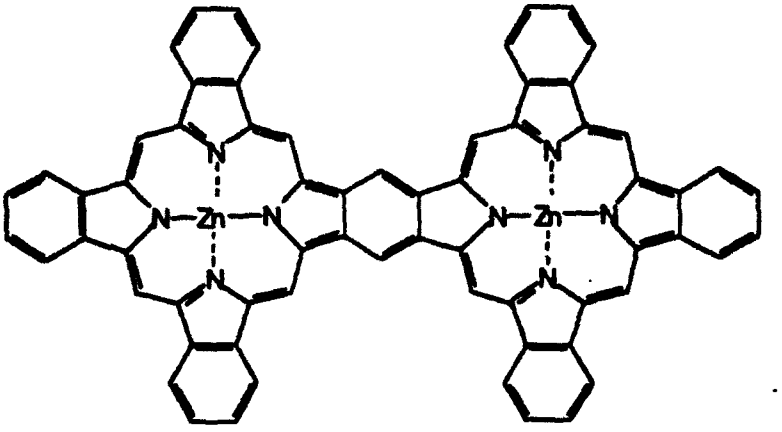

Figure 4. Zinc Fused-Ring Tetrabenzoporphyrin, Zn_2FRTBP.

The product obtained was separated into fractions by adsorption chromatography. ZnTBP was found in several of these fractions, but no Zn_2FRTBP was detected. At this point, work on fused-ring compounds was stopped.

Boron Subphthalocyanines. The work on $\chi^{(2)}$ materials was focused on the synthesis of phthalocyanines with both donor, D, and acceptor, A, groups, i.e., on "push-pull" phthalocyanines. The route chosen for the synthesis of these compounds involved the expansion of the ring of a substituted boron subphthalocyanine, $BsubPcR_3X$, with a substituted diiminoisoindoline,[4]

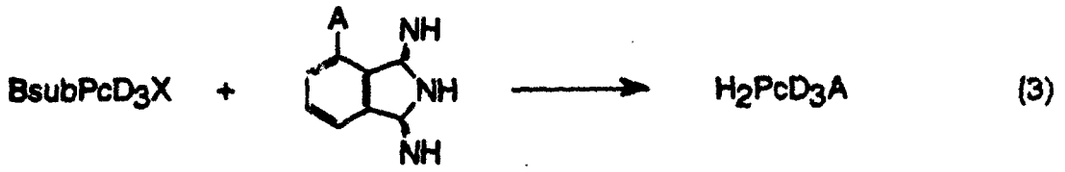

As a part of this effort, work was done on the synthesis and characterization of a series of boron subphthalocyanines. For the synthesis of these compounds, BsubPcCl was used as the starting material. This latter compound, Figure 5, is a known compound.[5,6]

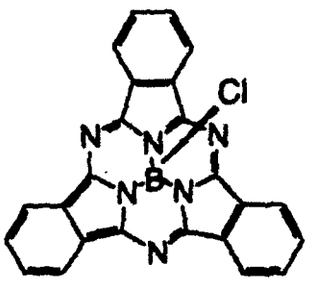

Figure 5. Chloroboron Subphthalocyanine, BsubPcCl.

The compounds made were BsubPcisoBu, BsubPcN(isoPr)$_2$, BsubPcOMe, BsubPcOEt, and BsubPcOSi(n-C_6H_{13})$_3$. For the synthesis of these compounds, the routes used were:

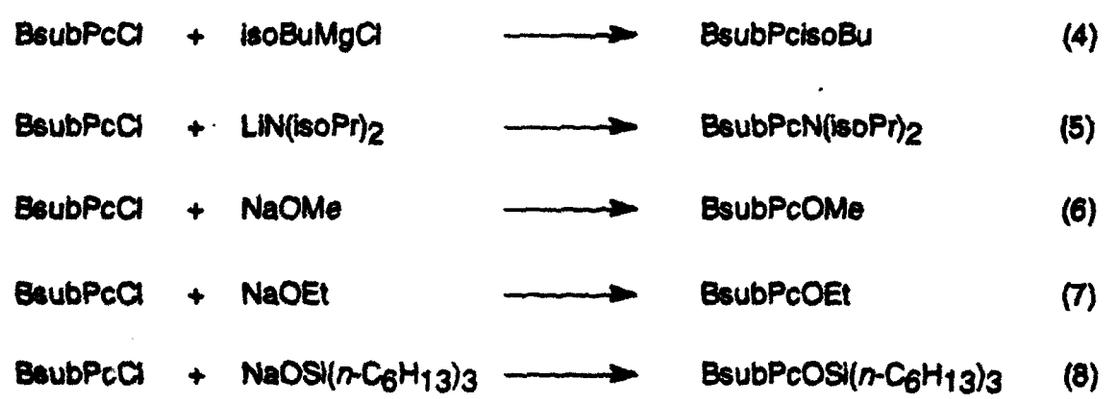

These compounds were purified by adsorption or gel permeation chromatography. Their composition was verified by high resolution mass spectroscopy.

These compounds were soluble in ordinary solvents such as toluene and were thus unlike BsubPcCl. The compounds gave the expected NMR resonances.

Push-Pull Phthalocyanines. Another part of the work on $\chi^{(2)}$ materials was aimed directly at the synthesis of a push-pull phthalocyanine. The compound chosen for this study was trifluoromethyltris-*t*-butylphthalocyanine, H_2TTPc, Figure 6. The route selected for this compound is shown in Scheme 1.

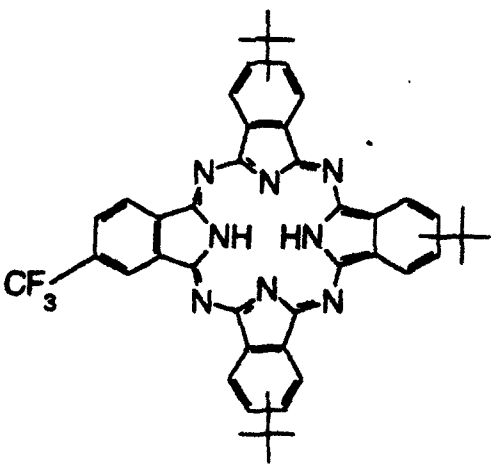

Figure 6. Trifluoromethyltris-*t*-butylphthalocyanine, H_2TTPc.

The 1,2-dimethyl-4-trifluoromethylbenzene, 1 needed for this synthesis was purchased (Lancaster). With it as a starting point, compounds 2 to 7 were made. The composition of each was verified by matching physical constants.[7] The BsubPc(*t*-Bu)$_3$Cl needed for the final step of the synthesis was made by a

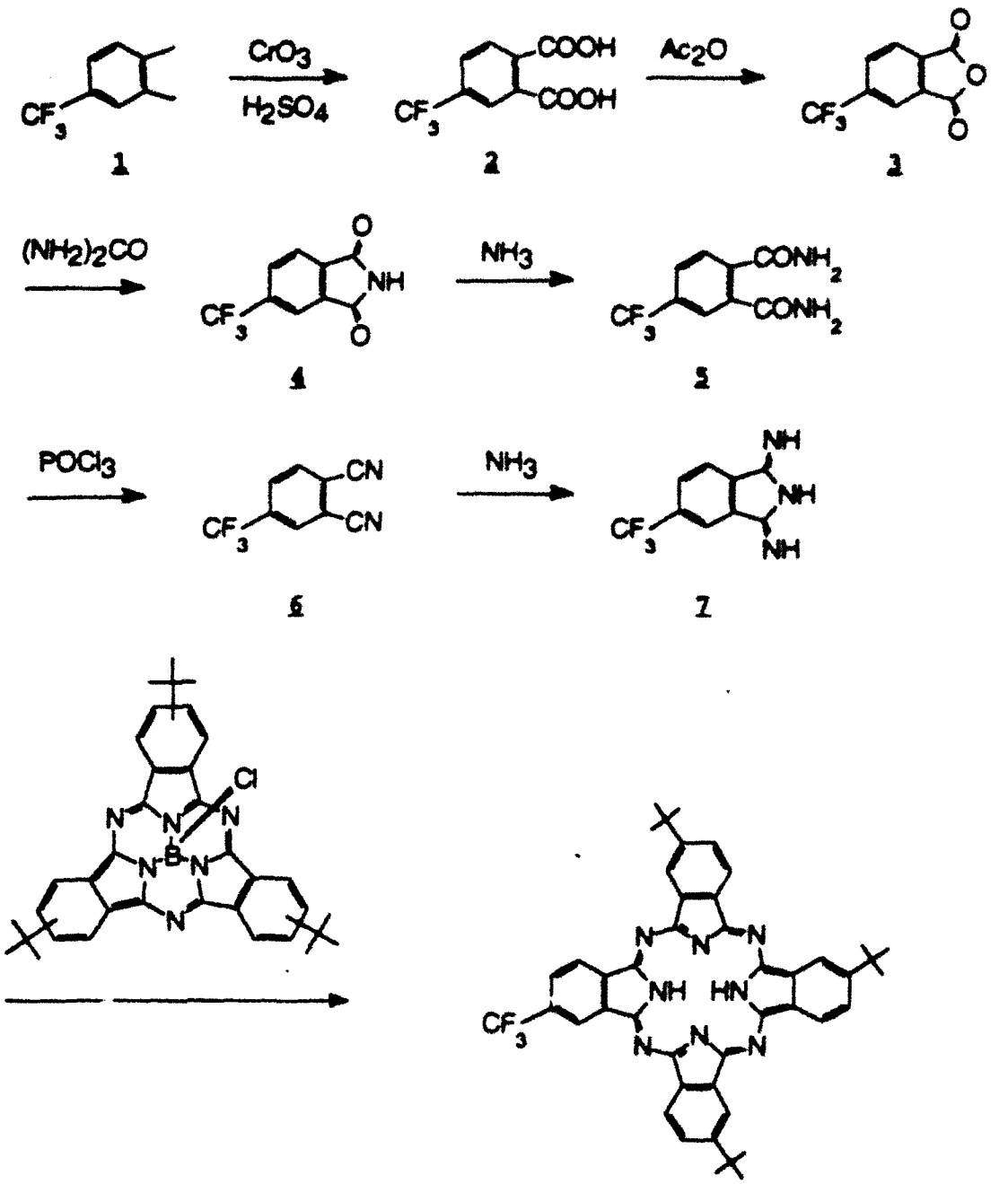

1 2 3 4 5 6 7 8

Scheme 1. Route chosen for synthesis of H_2TTPc.

procedure similar to that used by Meller and Ossko for BsubPcCl.[5] The yield of this step was low, but useful amounts of H_2TTPc were obtained. The H_2TTPc was purified by adsorption and column chromatography. Its composition was verified by mass spectroscopy. The compound showed a very complex NMR spectrum. This is attributable to the fact that the compound was an isomer mixture. The zinc compound was made from the H_2TTPc. This also gave a complex NMR spectrum.

References

1. Kobayashi, N.; Numao, M.; Kondo, R.; Nakajma, S.-i.; Osa, T. *Inorg. Chem.* **1991**, *30*, 2241-2244.
2. Kopraneenkov, V. N.; Makarova, E. A.; Luk'yanets, E. A. *J. Gen. Chem. (Engl. Transl.)* **1981**, *51*, 2353-2356.
3. Kopraneenkov, V. N.; Dashkevich, S. N.; Luk'yanets, E. A. *J. Gen. Chem. (Engl. Transl.)* **1981**, *51*, 2165-2168.
4. Kobayashi, N.; Kondo, R.; Nakajma, S.-i.; Osa, T. *J. Am. Chem. Soc.* **1990**, *112*, 9640-9641.
5. Meller, A.; Ossko, A. *Monatsh. Chem.* **1972**, *103*, 150-155.
6. Kietaibl, H. *Monatsh. Chem.* **1974**, *105*, 405-418.
7. Pawlowski, G.; Hanack, M. *Syn. Commun.* **1981**, *11*, 351-363.

Polymer Optical Fibers for Nonlinear Optics

Progress Report

Mark G. Kuzyk

Department of Physics, Washington State University, Pullman, WA 99164-2814

November 26, 1991

Contents

1 Project Summary

The purpose of the nonlinear optical polymer fiber project was to study the possibility of incorporating Hoechst-Celanese dye chromophores into the core of single-mode-dimensioned polymer optical fiber: a geometry that is well suited for a large variety of waveguiding devices. In particular, we have incorporated a PMMA copolymer of the monoacrylate material (notebook entry #37554-18C) in a fiber core. We report here on the methods and processing conditions used to make such fibers and the properties of the finished product. Enclosed with this report is a spool of fiber[*] and a variety of exhibits that represent various stages of the fiber-making process. Details are given in the text.

This summer project involved two students, Scott Townsend and Kurt Zimmerman, who are in the masters degree program in the Department of Physics. The work done at Washington State University was in close collaboration with Dr. Robert Norwood and Dr. Jim Sounik of Hoechst-Celanese.

2 Introduction

We have developed a fiber-drawing apparatus that is schematically outlined in Figure 1. In the drawing process, the preform is fed into an oven to soften the material which is subsequently pulled into a fiber. The preform is a solid rod of polymer with a dye-incorporated core region. In the drawing process, the preform diameter contracts leaving the core to cladding diameter ratio unchanged. Details of this process are described in one of our recent publications.[1]

The chromophores in the core define a waveguiding region of elevated refractive index and of high nonlinear-optical susceptibility, thus confining the high-intensity light to the region of high nonlinearity. Figure 2 shows a schematic representation of the fiber. Because the efficiencies of all nonlinear-optical processes depend on the intensity of light and the distance over which the light

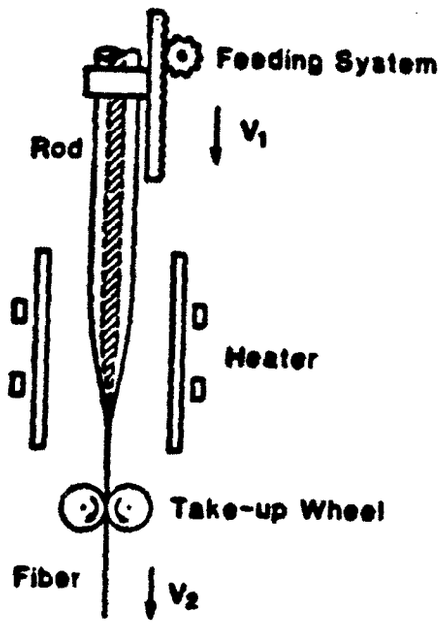

Figure 1: A schematic representation of the fiber drawing apparatus.

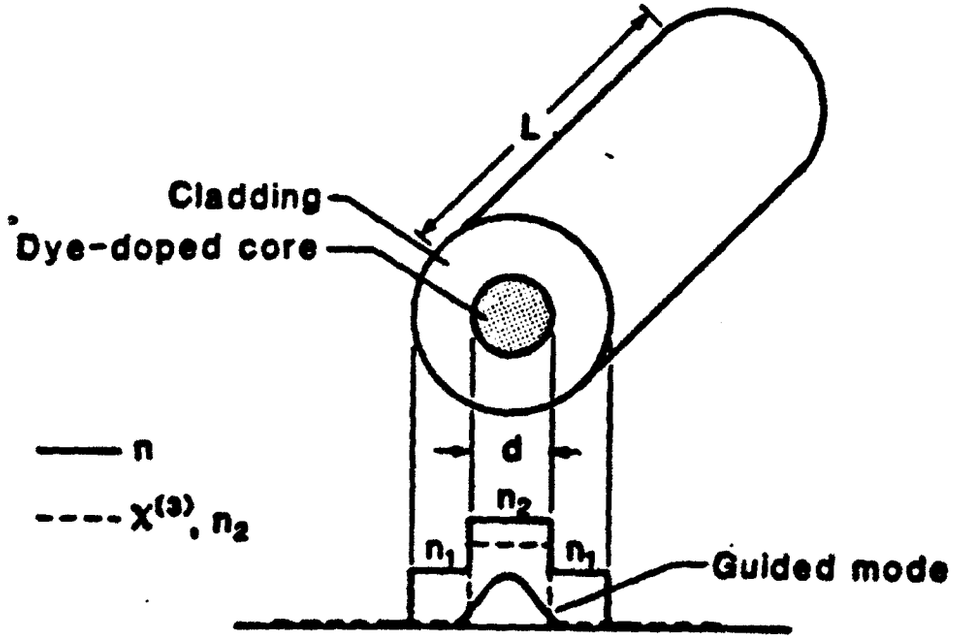

Figure 2: The cross-section of a polymer fiber.

propagates, optical fibers ideally suit the high-efficiency criteria by confining high light intensities to a small core over a long distance. In the sections that follow, we outline parts of the drawing apparatus that were developed for making Hoechst-Celanese fibers, methods for making preforms and properties of the final fibers.

3 Oven

The oven is an important part of the drawing process. The temperature distribution must be kept fixed during the whole drawing procedure. We have designed and built a glass oven chamber (for easy sample monitoring) with a resistive-wire coil heating element that is wound around the inner wall (See figure 3). The air space between the inner and outer chamber acts as an insulation layer. The air temperature inside the drawing region is stabilized by pulling a low rate of air-flow through the heat vent.

The oven temperature profile has been optimized to draw PMMA fiber by adjusting the coil spacing and voltage across the coil. We have measured both the air and preform temperature at the ideal drawing conditions as a function of vertical position down the middle of the central chamber. The top portion of Figure 4 shows the measured temperature profile and the bottom portion shows the corresponding position within the oven. The air temperature was measured by translating a thermistor probe down the shaft. The preform temperature was measured by physically imbedding the temperature probe into a preform, then, drawing the fiber. As the preform is fed into the oven, the probe moves down through the oven chamber until it reaches the neck down region, at which time the drawing process must be stopped to retrieve the thermistor.

Note that the air temperature rises up the oven shaft while the preform temperature peaks at the position of highest coil winding density. This is direct evidence that the dominant heating mechanism is that of radiative infrared heating as opposed to convective air heating. The fact

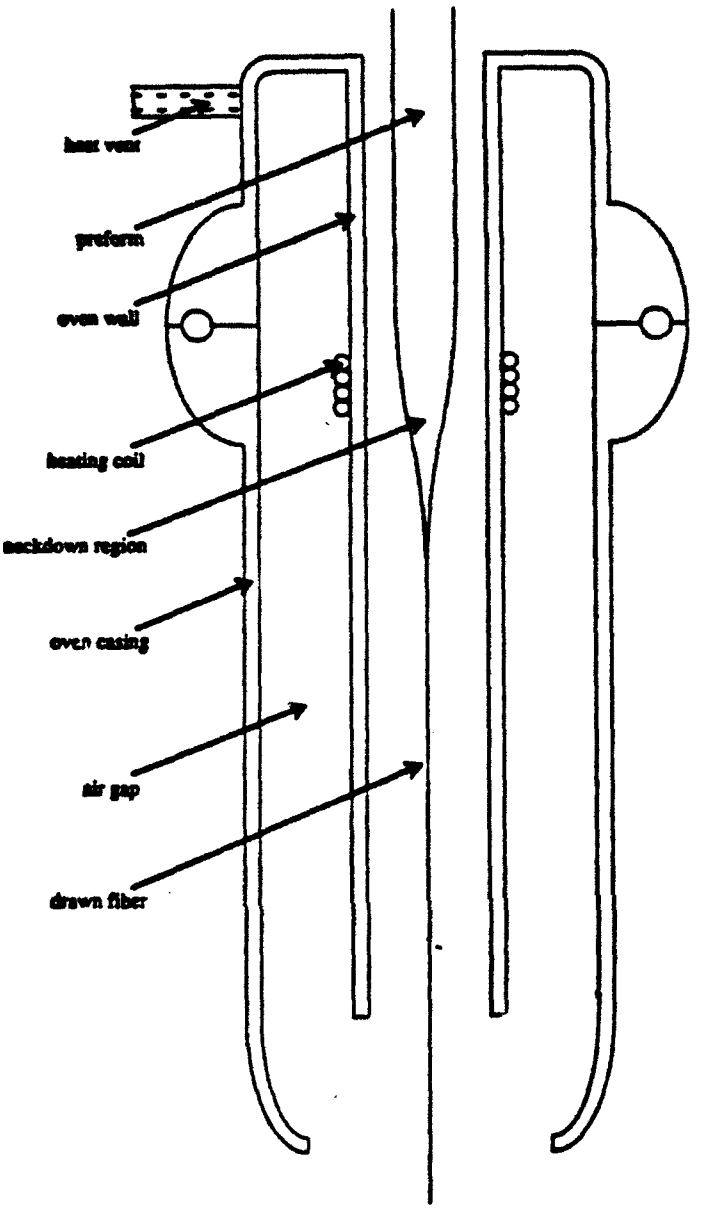

Figure 3: A cross-sectional view of the Oven.

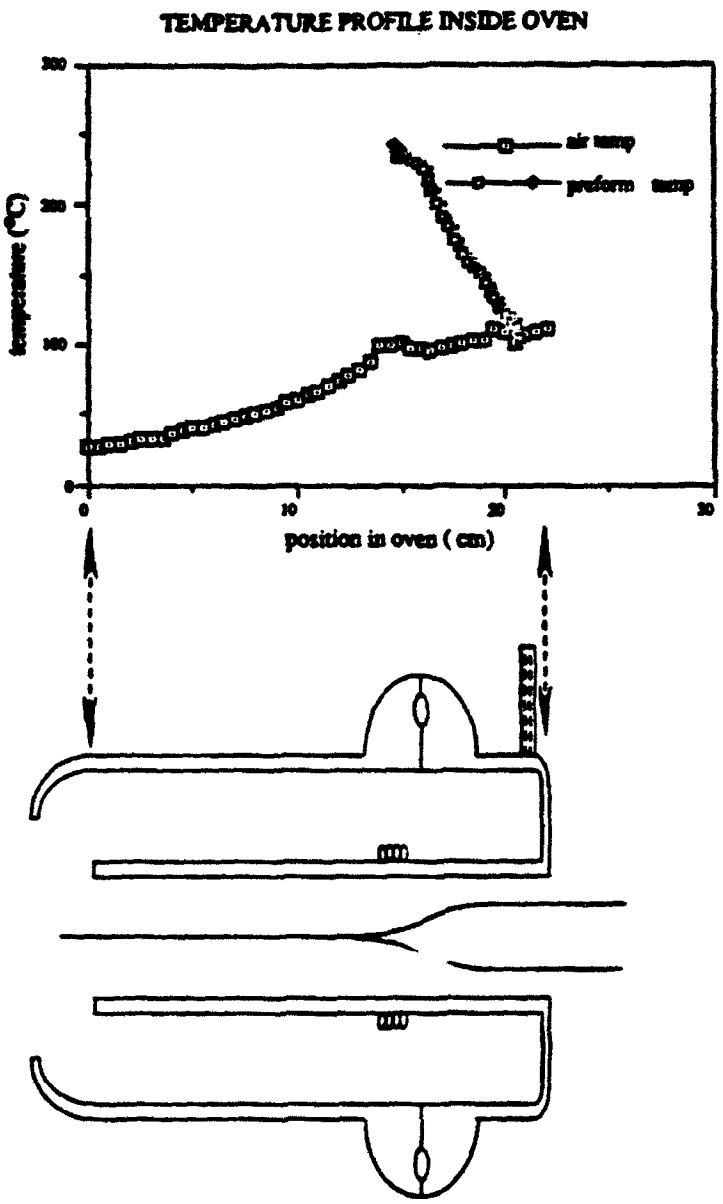

Figure 4: The vertical oven temperature profile.

that the neck-down region coincides with the point of highest coil density further strengthens this conclusion.

4 Draw Speed

The diameter of the fiber is determined from the feed velocity of the preform into the oven and the fiber drawing velocity. Because of mass conservation, the ratio of these two speeds is related to the ratio of the preform and fiber diameter:

$$d = D\left(\frac{V}{v}\right)^{1/2} \tag{1}$$

where v and d are the fiber velocity and diameter and V and D the preform feed velocity and diameter. It is also interesting to calculate the length of fiber, l, that can be drawn from a preform of length L:

$$l = \frac{D^2}{d^2}L. \tag{2}$$

Because the fiber diameter is much smaller than the preform diameter, it is typical for a $10cm$ preform to draw into a $1km$ fiber.

Figure 5 shows the measured fiber diameter as a function of draw speed ratio. The solid theoretical curve is calculated from Equation 1 with no adjustable parameters. The dashed curve through the data is fit with the preform diameter as the adjustable parameter. The inset shows the fiber diameter at low feed rate. Note that the data point for a very large fiber diameter is consistent with theory. With such calibration, we have found that we can produce a wide range of fiber diameters on demand. Figure 6 shows the reproducibility in fiber diameter over three separate runs that span a wide range of drawing speeds. Note that the scatter in the data is less than 5% of the mean.

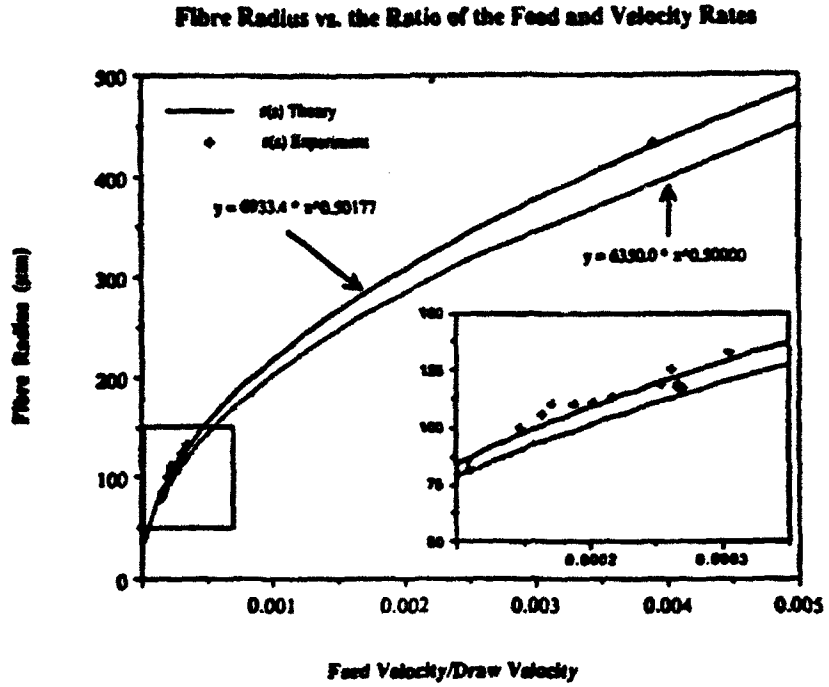

Figure 5: Fiber diameter dependence on draw/feed speed ratio. The diameter was measured with a micrometer after drawing.

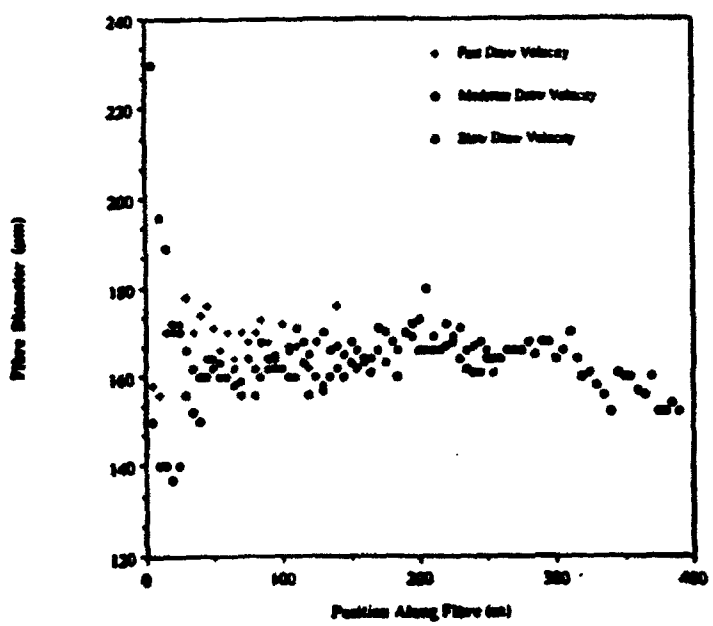

Figure 6: Reproducibility of fiber diameter with draw speed. The diameter was measured with a micrometer after drawing.

5 Fiber Draw Monitoring System

To make fiber of uniform quality over long lengths, it is important to monitor the drawing conditions. We are in the process of installing a laser-assisted optical diameter gauge and have already installed a fiber tension gauge. Calibrations of the tension with draw conditions are in progress. Because the preform temperature can not be directly monitored in the oven (for reasons described in 'Oven' section), the fiber thickness and tension monitor will be used to actively readjust the draw speeds and oven temperature to compensate for fluctuations. For short segments of fiber (tens of meters), the fiber diameters have been observed to be uniform. Fibers made to date were produced without monitoring.

Figure 7. shows the complete fiber drawing tower.

6 Preform Fabrication

The end quality of the polymer fiber is strongly dependent on the quality of the preform. Bubbles that are trapped in the preform, for example, will draw into long hollow regions. If such bubbles are trapped in the core, waveguiding may not be possible. For this reason, we have developed several methods of preform fabrication that have been specifically targeted at Hoechst-Celanese materials. In general, the preform fabrication process falls into two broad steps: cladding and core processing. The three procedures that we have developed are summarized below.

6.1 Core Injection

A solid cylindrical rod of PMMA is cut in half along the fiber axis and a semicircular grove is machined along the axis of both half-cylinders. The two halves are then bonded together with monomer and clamped together in a cylindrical fixture at elevated temperature. A wire, whose diameter matches the hole diameter, is used to both align the half-sections and to prevent

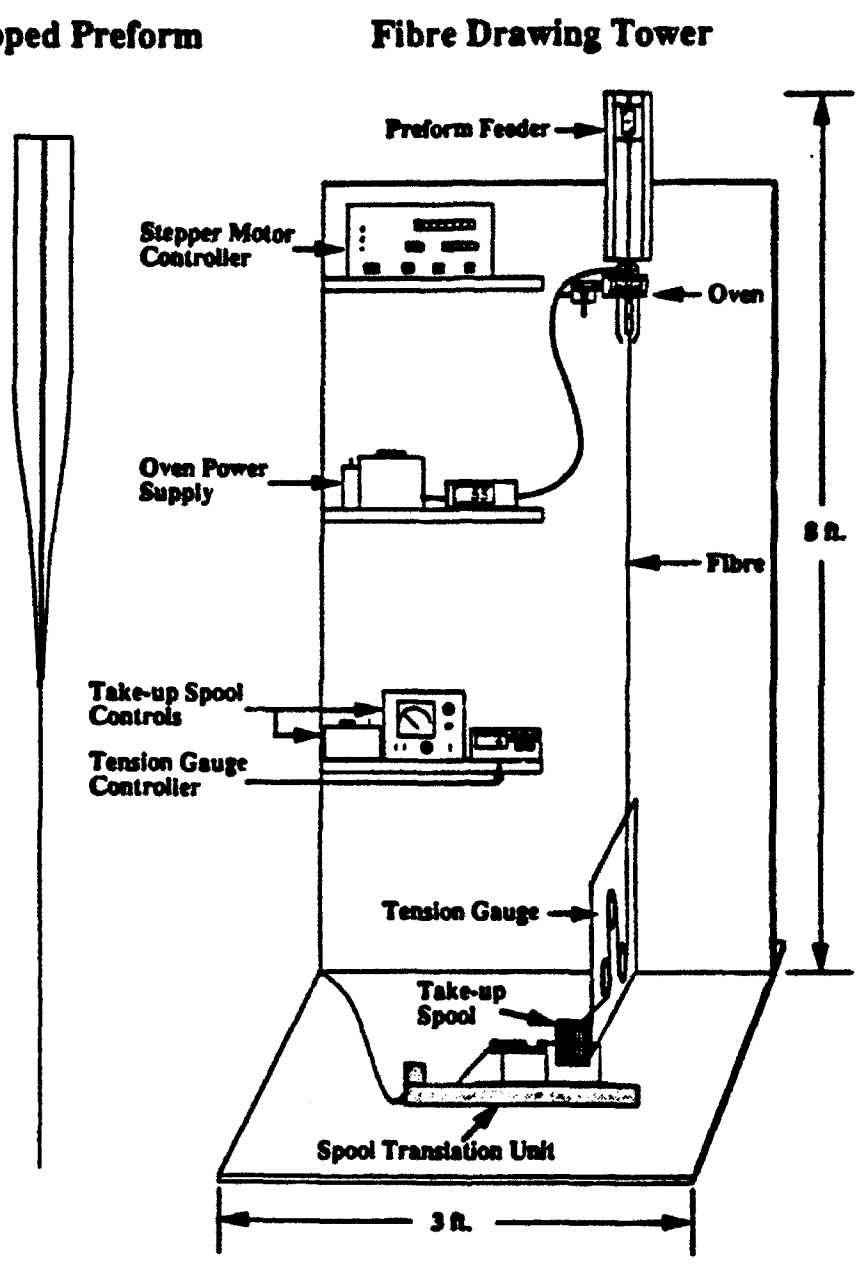

Figure 7: Fiber drawing tower.

monomer from leaking into the hole during the polymerization process. Exhibit A is a set of half-sections, Exhibit B the milled half sections, and Exhibit C the two bonded half sections. This seemingly complex process for 'drilling a hole' in the preform is necessary to prevent crazing and chipping that accompanies standard drilling. Furthermore, no drill bit is capable of making such a small diameter hole over such a long length.

Next, one end of the preform is sealed with epoxy. A liquid mixture of monomer, chromophore and initiator is inserted into the core with a microsyringe. After sealing the open end, the preform core is polymerized at elevated temperature in a cylindrical clamp to keep the preform from deforming. Exhibit D is a finished preform section and Exhibit E a thin polished section of a preform. The preform is then drawn into a fiber. Exhibit E is a cross-sectional piece of the remains of the neck-down region of a spent preform.

6.2 Capillary Filling

In the capillary method, the cladding region is prepared as in the previous subsection. The core, however, is formed separately and inserted into the hole of the solid preform as follows. A hollow preform is drawn in the tower to form a small capillary tube whose diameter matches the hole in the preform. The monomer solution is inserted into the capillary tube under capillary action and polymerized at elevated temperature. Exhibit F is the starting tube, Exhibit G the drawn capillary tube, and Exhibit H the final polymerized core. The capillary tube can be either inserted in the hole and drawn or inserted into the half-cylinders before they are bonded together.

6.3 Core Drawing

In the core drawing method, the core is also separately prepared. The monomer-chromophore solution is polymerized in a long test tube and the rod so formed is drawn into a fiber whose diameter matches the diameter of the cladding hole. The core is inserted into the preform hole

and drawn. The fiber core can be inserted into the core before or after the bonding procedure. Exhibit I is the polymerized tube used to draw the core and Exhibit J a drawn core.

7 Discussion

Each method of making preforms has advantages and disadvantages. The Hoechst-Celanese copolymer, however, has several advantages over the guest host solid solution system as follows.

- Higher doping concentrations are possible
- Faster polymerization rates (Dissolved dyes in the monomer inhibit polymerization)
- Greatly reduced diffusion of the dye chromophore out of the core and into the cladding

Figure 8 shows an example of dopant diffusion of a dye chromophore into PMMA polymer. The photographs (from left to right and down) show the core of a squarylium-doped fiber at ever increasing contrast levels. The upper left photograph shows a small but highly doped $8\mu m$ core and the bottom right photograph shows the broad range of diffusion in the same fiber core. Note that image truncation and grain is an artifact of the imaging system. While graded index profiles may be useful in some applications, a small-core step index is best suited for high intensity all-optical device applications.

The advantages of the Hoechst-Celanese material should lead to the development of high-quality waveguides that will someday be components in an all-optical device.

8 Work In Progress

We are continuing to improve the drawing process in an effort to make high-quality single-mode polymer fibers with Hoechst-Celanese materials. Two masters students will be involved with the project until the end of 1992. One of these students has been assigned a masters thesis project with

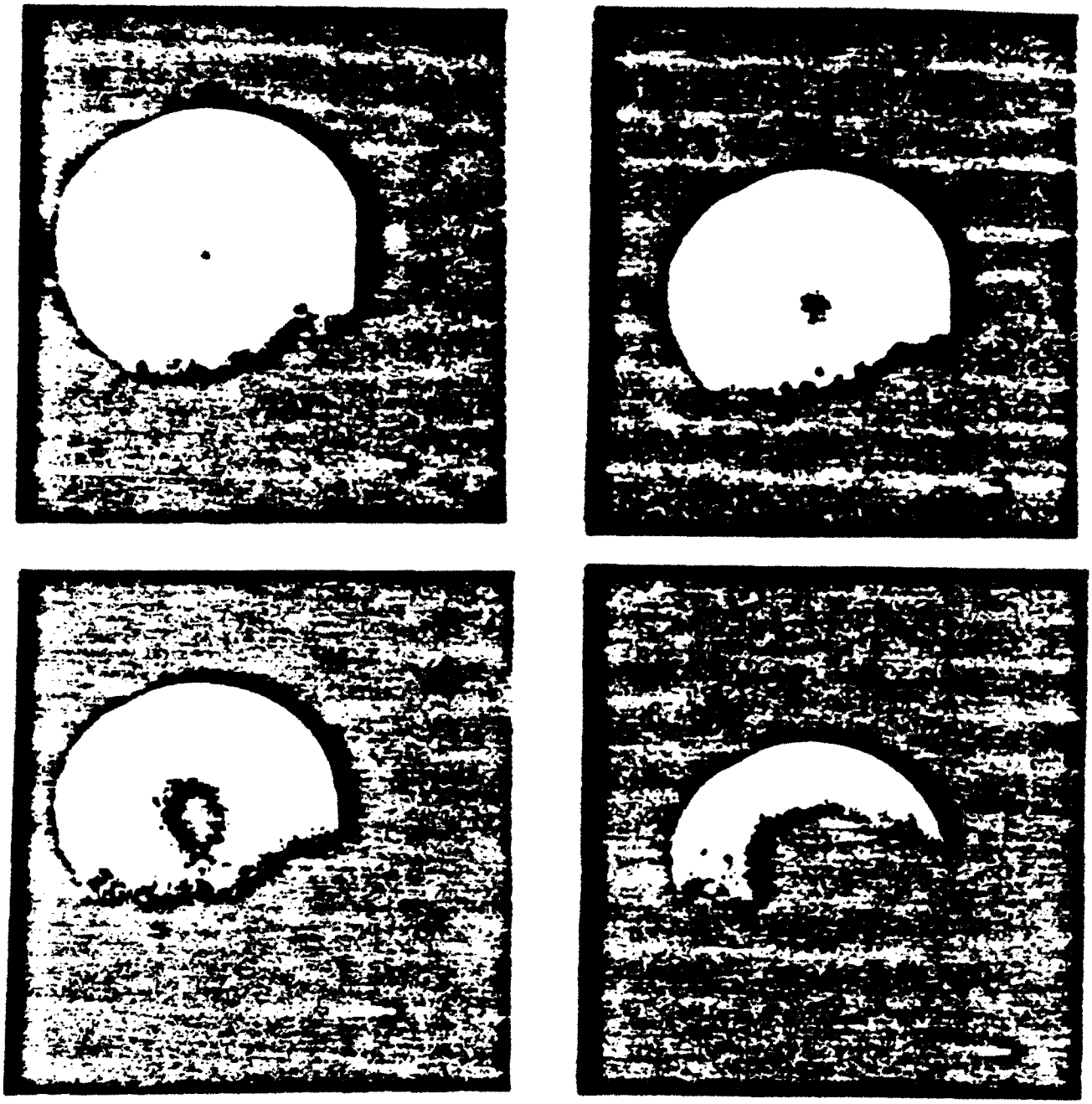

Figure 8: Photographs taken with a fiber imaging system of a squarylium-doped fiber with increasing levels of contrast.

the goal of observing third harmonic generation in the dye-chromophore-rich core region of a single or double-mode fiber. The experimental procedure involves applying a longitudinal stress to the fiber during the third harmonic measurements to induce a change in the optical path length which, as a function of this length, should result in maker fringes. Such measurements will determine the fast electronic response of the dyes in the waveguide. The second student is concentrating on improving the guiding modes of the fiber by improving the processing conditions. An infrared imaging system is being used under white-light exposure to record the surface quality of the fiber ends and to determine the core size. A coherent infrared source that excites a guided-mode will be imaged with the same system. The transverse beam profile of the light in the core will be used to determine the quality of the guided mode. The imaging apparatus is operational and the third harmonic generation experiments are being assembled. Both experiments are expected to yield new results by the end of 1992.

References

[*] Spool sent to Hoechst-Celanese 11/15/91.

[1] M. G. Kuzyk and C. W. Dirk, Appl. Phys. Lett 54, 1628 (1989).